Selective fluoride sensing by a novel series of lanthanide-based one-dimensional coordination polymers through intramolecular proton transfer

Vaibhav Singh,[a] *Lakshmi Thachanadan Suresh,*[a] *Jean-Pascal Sutter,**[b] *Arun Kumar Bar**[a]

[a]Indian Institute of Science Education and Research Tirupati, Tirupati-517507, AP, India.

[b]Laboratoire de Chimie de Coordination du CNRS (LCC-CNRS), Université de Toulouse, CNRS, Toulouse, France. E-mail: a.bar@iisertirupati.ac.in

---

SUPPORTING INFORMATION

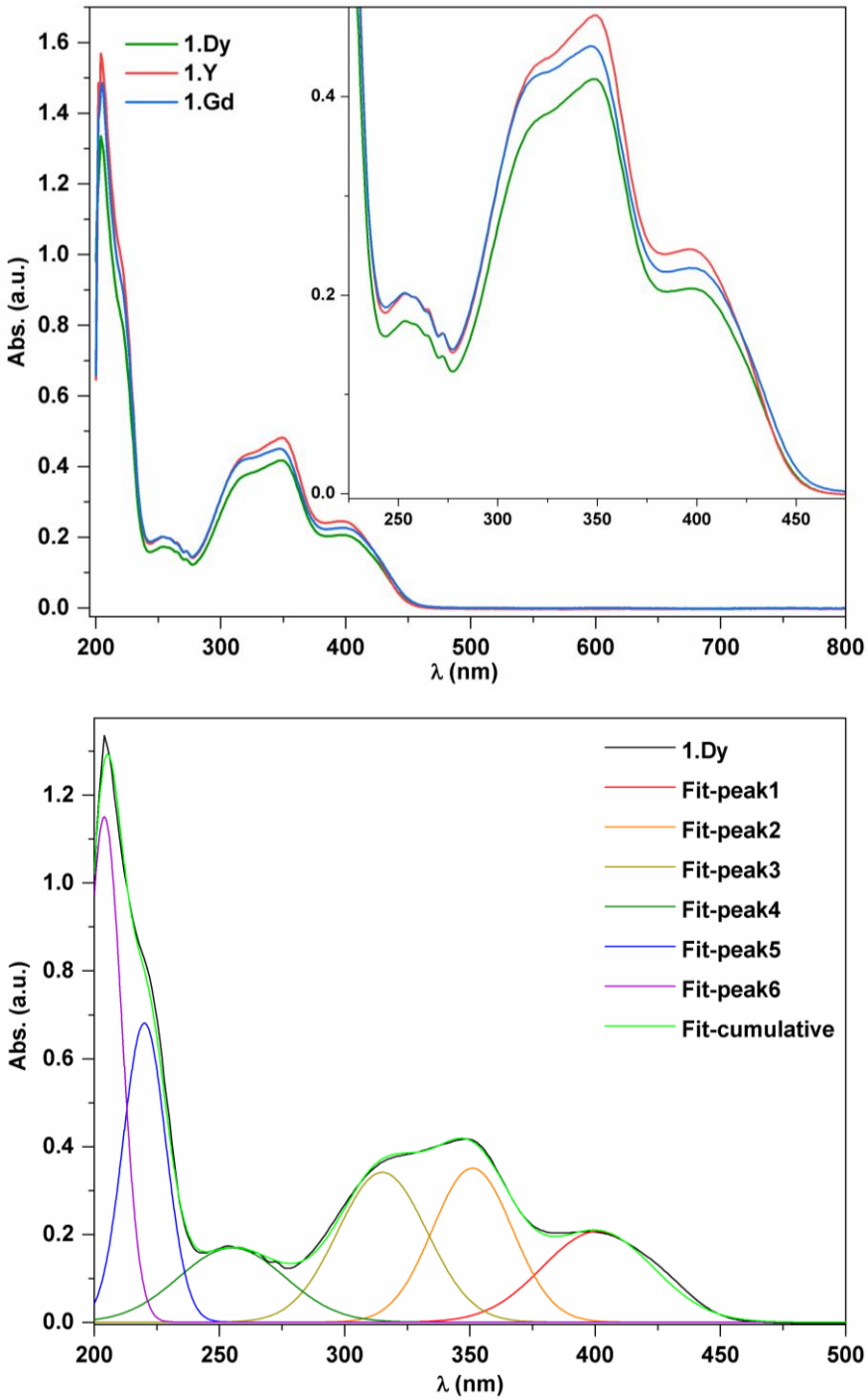

Figure S1: ***Top:*** The comparative UV-Vis absorption spectra of the methanolic solutions (12.5 μM) of **1·Y** (red), **1·Dy** (black) and **1·Gd** (blue), recorded at room temperature. The insets are the zoomed-in absorptions in the 225-475 nm regions. ***Bottom:*** The room temperature UV-Vis absorption spectrum of the methanolic solution (12.5 μM) of **1·Dy** (black) along with the best fit (fluorescent green) for its deconvoluted peaks at λ_{max}^{abs} (nm) = 401 (red); 351 (orange); 315 (yellow); 255 (green); 220 (blue) and 204 (violet); The characteristic data and measurement details are provided in experimental section.

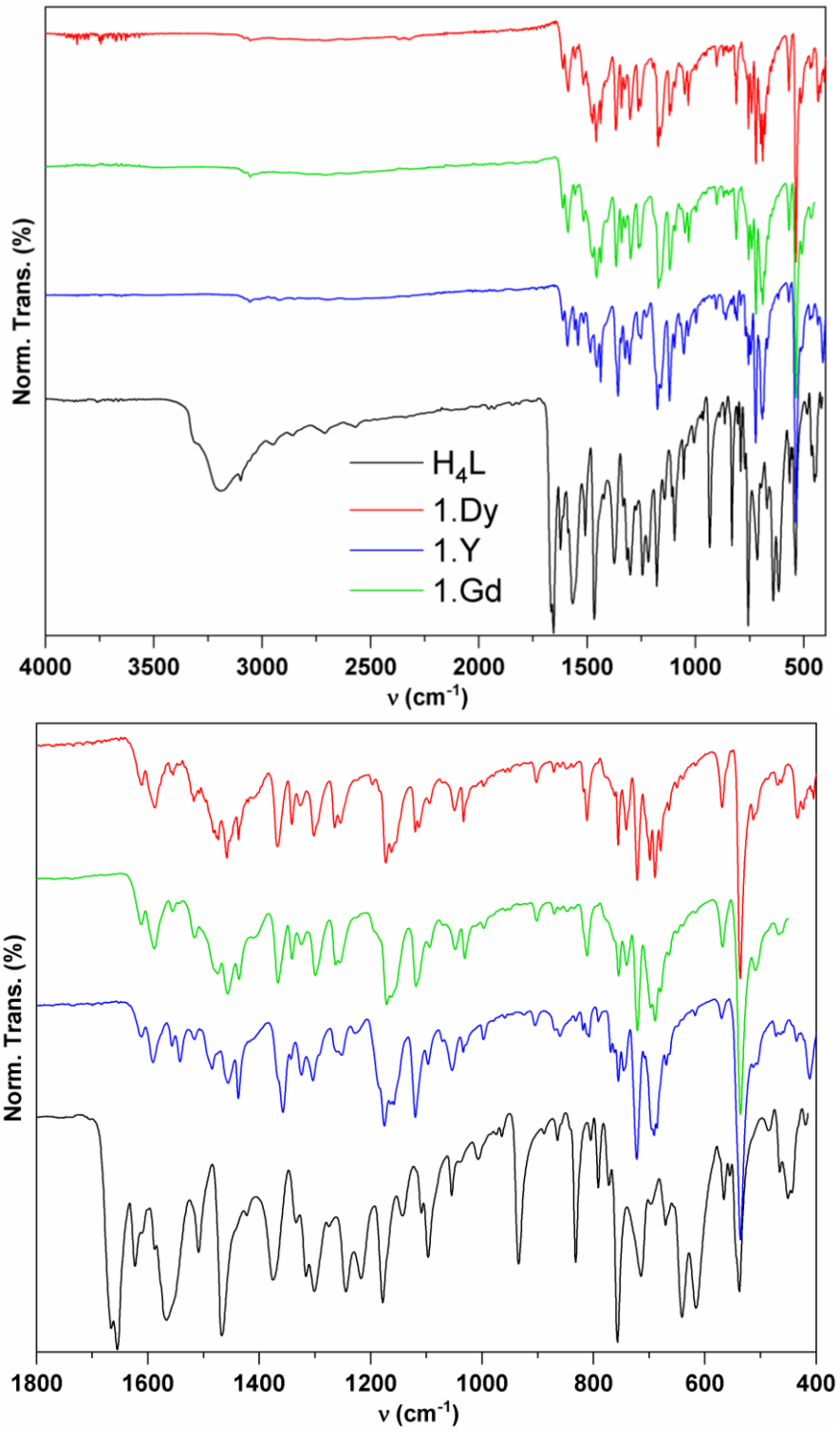

Figure S2. Comparative solid-state FT-IR spectra (4000 – 400 cm^{-1} on the top and 1800-400 cm^{-1} at the bottom) of the as synthesized Schiff base ligand **H_4L** (black), **1·Dy** (red), **1·Gd** (green) and **1·Y**(blue) recorded at room temperature.

Table S1: The characteristic stretching frequencies corresponding to the C=O and C=N functional groups in the Schiff base ligands and in the complexes. The assignment of the stretching frequencies is based on the reported literature.

Compound	$\upsilon_{C=0}(cm^{-1})$	$\upsilon_{C=N}(cm^{-1})$
H_4L	1640(vs),1608(s)	1573(m),1552(vs)
$[(H_2L)Y(NO_3)(TPPO)]_\infty$ **(1.Y)**	1557(w),1542(m)	1612(w),1591(m)
$[(H_2L)Dy(NO_3)(TPPO)]_\infty$**(1.Dy)**	1555(w)	1612(w) ,1590(m)
$[(H_2L)Gd(NO_3)(TPPO)]_\infty$**(1.Gd)**	1556(w)	1612(w),1588(m)

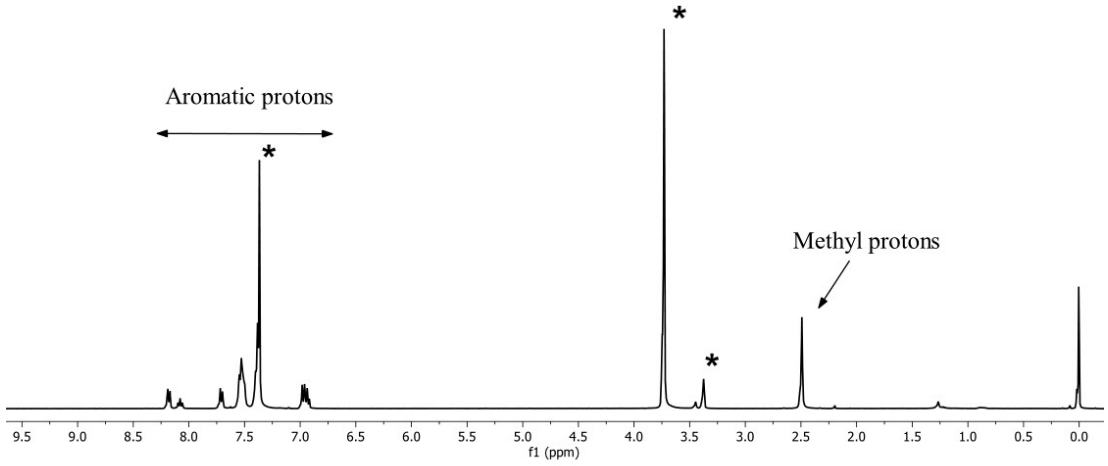

Figure S3: The room temperature solution ^{1}H NMR spectra of the complexes of Y analogue **1·Y** (top, recorded in $CDCl_3$/MeOD (5:1)). The solvent peaks/grease are indicated by asterisks

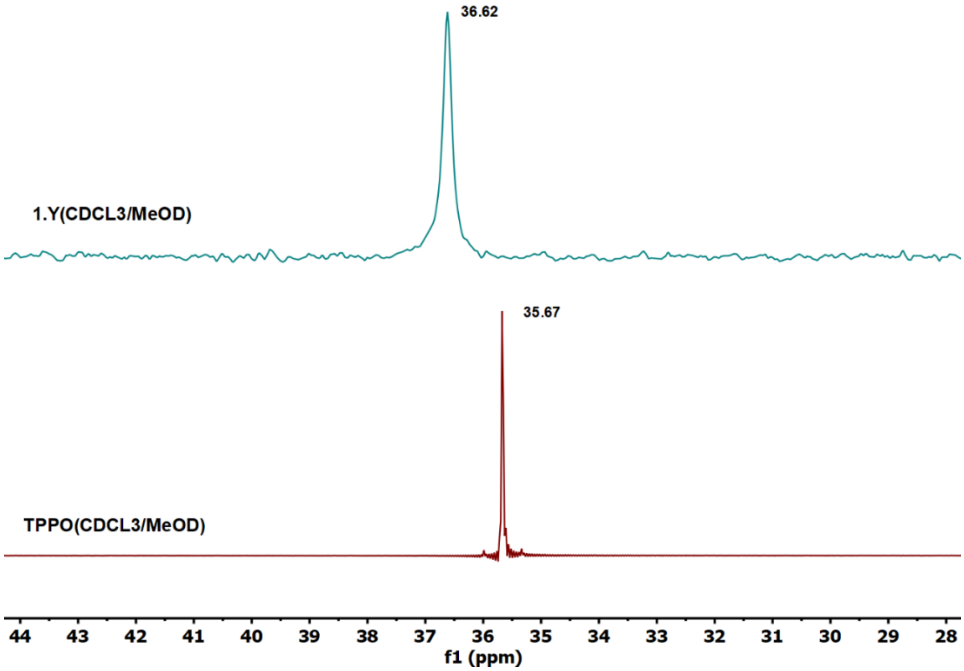

Figure S4: The comparative ^{31}P NMR spectra of TPPO (red) and **1·Y** (blue) recorded in CDCl3/MeOD(5:1) solution at room temperature.

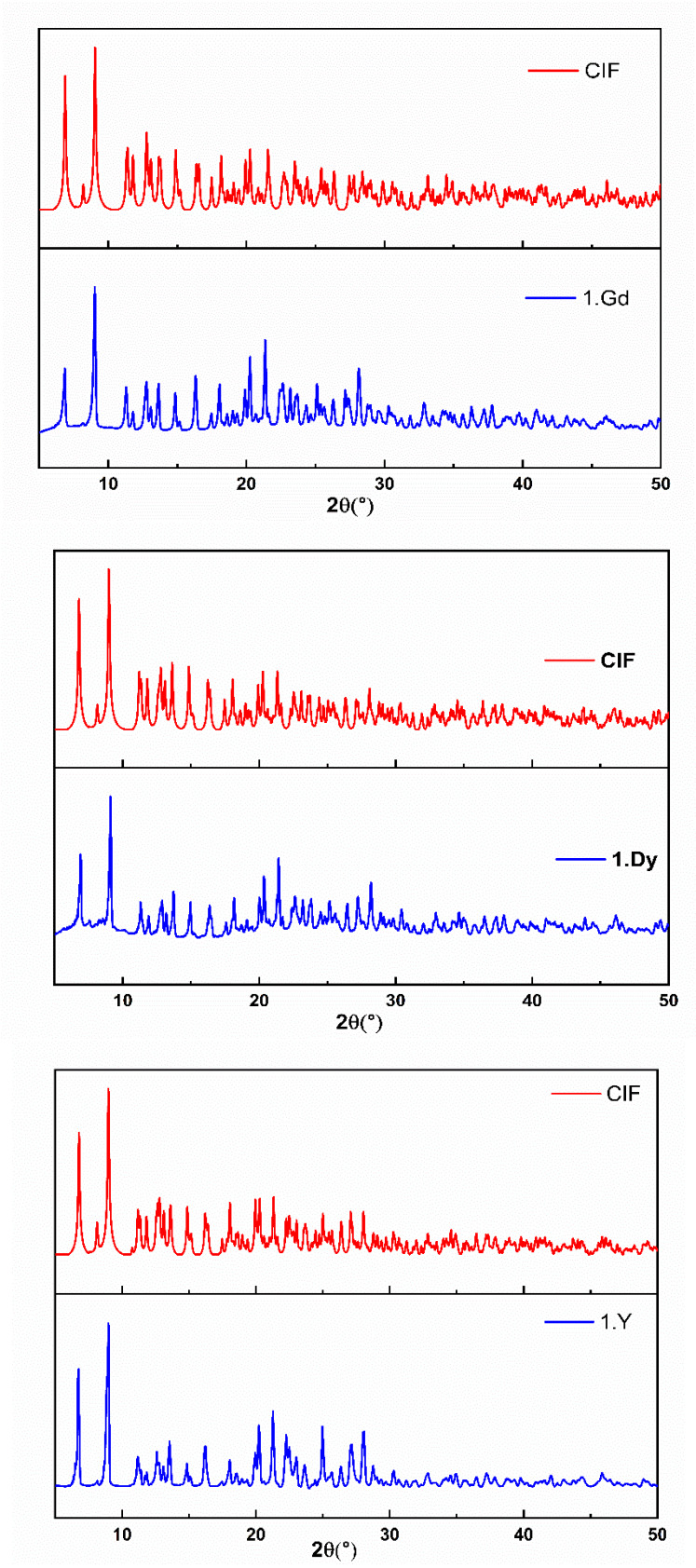

Figure S5: The powder X-ray diffraction patterns of the complexes **1·Gd** (*top*), **1·Dy** (*middle*) and **1·Y** (*bottom*) recorded at room temperature. Colour codes: experimental, blue; and simulated, red.

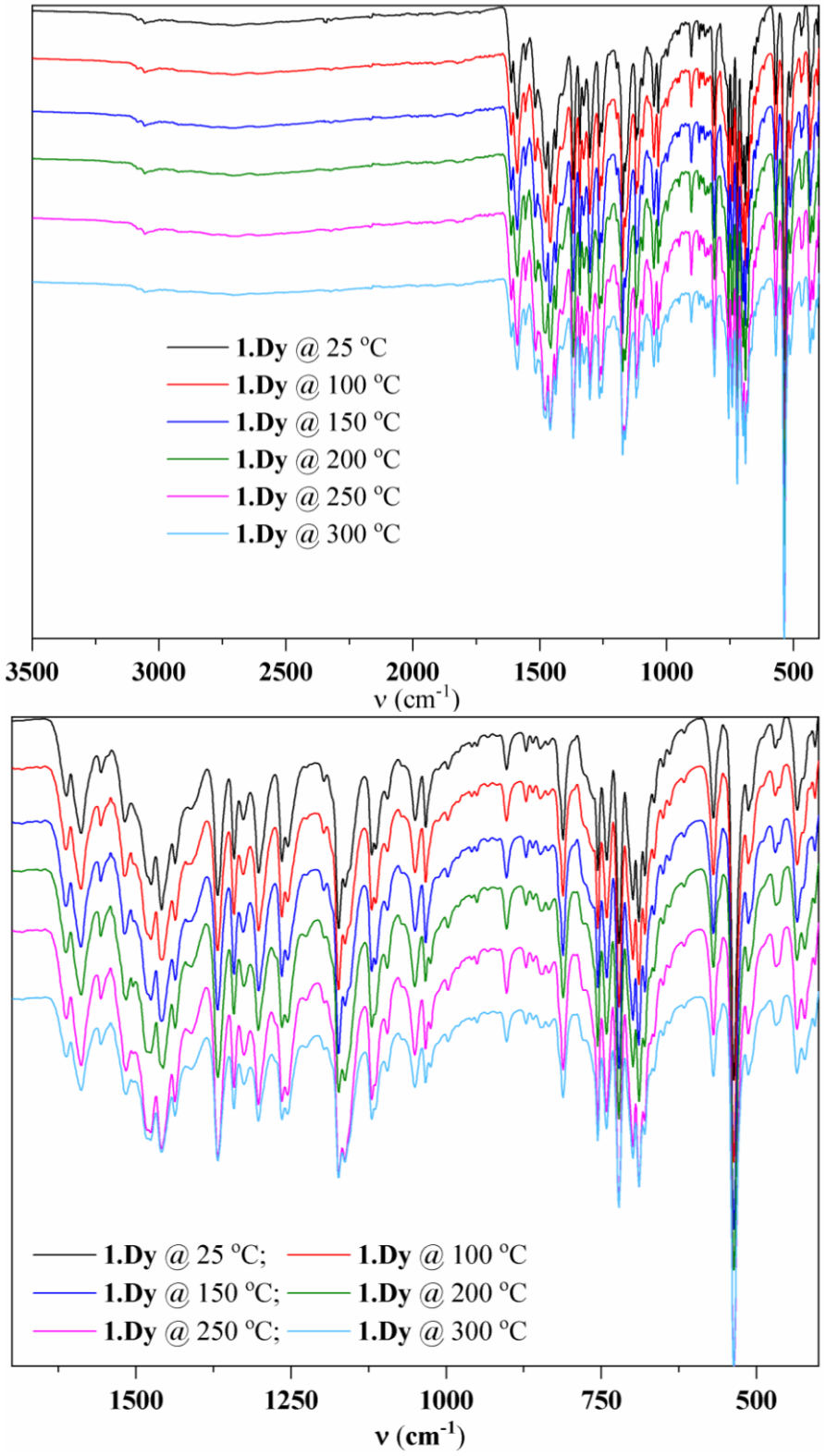

Figure S6: The variable temperature comparative solid-state FT-IR spectra (3500 – 400 cm^{-1} on the top and 1700-400 cm^{-1} at the bottom) of the complex **1·Dy** recorded at 25 °C (black), 100 °C (red), 150 °C (blue), 200 °C (green) 250 °C (magenta) and 300 °C (cyan).

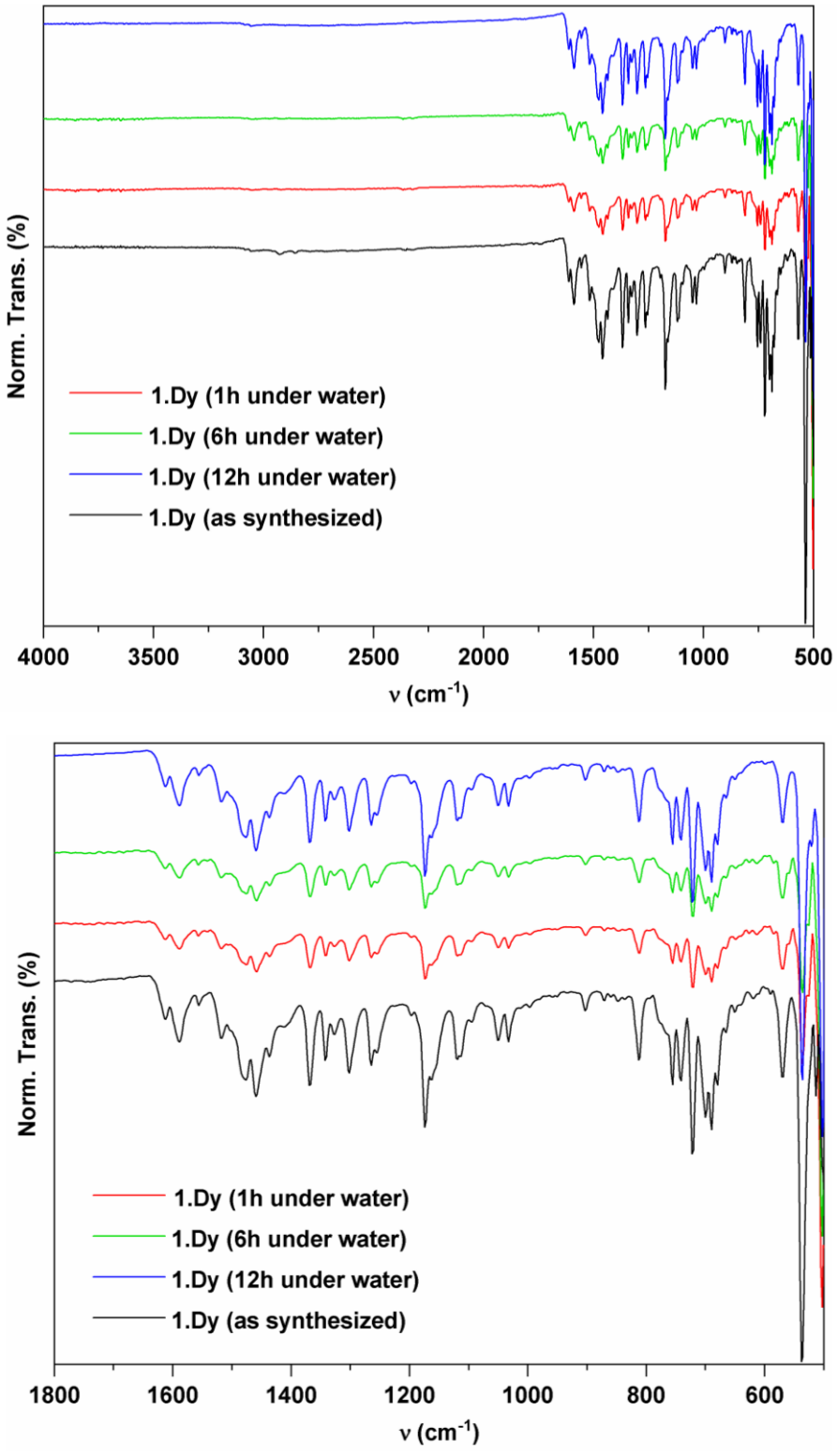

Figure S7: The comparative time-dependent solid-state FT-IR spectra (4000 – 400 cm^{-1} on the top and 1800-400 cm^{-1} at the bottom) of the complex **1.Dy** recorded at room temperature upon soaking under water instantly 0h (black) and after 1h (red), 6h (green), and 12h (blue).

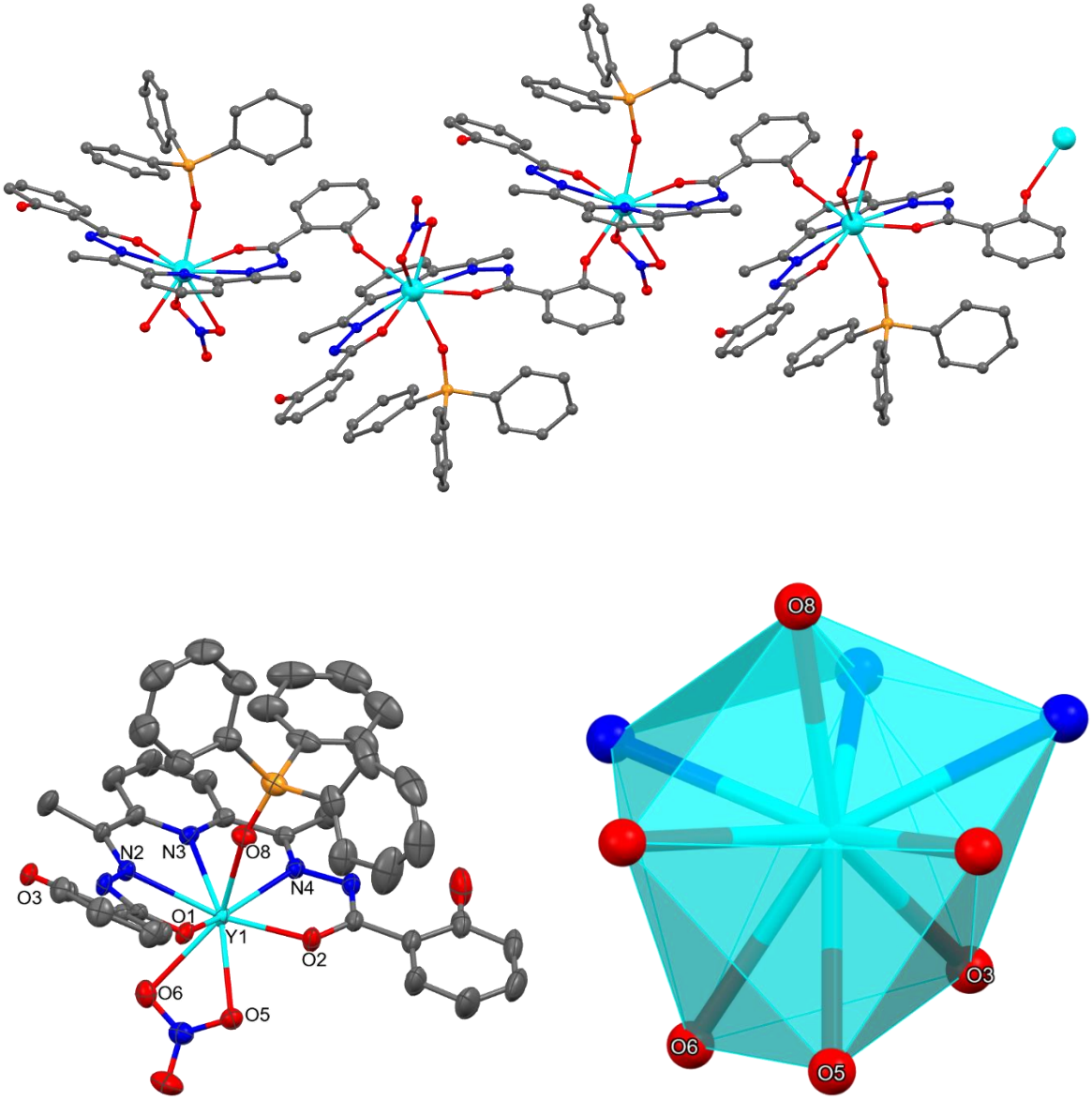

Figure S8*:* Top: The *ball-and-stick* models of the single-crystal X-ray molecular structures of the **1·Y** (displayed up to four consecutive repeat units) **Bottom left:** Ellipsoid models with 40% probability for the single crystal X-ray molecular structure of **1·Y** in solid state. H atoms in **1·Y** are omitted for clarity. Colour codes: cyan, Y; yellow, P; red, O; blue, N; grey, C. **Bottom *Right:*** The coordination polyhedron around the Y centre of **1·Y**. The oxygen atoms of the meridionally coordinated ancillary ligands are labelled.

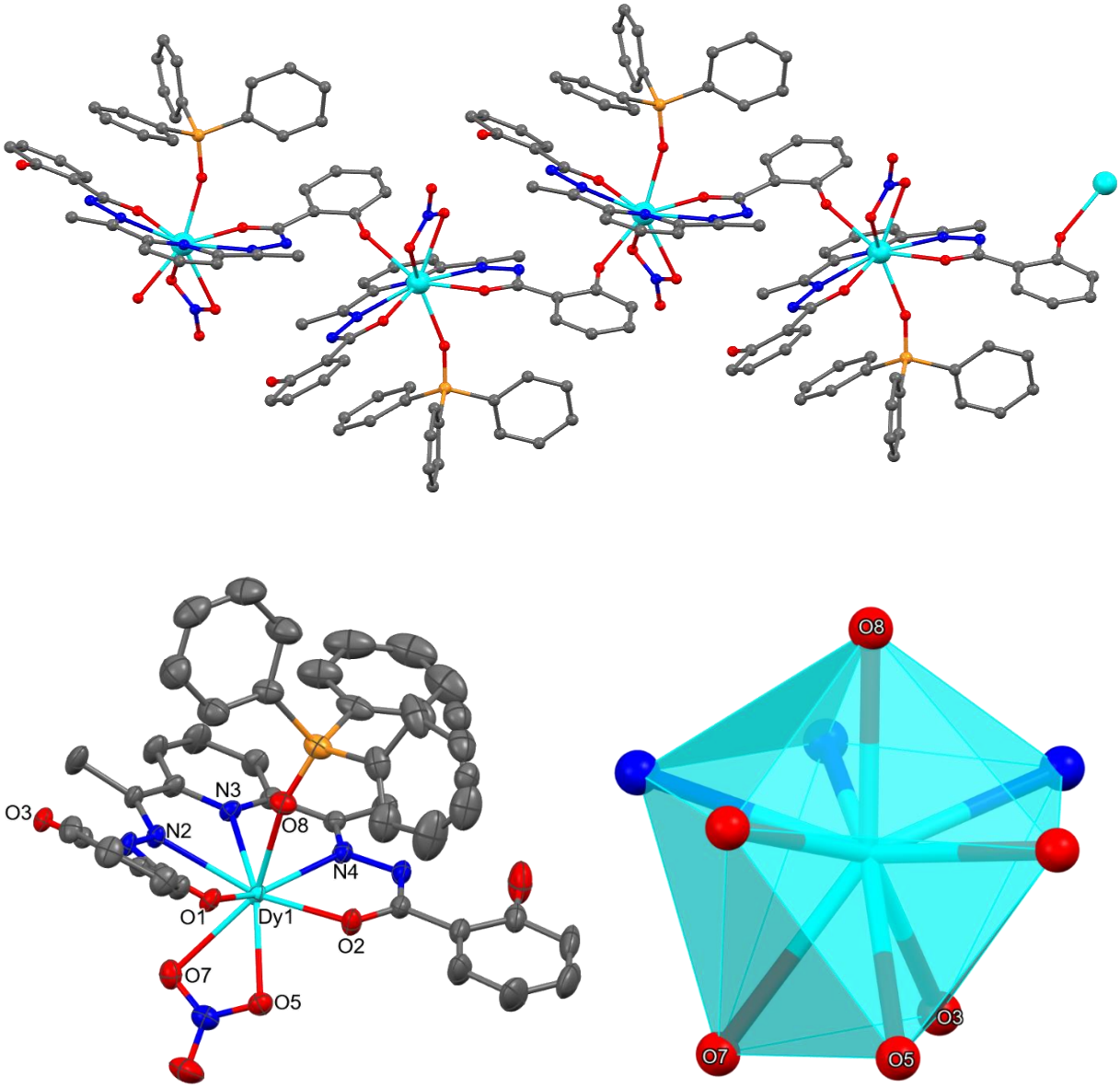

Figure S9*:* Top: The *ball-and-stick* models of the single-crystal X-ray molecular structures of the **1·Dy** (displayed up to four consecutive repeat units) **Bottom left:** Ellipsoid models with 40% probability for the single crystal X-ray molecular structure of **1·Dy** in solid state. H atoms in **1·Dy** are omitted for clarity. Colour codes: cyan, Y; yellow, P; red, O; blue, N; grey, C. **Bottom *Right:*** The coordination polyhedron around the Dy centre of **1·Dy**. The oxygen atoms of the meridionally coordinated ancillary ligands are labelled.

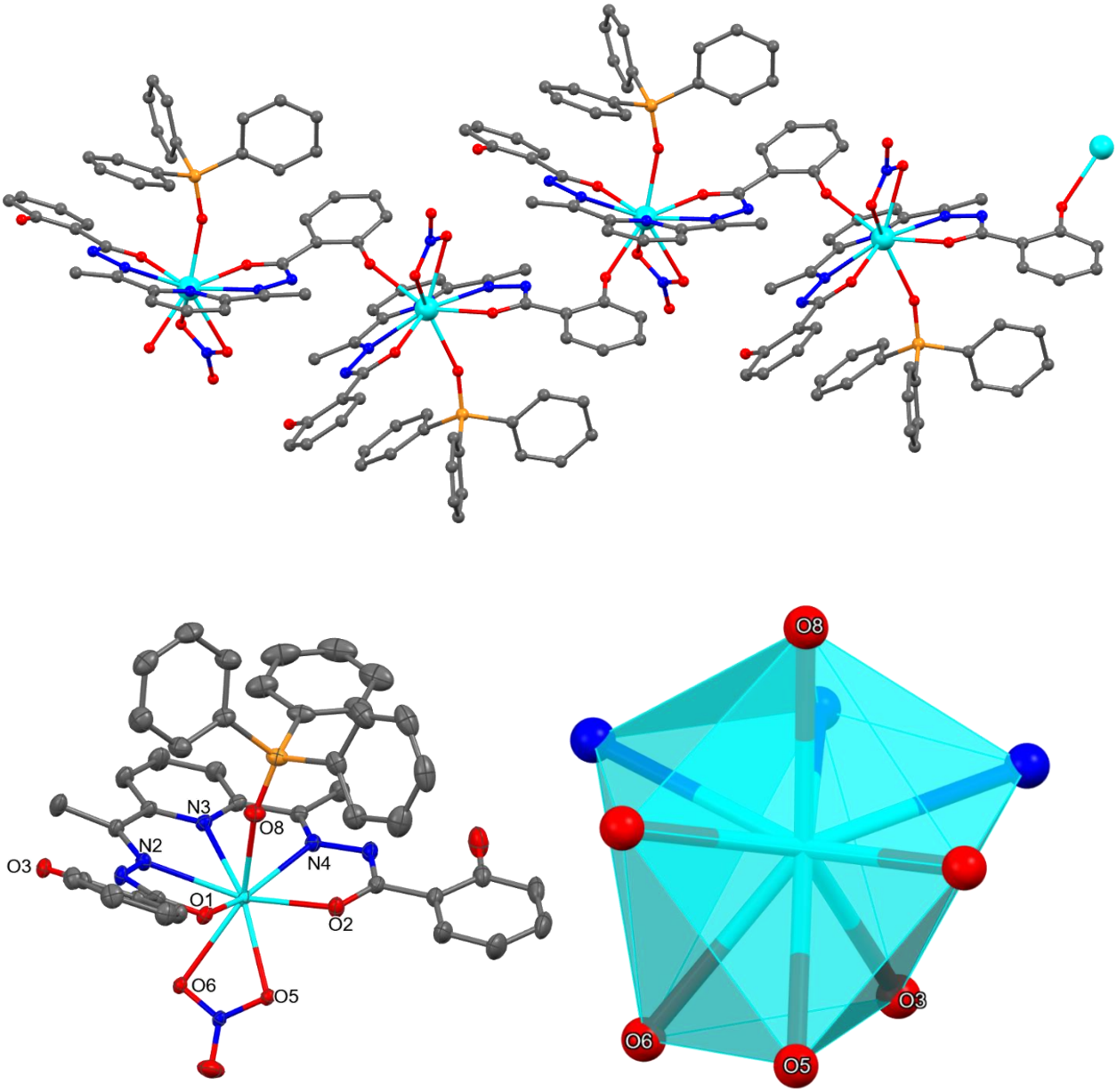

Figure S10*:* Top:The ball-and-stick models of the single-crystal X-ray molecular structures of the **1·Gd** (displayed up to four consecutive repeat units) **Bottom left:** Ellipsoid models with 50% probability for the single crystal X-ray molecular structure of **1·Gd** in solid state. H atoms in **1·Gd** are omitted for clarity. Colour codes: cyan, Gd; yellow, P; red, O; blue, N; grey, C. **Bottom *Right:*** The coordination polyhedron around the Gd centre of **1·Gd**. The oxygen atoms of the meridionally coordinated ancillary ligands are labelled.

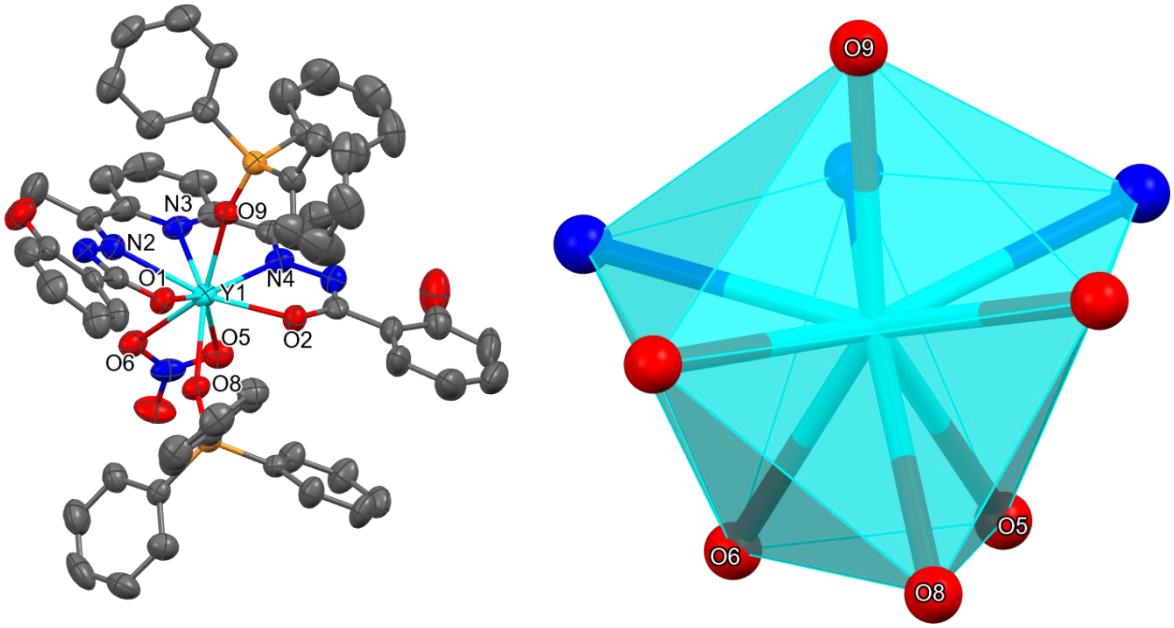

Figure S11*:* Top: Ellipsoid models with 40% probability for the single crystal X-ray molecular structure of **2·Y** in solid state. H atoms in **2·Y** are omitted for clarity. Colour codes: cyan, Y; yellow, P; red, O; blue, N; grey, C. **Bottom*:*** The coordination polyhedron around the Y centre of **2·Y**. The oxygen atoms of the meridionally coordinated ancillary ligands are labelled.

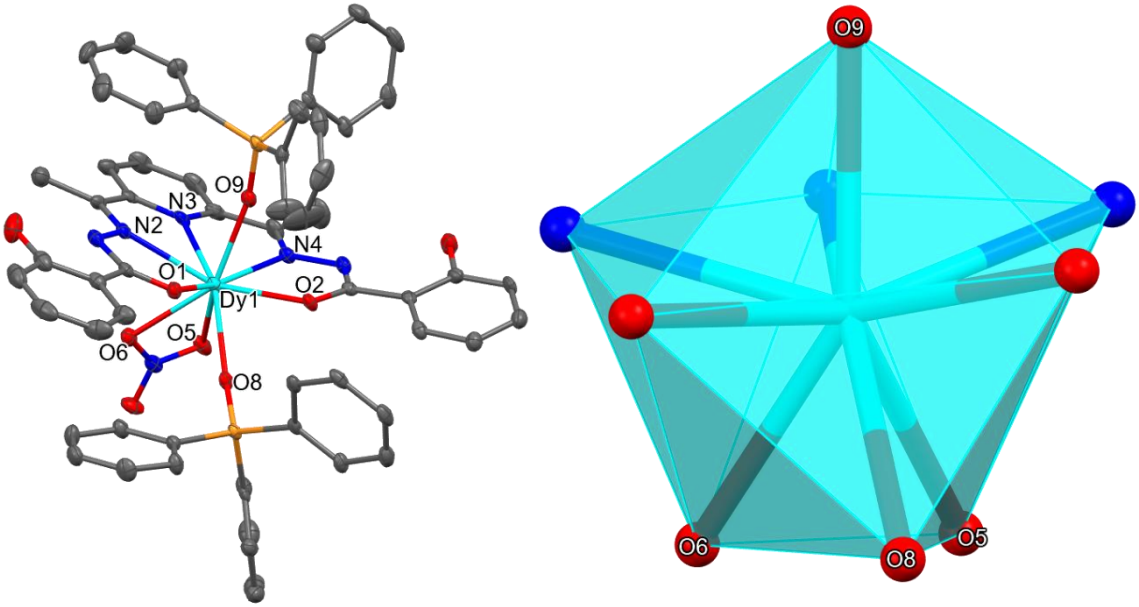

Figure S12*:* Top: Ellipsoid models with 40% probability for the single crystal X-ray molecular structure of **2·Dy** in solid state. H atoms in **2·Dy** are omitted for clarity. Colour codes: cyan, Dy; yellow, P; red, O; blue, N; grey, C. **Bottom*:*** The coordination polyhedron around the Dy centre of **2·Dy**. The oxygen atoms of the meridionally coordinated ancillary ligands are labelled.

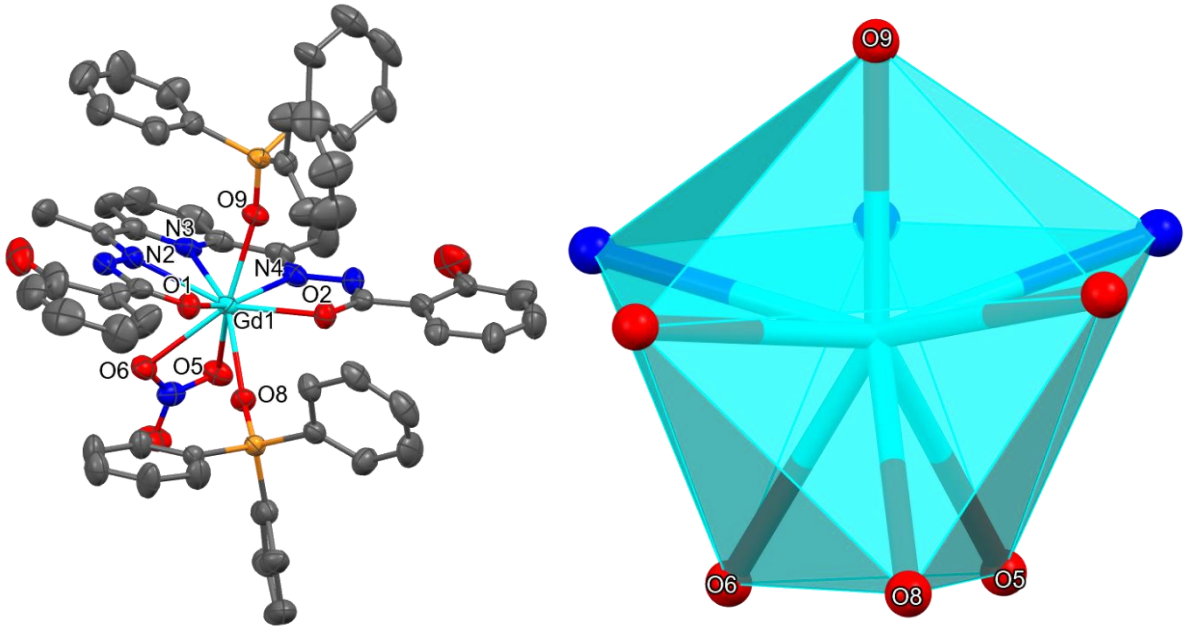

Figure S13*:* Top: Ellipsoid models with 40% probability for the single crystal X-ray molecular structure of **2·Gd** in solid state. H atoms in **2·Gd** are omitted for clarity. Colour codes: cyan, Gd; yellow, P; red, O; blue, N; grey, C. **Bottom*:*** The coordination polyhedron around the Gd centre of **2·Gd**. The oxygen atoms of the meridionally coordinated ancillary ligands are labelled.

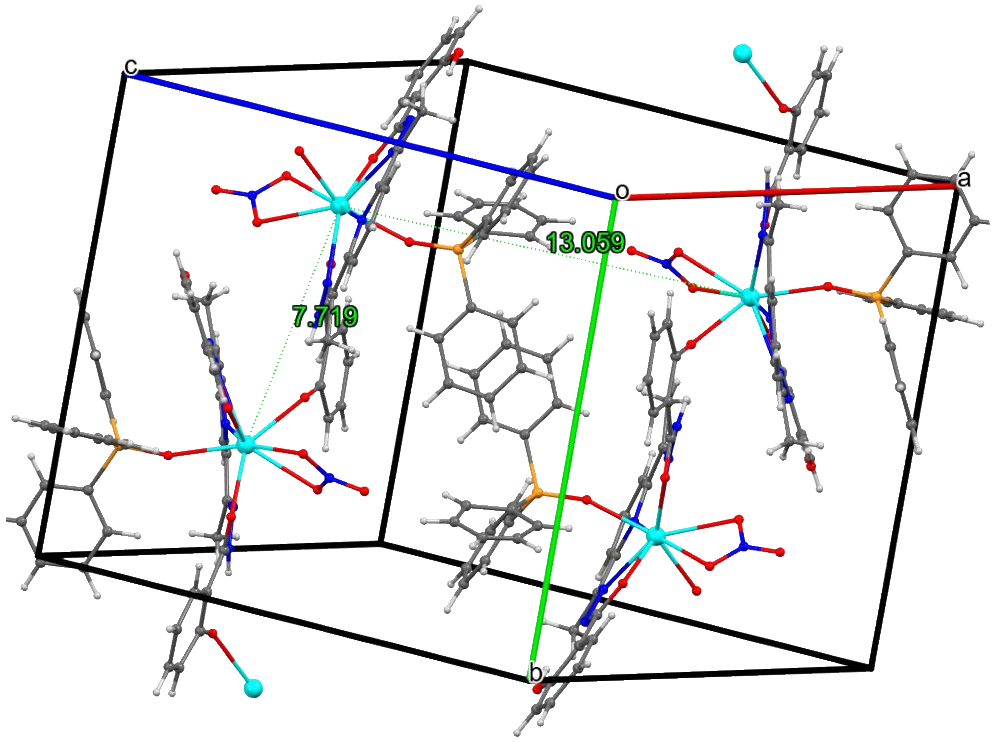

Figure S14: Unit cell contents of **1·Y .** Colour codes: cyan, Y; red, O; blue, N; grey, C; off-white, H. The dotted green lines correspond to the Y---Y distances in the unit cells.

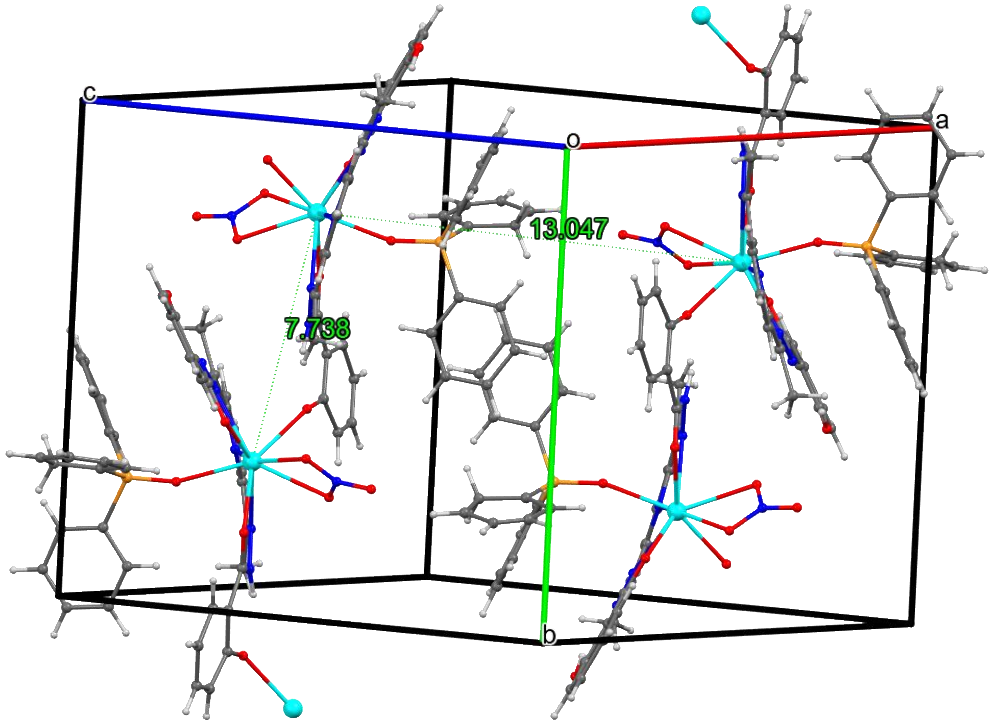

Figure S15: Unit cell contents of **1·Dy**. Colour codes: cyan, Dy; red, O; blue, N; grey, C; off-white, H. The dotted green lines correspond to the Dy---Dy distances in the unit cells.

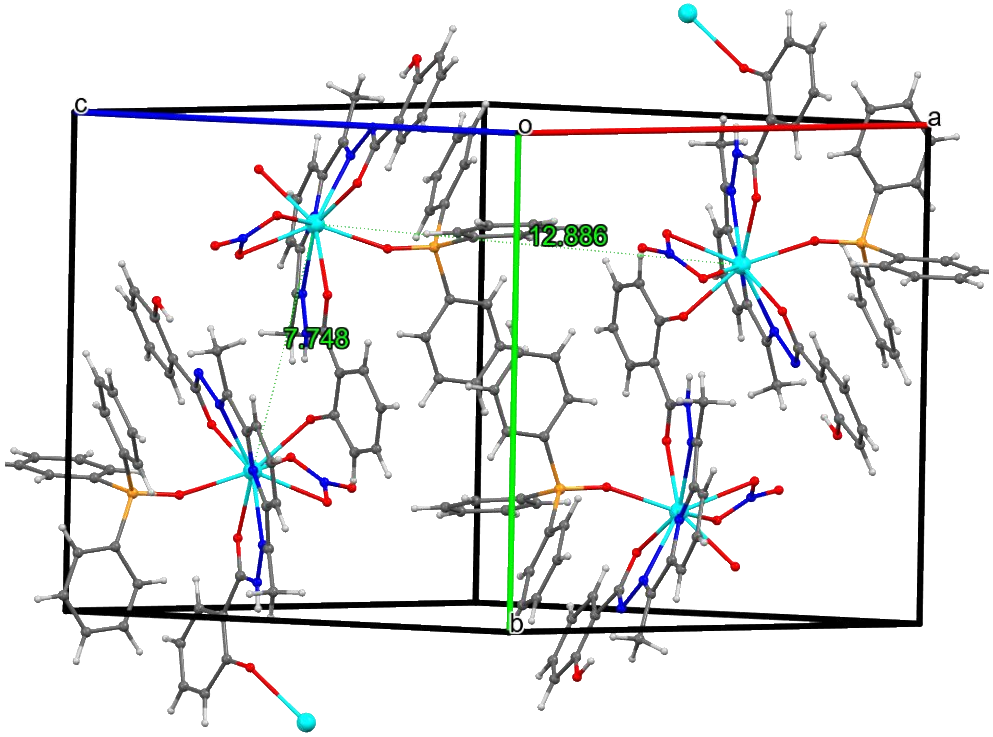

Figure S16: Unit cell contents of **1·Gd**. Colour codes: cyan, Gd; red, O; blue, N; grey, C; off-white, H. The dotted green lines correspond to the Gd---Gd distances in the unit cells.

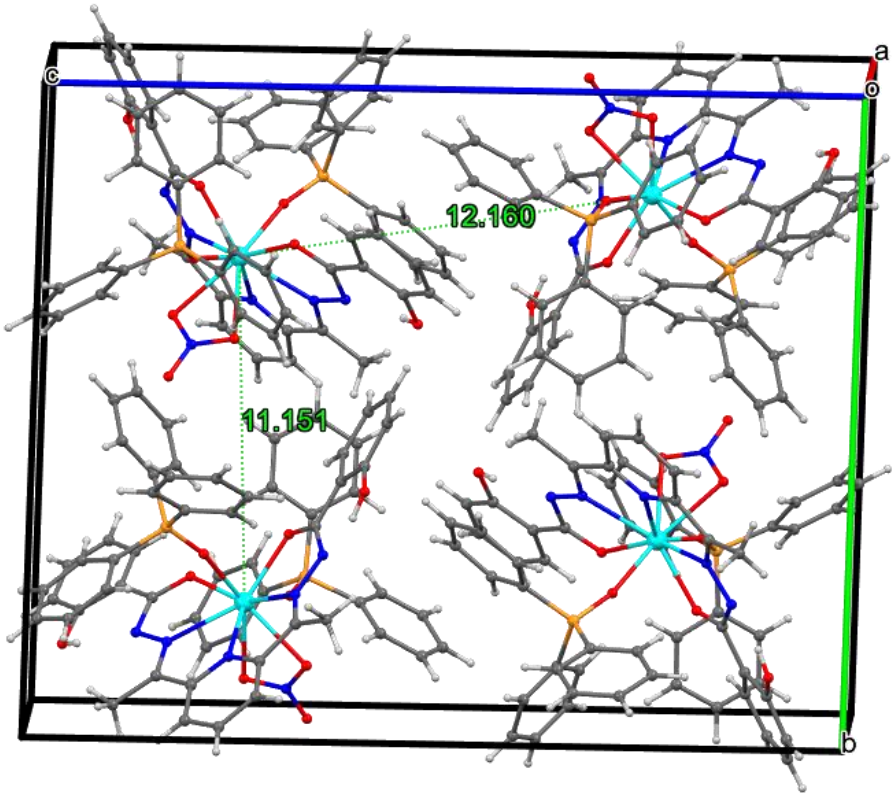

Figure S17: Unit cell contents of **2·Y**. Colour codes: cyan, Y; red, O; blue, N; grey, C; off-white, H. The dotted green lines correspond to the Y---Y distances in the unit cells.

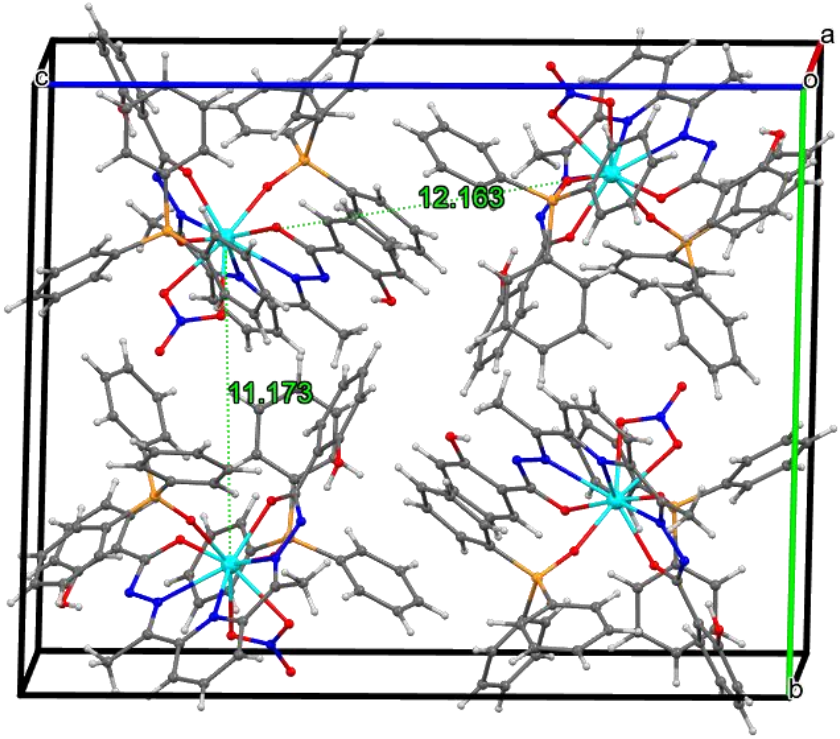

Figure S18: Unit cell contents of **2·Dy**. Colour codes: cyan, Dy; red, O; blue, N; grey, C; off-white, H. The dotted green lines correspond to the Dy---Dy distances in the unit cells.

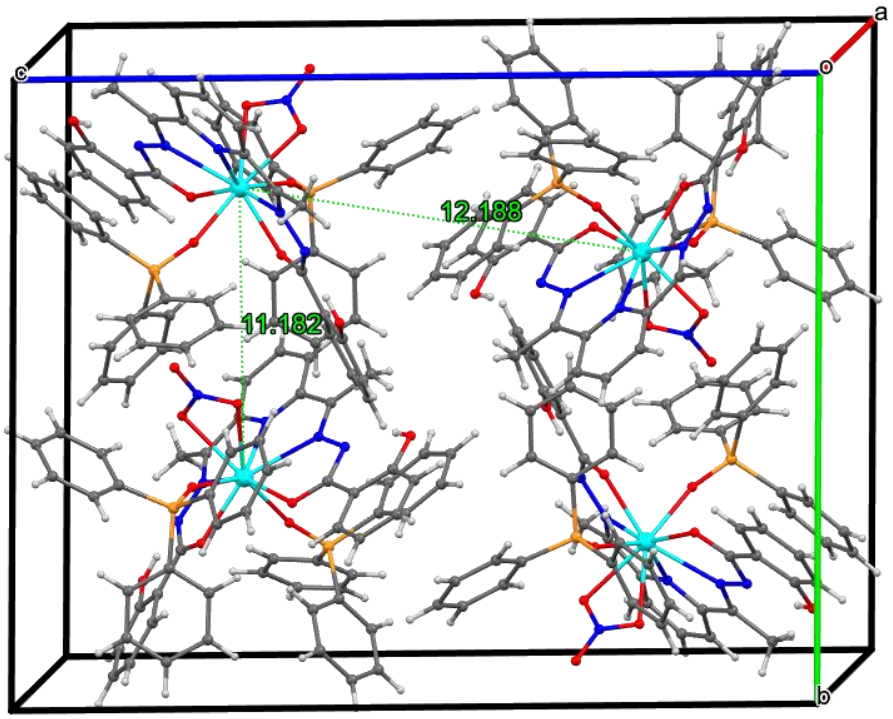

Figure S19: Unit cell contents of **2·Gd**. Colour codes: cyan, Gd; red, O; blue, N; grey, C; off-white, H. The dotted green lines correspond to the Gd---Gd distances in the unit cells.

Table S2. Selected crystallographic data and refinement parameters for **1·Ln** and **2·Ln** (Ln = Y, Gd and Dy).

	1·Dy	**1·Y**	**1·Gd**
Formula[a]	$C_{41}H_{34}DyN_6O_8P$	$C_{41}H_{34}YN_6O_8P$	$C_{41}H_{34}GdN_6O_8P$
Mr (g mol^{-1})[a]	932.21	858.62	926.96
crystal system	Monoclinic	Monoclinic	Monoclinic
space group	P 21/n	P 21/n	P 21/n
T (K)	150	150	150
a (Å)	16.2035(4)	16.1937(4)	16.0840(4)
b (Å)	14.9875(4)	14.9487(3)	14.9967(3)
c (Å)	16.3982(4)	16.4338(4)	16.1977(4)
α (°)	90	90	90
β (°)	105.806(2)	105.832(3)	105.453(1)
γ (°)	90	90	90
V (Å^3)	3831.73(17)	3827.30(16)	3765.76(15)
Z	4	4	4
$\rho_{calcd.}$ (g cm^{-3})	1.616	1.490	1.635
μ (mm^{-1})	2.054	1.628	1.867
collected reflns	31126	38058	67528
unique reflns	8286	8852	8315
No. of parameters	544	546	503
Refinement Reflections.	31126	38058	67528
R (I > 3σ(I))[b]	0.0228	0.0383	0.0236
wR (I > 3σ(I))[c]	0.0573	0.0895	0.0576
GOF on *F*	1.031	1.020	1.046
	2·Dy	**2·Y**	**2·Gd**
Formula[a]	$C_{59}H_{49}DyN_6O_9P_2$	$C_{59}H_{49}YN_6O_9P_2$	$C_{59}H_{49}GdN_6O_9P_2$
Mr (g mol^{-1})[a]	1210.48	1136.89	1205.23
crystal system	Monoclinic	Monoclinic	Monoclinic
space group	P 21/c	P 21/c	P 21/c
T (K)	100	100	100
a (Å)	12.7507(4)	12.7183(8)	12.7779(4)
b (Å)	18.8420(6)	18.8005(11)	18.8824(5)
c (Å)	23.9856(9)	23.9922(15)	24.0303(6)
α (°)	90	90	90
β (°)	103.0270(10)	102.962(2)	103.1190(10)
γ (°)	90	90	90
V (Å^3)	5614.2(3)	5590.6(6)	5646.6(3))
Z	4	4	4
$\rho_{calcd.}$ (g cm^{-3})	1.432	1.351	1.418
μ (mm^{-1})	1.449	1.162	1.292
collected reflns	104895	53310	74873
unique reflns	12889	9913	13985
No. of parameters	698	699	675
Refinement Reflections.	104895	53310	37008
R (I > 3σ(I))[b]	0.0202	0.0644	0.0375
wR (I > 3σ(I))[c]	0.0534	0.1838	0.1043
GOF on *F*	1.032	0.956	0.996

[a] Excluding co-crystallized solvent molecules. [b] $R = \Sigma||F_o| - |F_c||/\Sigma|F_o|$, [c] $wR = [\Sigma(w(F_o^2 - F_c^2)^2)/\Sigma ([w(F_o^2)^2]^{1/2}$ where $w = 1/(\sigma^2(F_o^2) + (aP)^2 + bP)$ with $P = (2F_c^2 + \max(F_o^2,0))/3$.

Table S3. Selected bond lengths (Å) and bond angles (°) of the complexes **1·Ln** (Ln = Y, Dy, Gd) and **2·Ln** (Ln = Y, Dy, Gd)

Complex **1·Y**

Y1 O3	2.3560(14)	Y1 O1	2.3912(14)	Y1 O2	2.2629(15)	Y1 O6	2.5417(17)
Y1 O5	2.4307(15)	Y1 N4	2.4717(18)	Y1 O8	2.3573(16)	Y1 N2	2.5352(17)
Y1 N3	2.5120(16)	Y1 N6	2.903(2)				

O3 Y1 O1	141.58(5)	O3 Y1 O6	70.53(5)	O3 Y1 O5	73.31(5)
O3 Y1 N4	71.09(6)	O3 Y1 O8	145.47(5)	O3 Y1 N2	112.55(5)
O3 Y1 N3	77.81(5)	O3 Y1 N6	69.27(6)	O1 Y1 O6	72.28(5)
O1 Y1 O5	76.19(5)	O1 Y1 N4	145.40(6)	O1 Y1 N2	64.07(5)
O1 Y1 N3	122.99(5)	O1 Y1 N6	73.12(6)	O2 Y1 O3	95.83(6)
O2 Y1 O1	94.44(5)	O2 Y1 O6	120.08(6)	O2 Y1 O5	68.90(6)
O2 Y1 N4	64.79(6)	O2 Y1 O8	81.03(6)	O2 Y1 N2	151.61(6)
O2 Y1 N3	127.04(6)	O2 Y1 N6	94.24(6)	O6 Y1 N6	25.87(6)
O5 Y1 O6	51.19(5)	O5 Y1 N4	116.65(6)	O5 Y1 N2	118.97(5)
O5 Y1 N3	148.55(6)	O5 Y1 N6	25.34(6)	N4 Y1 O6	141.61(6)
N4 Y1 N2	122.55(6)	N4 Y1 N3	63.48(6)	N4 Y1 N6	132.44(6)
O8 Y1 O1	72.78(5)	O8 Y1 O6	140.20(6)	O8 Y1 O5	134.40(6)
O8 Y1 N4	76.65(6)	O8 Y1 N2	75.10(6)	O8 Y1 N3	77.05(6)
O8 Y1 N6	145.05(6)	N2 Y1 O6	72.91(6)	N2 Y1 N6	96.56(6)
N3 Y1 O6	107.22(6)	N3 Y1 N2	61.98(5)	N3 Y1 N6	129.45(6)

Complex **1·Gd**

Gd1 O1	2.4232(15)	Gd1 O3	2.3858(15)	Gd1 O8	2.3876(16)	Gd1 O6	2.5670(15)
Gd1 O5	2.4601(14)	Gd1 O2	2.2994(15)	Gd1 N3	2.5325(18)	Gd1 N4	2.4991(18)
Gd1 N6	2.9379(18)	Gd1 N2	2.5623(18)				

O1 Gd1 O6	71.78(5)	O1 Gd1 O5	76.71(5)	O1 Gd1 N3	122.08(5)
O1 Gd1 N4	145.75(6)	O1 Gd1 N6	71.87(5)	O1 Gd1 N2	63.50(5)
O3 Gd1 O1	141.72(5)	O3 Gd1 O8	145.10(6)	O3 Gd1 O6	70.58(5)
O3 Gd1 O5	74.48(5)	O3 Gd1 N3	77.42(6)	O3 Gd1 N4	71.16(6)
O3 Gd1 N6	71.27(5)	O3 Gd1 N2	112.12(6)	O8 Gd1 O1	72.79(6)
O8 Gd1 O6	140.63(5)	O8 Gd1 O5	133.59(5)	O8 Gd1 N3	76.50(6)
O8 Gd1 N4	76.54(6)	O8 Gd1 N6	143.41(5)	O8 Gd1 N2	74.32(6)
O6 Gd1 N6	25.71(5)	O5 Gd1 O6	50.97(5)	O5 Gd1 N3	149.88(5)
O5 Gd1 N4	116.11(5)	O5 Gd1 N6	25.27(5)	O5 Gd1 N2	120.69(5)
O2 Gd1 O1	95.55(5)	O2 Gd1 O3	96.94(6)	O2 Gd1 O8	80.24(6)
O2 Gd1 O6	119.70(5)	O2 Gd1 O5	68.74(5)	O2 Gd1 N3	125.90(6)
O2 Gd1 N4	64.17(6)	O2 Gd1 N6	93.99(5)	O2 Gd1 N2	150.79(6)
N3 Gd1 O6	108.97(5)	N3 Gd1 N6	131.79(5)	N3 Gd1 N2	61.47(6)
N4 Gd1 O6	141.72(5)	N4 Gd1 N3	63.19(6)	N4 Gd1 N6	133.17(5)
N4 Gd1 N2	121.69(6)	N2 Gd1 O6	74.93(5)	N2 Gd1 N6	97.88(5)

Complex **1·Dy**

Dy1 O1	2.4062(15)	Dy1 O3	2.3718(15)	Dy1 O8	2.3704(17)	Dy1 O5	2.4413(17)
Dy1 O2	2.2757(16)	Dy1 O7	2.5515(18)	Dy1 N3	2.5154(18)	Dy1 N2	2.5409(18)
Dy1 N4	2.4770(19)	Dy1 N6	2.912(2)				

O1 Dy1 O5	76.43(6)	O1 Dy1 O7	72.18(6)	O1 Dy1 N3	122.69(5)
O1 Dy1 N2	63.87(6)	O1 Dy1 N4	145.42(6)	O1 Dy1 N6	73.08(6)
O3 Dy1 O1	141.62(5)	O3 Dy1 O5	73.28(6)	O3 Dy1 O7	70.56(5)
O3 Dy1 N3	77.97(6)	O3 Dy1 N2	112.68(6)	O3 Dy1 N4	71.12(6)
O3 Dy1 N6	69.40(6)	O8 Dy1 O1	72.68(6)	O8 Dy1 O3	145.52(6)
O8 Dy1 O5	134.27(6)	O8 Dy1 O7	140.30(6)	O8 Dy1 N3	76.96(6)
O8 Dy1 N2	74.96(6)	O8 Dy1 N4	76.63(6)	O8 Dy1 N6	144.86(6)
O5 Dy1 O7	50.98(6)	O5 Dy1 N3	148.77(6)	O5 Dy1 N2	119.30(6)
O5 Dy1 N4	116.54(6)	O5 Dy1 N6	25.40(6)	O2 Dy1 O1	94.76(6)
O2 Dy1 O3	95.80(6)	O2 Dy1 O8	80.87(7)	O2 Dy1 O5	68.91(6)
O2 Dy1 O7	119.88(6)	O2 Dy1 N3	126.79(6)	O2 Dy1 N2	151.49(6)
O2 Dy1 N4	64.62(6)	O2 Dy1 N6	94.31(6)	O7 Dy1 N6	25.60(6)
N3 Dy1 O7	107.70(6)	N3 Dy1 N2	61.87(6)	N3 Dy1 N6	129.75(6)
N2 Dy1 O7	73.41(6)	N2 Dy1 N6	96.79(6)	N4 Dy1 O7	141.68(6)
N4 Dy1 N3	63.44(6)	N4 Dy1 N2	122.38(6)	N4 Dy1 N6	132.53(6)

Complex **2·Y**

Y1 O9	2.291(3)	Y1 O1	2.325(3)	Y1 O2	2.335(4)	Y1 O8	2.319(3)
Y1 O6	2.544(3)	Y1 O5	2.493(3)	Y1 N2	2.498(4)	Y1 N3	2.506(4)
Y1 N4	2.495(4)	Y1 N6	2.919(4)				

O9 Y1 O1	75.22(11)	O9 Y1 O2	83.73(12)	O9 Y1 O8	138.12(11)
O9 Y1 O6	143.00(12)	O9 Y1 O5	145.07(11)	O9 Y1 N2	75.24(13)
O9 Y1 N3	79.25(12)	O9 Y1 N4	79.06(12)	O9 Y1 N6	157.81(12)
O1 Y1 O2	97.56(12)	O1 Y1 O6	102.37(11)	O1 Y1 O5	139.54(11)
O1 Y1 N2	64.26(13)	O1 Y1 N3	125.35(13)	O1 Y1 N4	150.09(12)
O1 Y1 N6	120.02(12)	O2 Y1 O6	132.48(12)	O2 Y1 O5	87.03(12)
O2 Y1 N2	154.96(13)	O2 Y1 N3	126.66(12)	O2 Y1 N4	64.38(12)
O2 Y1 N6	108.17(13)	O8 Y1 O1	70.60(11)	O8 Y1 O2	77.63(12)
O8 Y1 O6	69.36(11)	O8 Y1 O5	71.26(11)	O8 Y1 N2	109.39(13)
O8 Y1 N3	141.13(12)	O8 Y1 N4	123.38(13)	O8 Y1 N6	63.93(11)
O6 Y1 N6	25.92(12)	O5 Y1 O6	50.81(12)	O5 Y1 N2	118.01(12)
O5 Y1 N3	79.58(12)	O5 Y1 N4	66.61(12)	O5 Y1 N6	25.53(12)
N2 Y1 O6	70.91(12)	N2 Y1 N3	62.83(13)	N2 Y1 N6	96.23(13)
N3 Y1 O6	72.38(12)	N3 Y1 N6	78.65(12)	N4 Y1 O6	107.35(12)
N4 Y1 N2	123.01(14)	N4 Y1 N3	62.89(14)	N4 Y1 N6	89.16(13)

Complex **2·Gd**

Gd1 O8	2.358(2)	Gd1 O5	2.542(2)	Gd1 O9	2.336(2)	Gd1 O2	2.377(2)
Gd1 O6	2.584(2)	Gd1 O1	2.360(2)	Gd1 N6	2.959(3)	Gd1 N3	2.550(3)
Gd1 N2	2.534(3)	Gd1 N4	2.537(3)				

O8 Gd1 O5	71.20(7)	O8 Gd1 O2	78.58(8)	O8 Gd1 O6	69.53(7)
O8 Gd1 O1	70.58(7)	O8 Gd1 N6	64.14(7)	O8 Gd1 N3	141.69(8)
O8 Gd1 N2	110.08(8)	O8 Gd1 N4	123.68(8)	O5 Gd1 O6	49.97(7)
O5 Gd1 N6	25.17(7)	O5 Gd1 N3	80.08(8)	O9 Gd1 O8	137.41(7)
O9 Gd1 O5	146.09(7)	O9 Gd1 O2	83.53(8)	O9 Gd1 O6	143.25(8)
O9 Gd1 O1	74.90(8)	O9 Gd1 N6	158.23(8)	O9 Gd1 N3	79.23(8)
O9 Gd1 N2	74.39(8)	O9 Gd1 N4	79.74(8)	O2 Gd1 O5	86.93(8)
O2 Gd1 O6	132.27(8)	O2 Gd1 N6	108.15(8)	O2 Gd1 N3	125.39(8)
O2 Gd1 N2	155.01(8)	O2 Gd1 N4	63.54(8)	O6 Gd1 N6	25.42(7)
O1 Gd1 O5	138.93(7)	O1 Gd1 O2	99.73(8)	O1 Gd1 O6	101.89(7)
O1 Gd1 N6	119.37(8)	O1 Gd1 N3	124.23(8)	O1 Gd1 N2	63.60(8)
O1 Gd1 N4	151.16(8)	N3 Gd1 O6	72.66(8)	N3 Gd1 N6	79.04(8)
N2 Gd1 O5	117.97(8)	N2 Gd1 O6	71.76(8)	N2 Gd1 N6	96.56(8)
N2 Gd1 N3	62.17(9)	N2 Gd1 N4	122.05(9)	N4 Gd1 O5	66.91(8)
N4 Gd1 O6	106.65(8)	N4 Gd1 N6	88.99(8)	N4 Gd1 N3	62.55(9)

Complex **2·Dy**

Dy1 O9 2.3032(11)	Dy1 O8 2.3334(11)	Dy1 O1 2.3338(11)	Dy1 O6 2.5684(12)
Dy1 O2 2.3493(12)	Dy1 O5 2.5115(12	Dy1 N4 2.5085(14)	Dy1 N2 2.5066(14)
Dy1 N6 2.9353(14)	Dy1 N3 2.5212(14)		

O9 Dy1 O8	138.02(4)	O9 Dy1 O1	75.07(4)	O9 Dy1 O6	143.07(4)
O9 Dy1 O2	83.78(4)	O9 Dy1 O5	145.38(4)	O9 Dy1 N4	79.43(4)
O9 Dy1 N2	74.70(4)	O9 Dy1 N6	157.84(4)	O9 Dy1 N3	79.10(4)
O8 Dy1 O1	70.69(4)	O8 Dy1 O6	69.29(4)	O8 Dy1 O2	77.95(4)
O8 Dy1 O5	71.26(4)	O8 Dy1 N4	123.26(4)	O8 Dy1 N2	109.71(4)
O8 Dy1 N6	63.96(4)	O8 Dy1 N3	141.34(4)	O1 Dy1 O6	102.29(4)
O1 Dy1 O2	98.27(4)	O1 Dy1 O5	139.43(4)	O1 Dy1 N4	150.44(4)
O1 Dy1 N2	63.96(4)	O1 Dy1 N6	119.84(4)	O1 Dy1 N3	125.04(4)
O6 Dy1 N6	25.61(4)	O2 Dy1 O6	132.30(4)	O2 Dy1 O5	87.07(4)
O2 Dy1 N4	63.96(4)	O2 Dy1 N2	154.84(4)	O2 Dy1 N6	108.20(4)
O2 Dy1 N3	126.12(4)	O5 Dy1 O6	50.39(4)	O5 Dy1 N6	25.41(4)
O5 Dy1 N3	79.64(4)	N4 Dy1 O6	107.08(4)	N4 Dy1 O5	66.58(4)
N4 Dy1 N6	89.05(4)	N4 Dy1 N3	62.82(5)	N2 Dy1 O6	71.46(4)
N2 Dy1 O5	118.07(4)	N2 Dy1 N4	122.87(5)	N2 Dy1 N6	96.45(4)
N2 Dy1 N3	62.75(5)	N3 Dy1 O6	72.63(4)	N3 Dy1 N6	78.80(4)

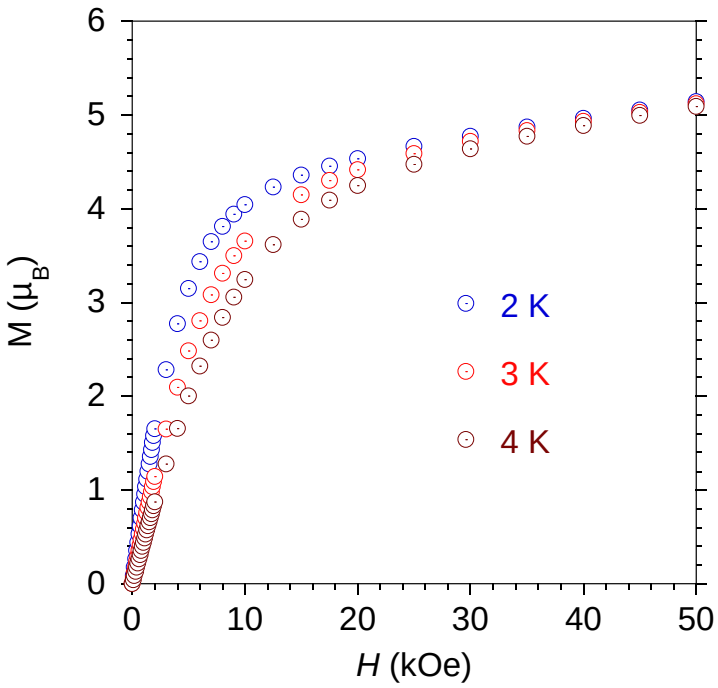

Figures S20: The variable temperature (2K, blue circles; 3K, red circles; 4K, purple) field dependence of the magnetization measured on the polycrystalline solid sample of **1.Dy**.

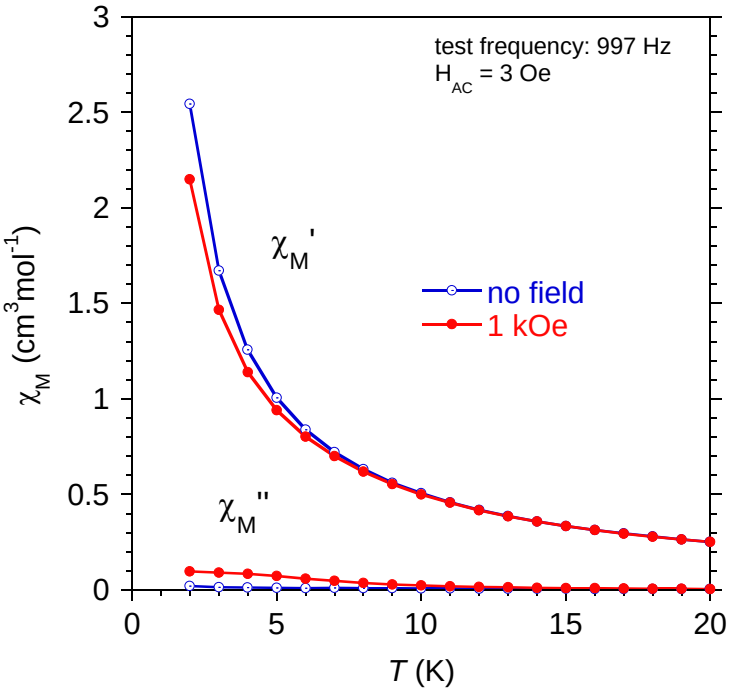

Figure S21: The AC susceptibility for **1·Dy** recorded without and with an applied DC field.

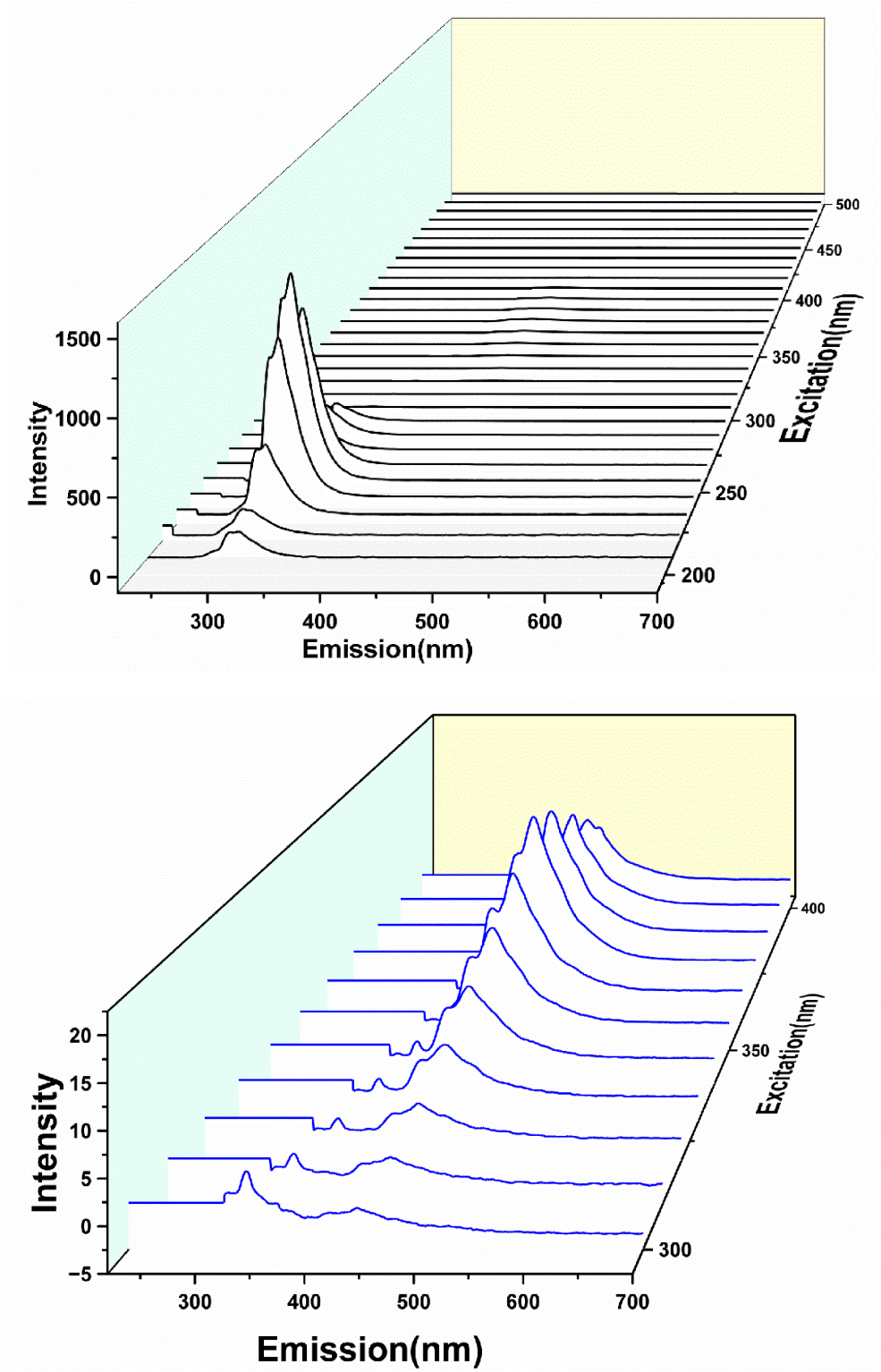

Figure S22: The excitation PL spectra for the 12.5 μM methanolic solution of **1·Dy** ranging from 200 nm to 500 nm (top) and the zoomed-in plot covering 300-400 nm (bottom) (Excitation and emission bandwidth = 2.5 nm).

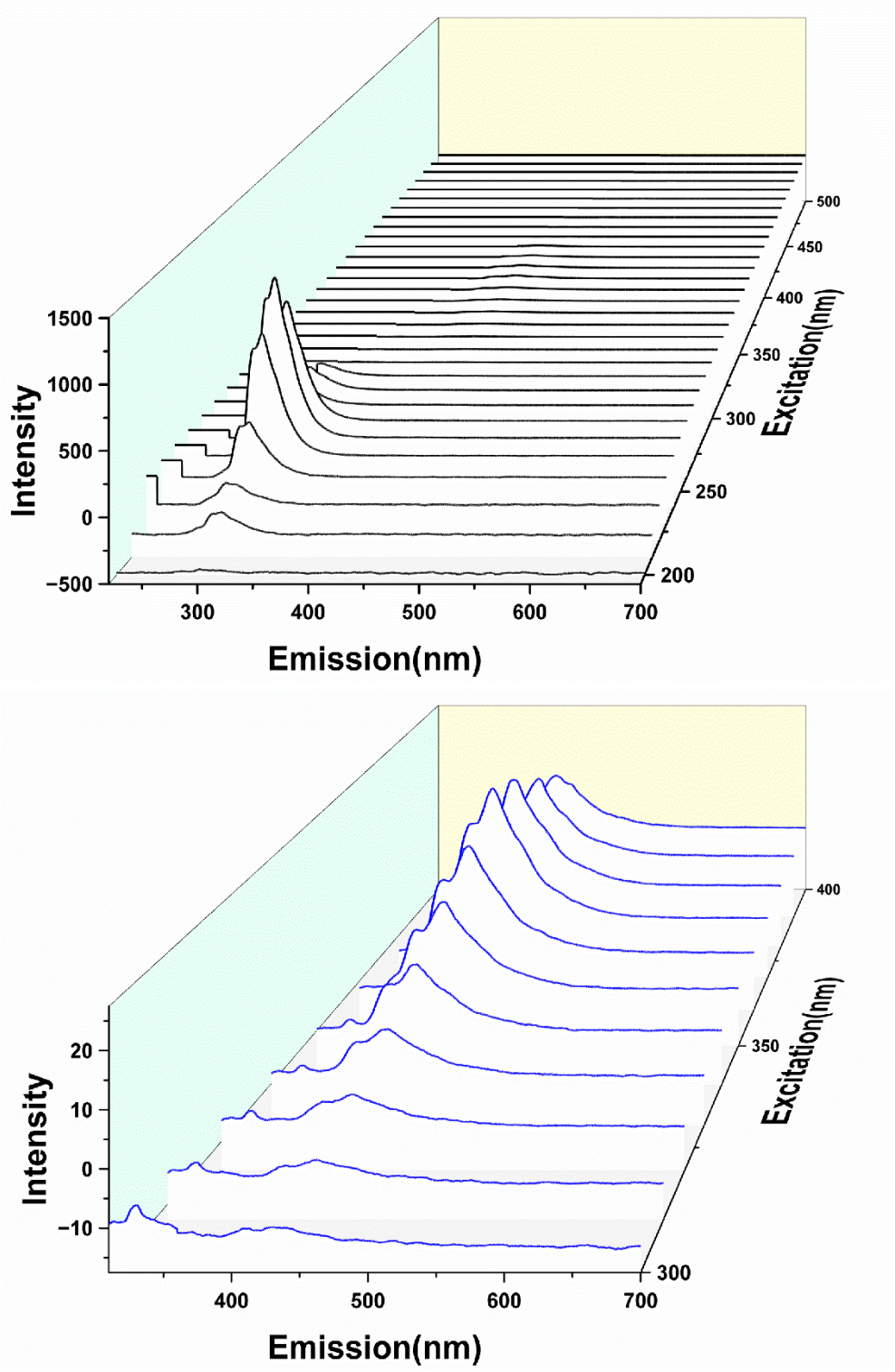

Figure S23: The excitation PL spectra for the 2mL of 12.5 μM methanolic solution of **1·Dy** in the presence of 5 equivalents (w.r.t. Dy ion) of NH_4F in the range of 200 nm to 500 nm (top) and its zoomed-in plot covering 300-400 nm (bottom) (Excitation and emission bandwidth = 2.5 nm).

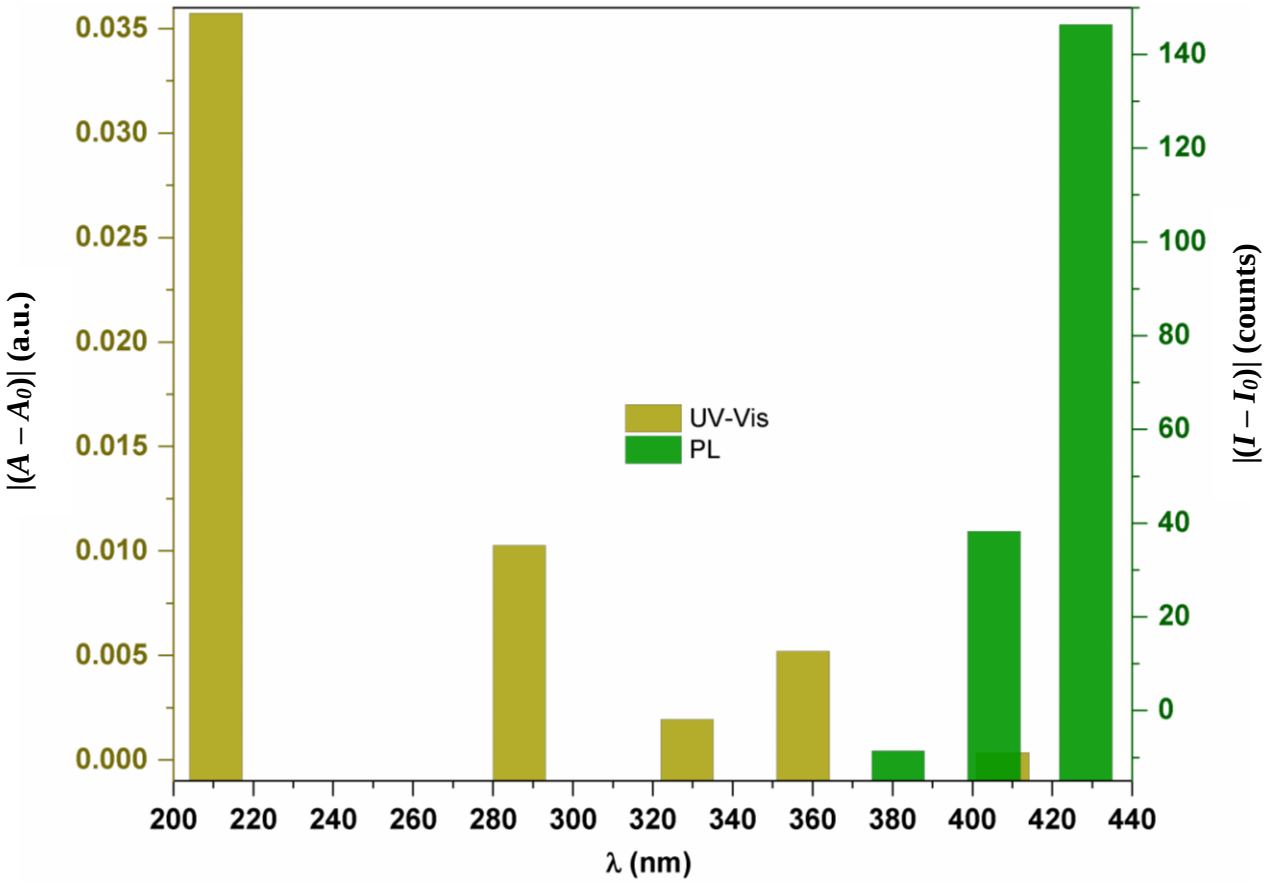

Figure S24: The relative changes in the UV-vis absorbance ($|A - A_0|$; dark yellow bars) and the PL photon counts ($|I - I_0|$; green bars) for the 2mL of 12.5 μM methanolic solution of **1·Dy** in the presence of 5 equivalents (with respect to Dy ion) of NH_4F at room temperature.

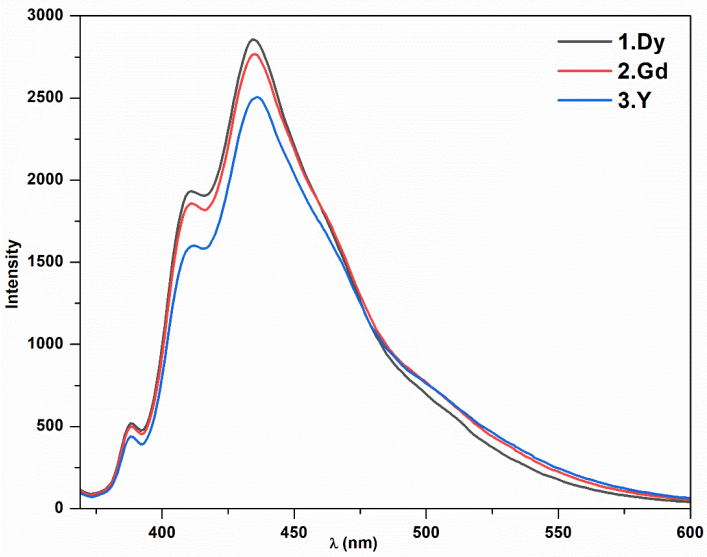

Figure S25: The comparative photoluminescence spectra of the methanolic solutions of **1·Y** (red), **1·Dy** (black) and **1·Gd** (blue), recorded in MeOH at room temperature upon excitation at 397 nm. The characteristic data and measurement details are provided in experimental section.

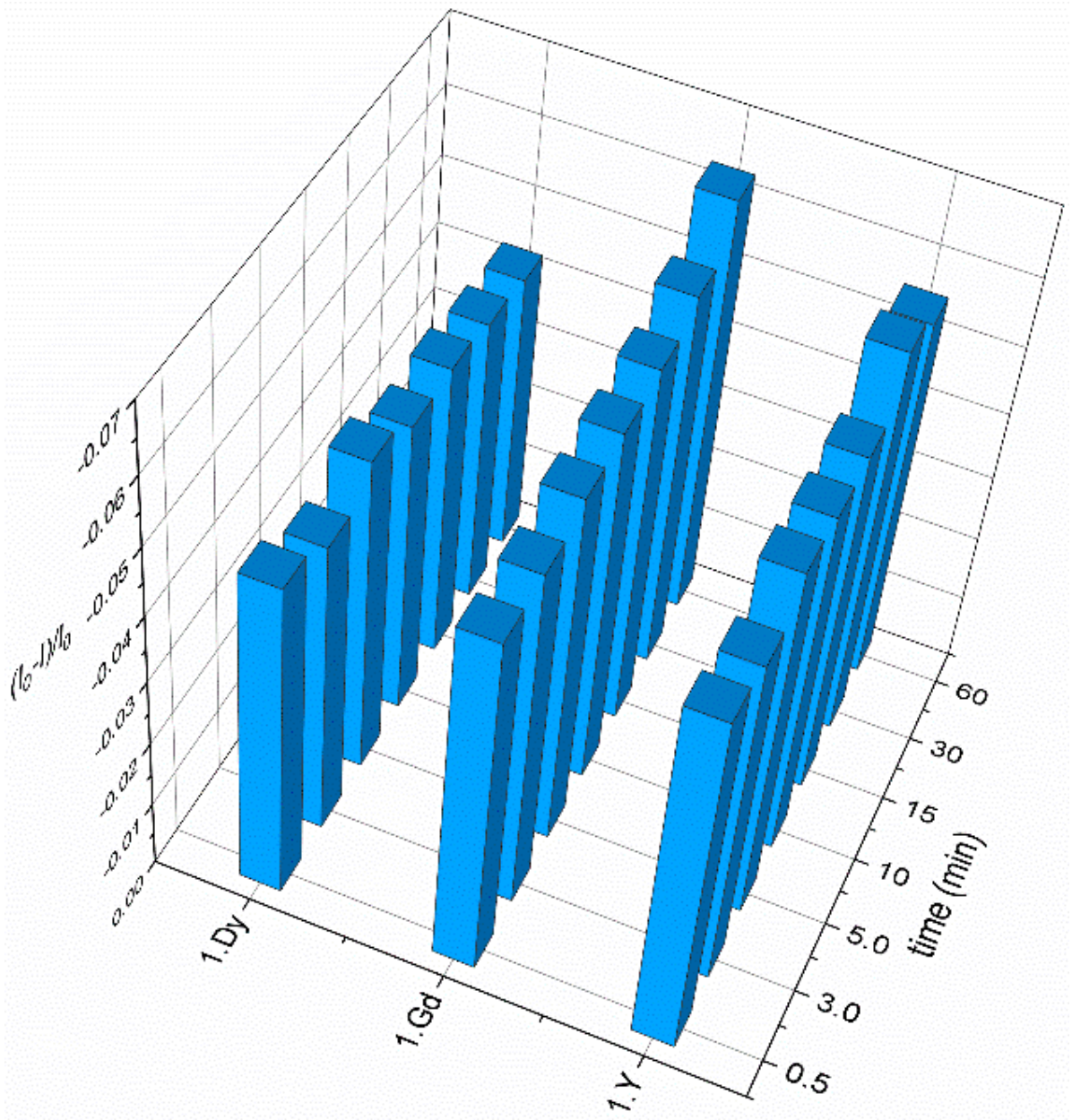

Figure S26: The time-dependent changes of the relative photon counts, $(I_0 - I)/I_0$, at $\lambda_{max}^{em.}$ = 435 nm in the PL spectra for the 12.5 μM solutions of **1·Ln** (Ln = Y, Gd and Dy) in the presence of 5 equivalents of F^- per Ln ion of the 1D coordination polymers, **1·Ln**. The time (*t*) was varied between 30 seconds – 2h at room temperature. I_0 corresponds to the photon counts in the absence of F^- ion, while *I* correspond to the photon counts at time *t* after addition of 5 equivalents (with respect to the Ln centre) of F- ion in aqueous methanolic (1:1, v/v) into the respective solution of **1·Ln**.

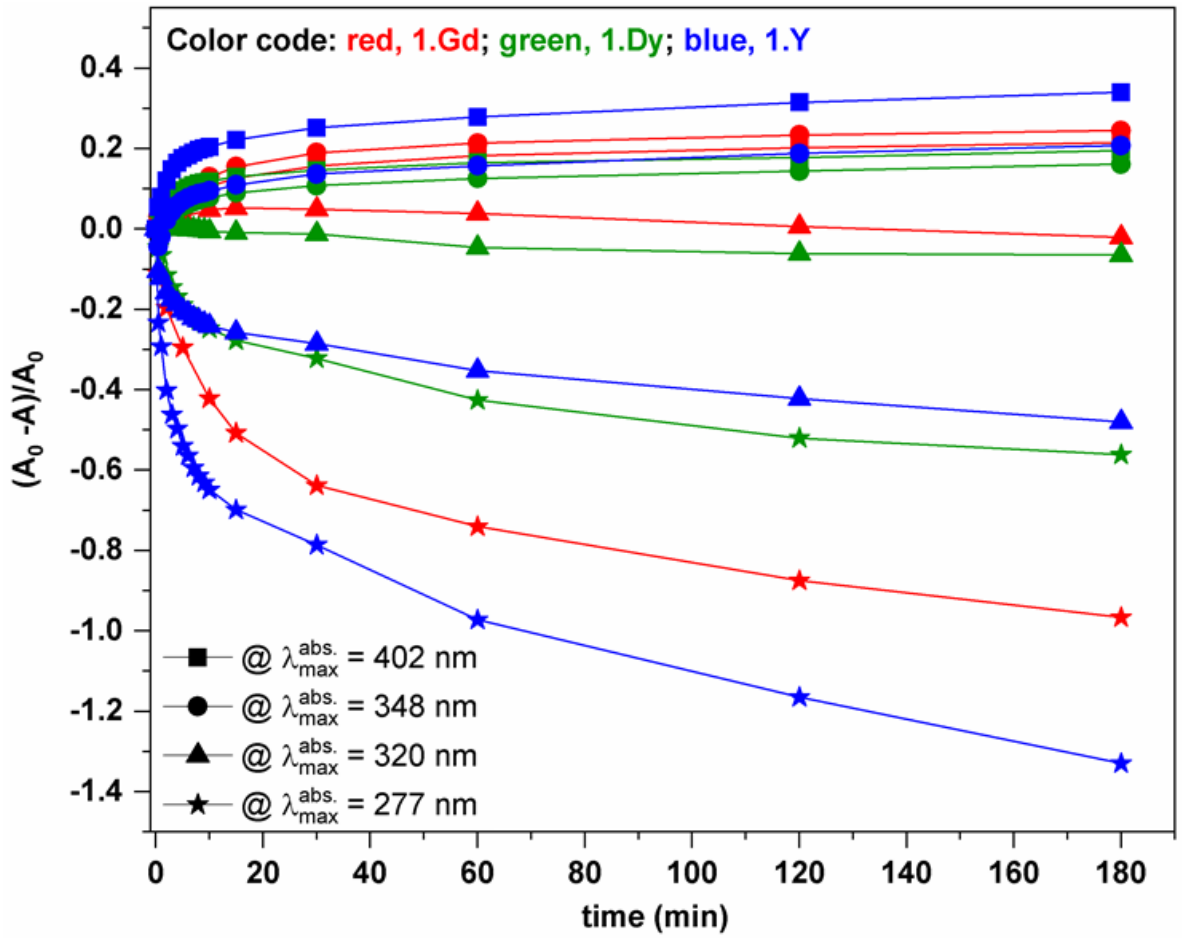

Figure S27: The time-dependent UV-Vis absorption changes (relative; $(A_0 - A)/A_0$) for 12.5 μM (with respect to Ln centre) methanolic solutions of **1·Dy** (green), **1·Gd** (red) and **1·Y** (blue) at $\lambda_{max}^{abs.}$ = 277 nm (solid stars), 320 nm (solid up-triangles), 348 nm (solid circles), and 402 nm (solid squares) upon treatment with 25 equivalents of NH_4F in aqueous methanolic (1:1 v/v) solution at room temperature. The solid lines are eye-guides only. A_0 corresponds to the absorbance in the absence of F^- ion, while A corresponds to the absorbance at time t.

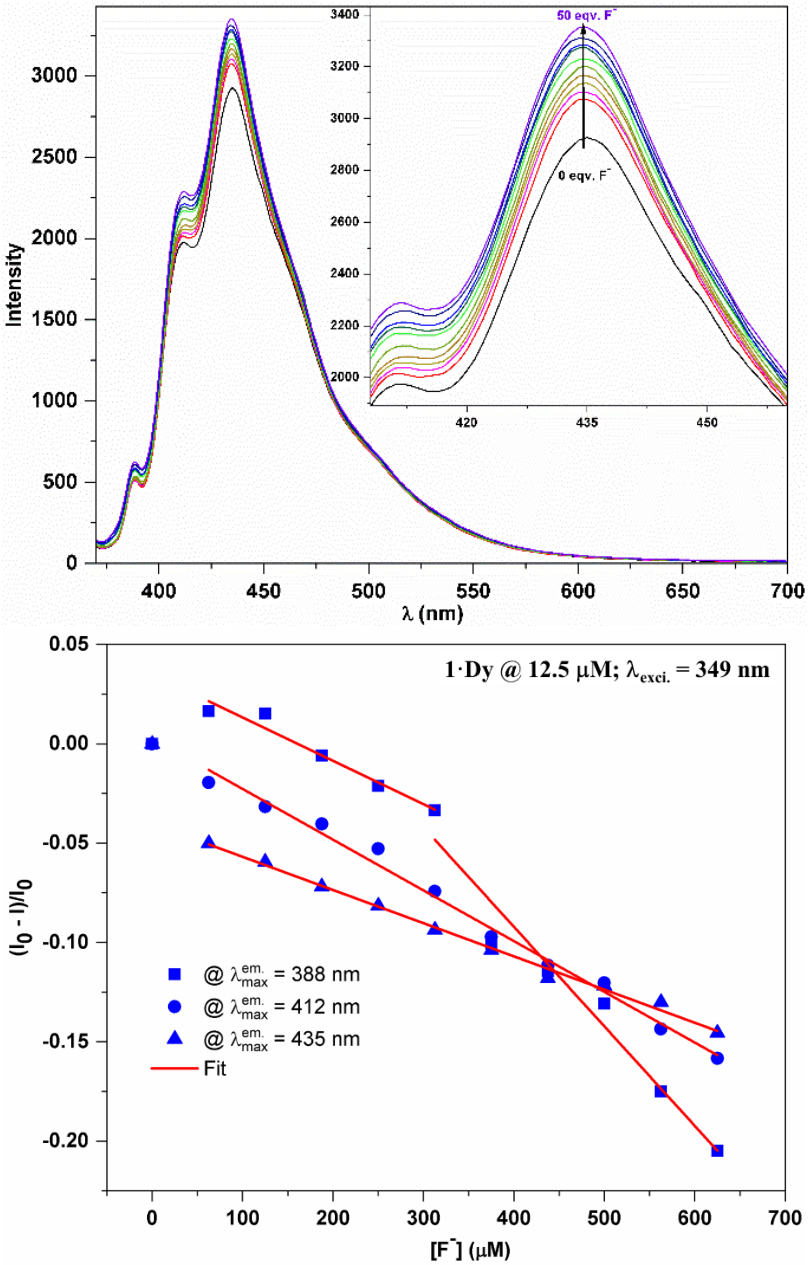

Figure S28: The room temperature steady-state PL spectral change (*top*) and the corresponding calibration plots (*bottom*) with 12.5 μM (with respect to Ln centre) methanolic solutions of **1·Dy** at the excitation wavelength of 349 nm upon titration with aqueous methanolic (1:1 v/v) solution of NH_4F in the range of 0 – 650 μM. The inset is the expanded region in the ranges as mentioned in the ordinate and abscissa. The relative change in photon counts, $(I_0 - I)/I_0$, at emission maxima $\lambda_{max}^{em.}$ = 388 nm (solid squares), 412 nm (solid circles), and 435 nm (solid triangles) along with the best fits (the solid red lines) are plotted against the concentration of F^-, where I_0 and I stand for the photon counts of the 12.5 μM solutions of the 1D coordination polymers **1·Ln** (Ln = Y, Gd and Dy) in the absence of NH_4F and in the presence of NH_4F, respectively. The limit of detections (LoD's) for different 1D coordination polymers at different emission maxima are tabulated below (Table S4).

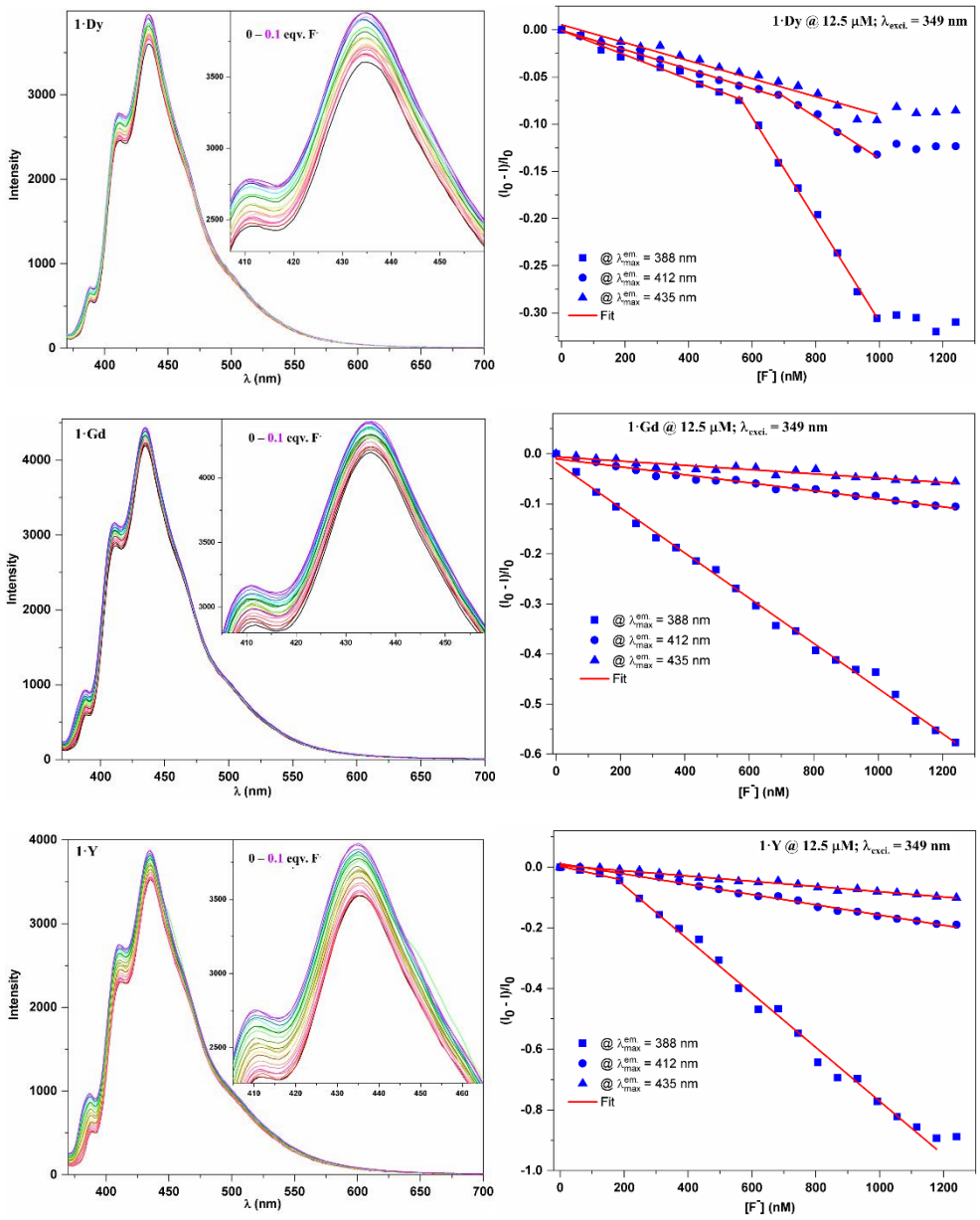

Figure S29: The room temperature steady-state PL spectral change (left) and the corresponding calibration plots (right) with solutions of **1·Dy** (top), **1·Gd** (middle) and **1·Y** (bottom) at the excitation wavelength of 349 nm upon titration with NH_4F. The micromolar (μM; with respect to Ln centre in the 1D coordination polymers) stock solutions in methanol are titrated with millimolar (mM) aqueous methanolic (1:1 v/v) solution of NH_4F such that the 1D coordination polymers are at 12.5 μM strengths and the concentrations of F^- are varied between 0 – 1250 nM in the study solutions. The inset is the expanded region in the ranges as mentioned in the ordinate and abscissa. The relative change in photon counts, $(I_0 – I)/I_0$, at emission maxima $\lambda_{max}^{em.}$ = 388 nm (solid squares), 412 nm (solid circles), and 435 nm (solid triangles) along with the best fits (the solid red lines) are plotted against the concentration of F^-, where I_0 and I stand for the photon counts of the 12.5 μM solutions of the 1D coordination polymers **1·Ln** (Ln = Y, Gd and Dy) in the absence of NH_4F and in the presence of NH_4F, respectively. The limit of detections (LoD's) for different 1D coordination polymers at different emission maxima are tabulated below (Table S5).

Table S4. The limit of detections (LoD's) of F^- by **1·Dy** at different emission maximum and different F- concentration domains micromolar (μM) range. The calculations are based on the conventional $3\sigma/m$ method where σ stands for the standard deviation of the blank and m stands for the slope of the calibration plots with respect to the relative change in photon counts. The experimental conditions are as described in the figure above (Figure S28).

LoD (μM) $[F^-]$	$\lambda_{max}^{em.}$ = 435 nm	$\lambda_{max}^{em.}$ = 412 nm	$\lambda_{max}^{em.}$ = 388 nm
60 – 300 μM			3.067823
300 – 625 μM			1.336479
60 – 625 μM (average)	31.5982	37.29363	2.202151

Table S5. The limit of detection (LoD) of F^- by **1·Ln** (Ln = Y, Gd and Dy) at different emission maximum for the F- concentrations in the nanomolar (nM) range. The calculations are based on the conventional $3\sigma/m$ method where σ stands for the standard deviation of the blank and m stands for the slope of the calibration plots with respect to the relative change in photon counts. The experimental conditions are as described in the figure above (Figure S29).

LoD (μM)	$\lambda_{max}^{em.}$ = 435 nm	$\lambda_{max}^{em.}$ = 412 nm	$\lambda_{max}^{em.}$ = 388 nm
1·Y	722.834	473.436	7.54
1·Gd		1001.386	14.842
1·Dy	1466.15	313.399	16.083

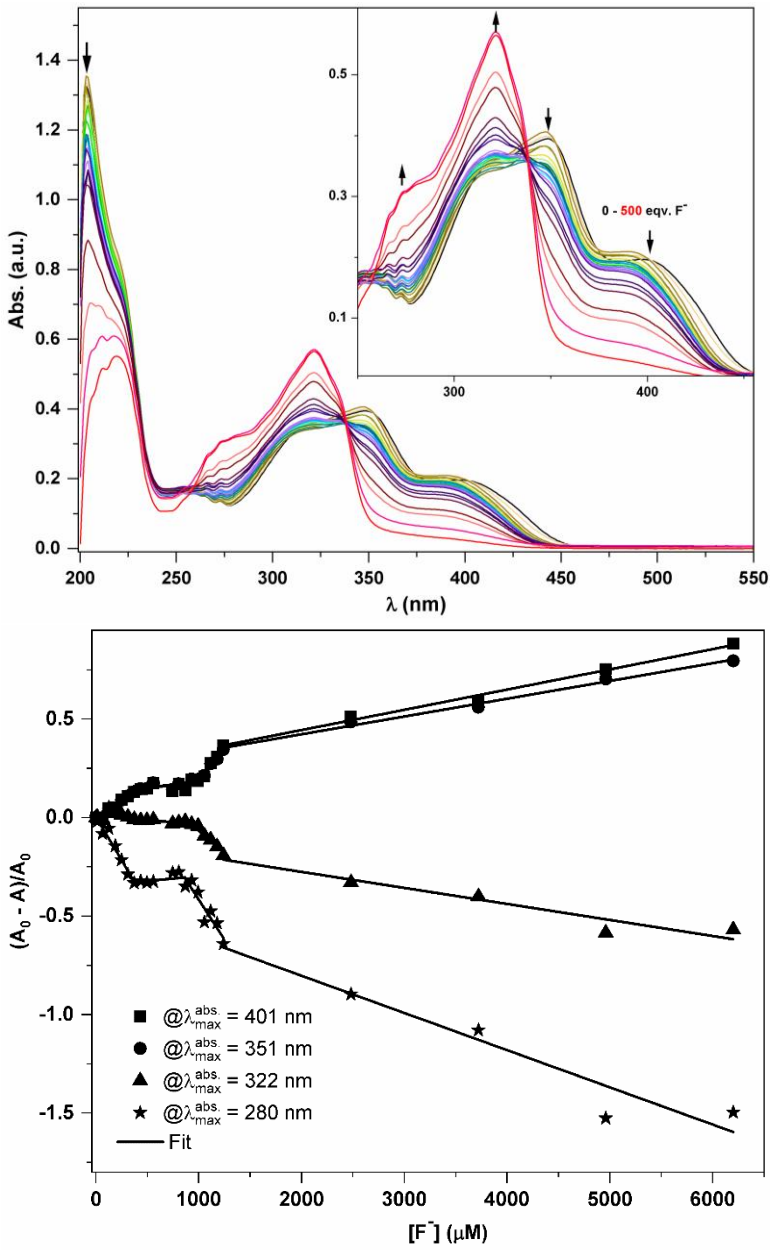

Figure S30: ***Top:*** The UV-Vis absorption spectral changes for 12.5 μM (with respect to Ln centre) methanolic solutions of **1·Dy** at room temperature upon titration with aqueous methanolic (1:1, v/v) solution of NH_4F ranging between 0–500 equivalents (with respect to the Dy centre). The inset is the expanded region in the ranges as mentioned in the ordinate and abscissa. ***Bottom:*** The relative change in absorptions, $(A_0 - A)/A_0$, at the absorption maxima $\lambda_{max}^{abs.}$ = 280 nm (solid stars), 322 nm (solid up-triangles), 351 nm (solid circles), and 401 nm (solid squares) are plotted against the concentration of F^- upon titration with 2 mL of 12.5 μM solutions of the 1D coordination polymer **1·Dy**, where A_0 and A stand for the absorbances of the 12.5 μM solution in the absence of NH_4F and in the presence of NH_4F, respectively. The solid lines represent the best fits. The sensitivity for F^- is observed to be different at different absorption maximum as well as in different F- concentration domains, which are tabulated below (Table S6).

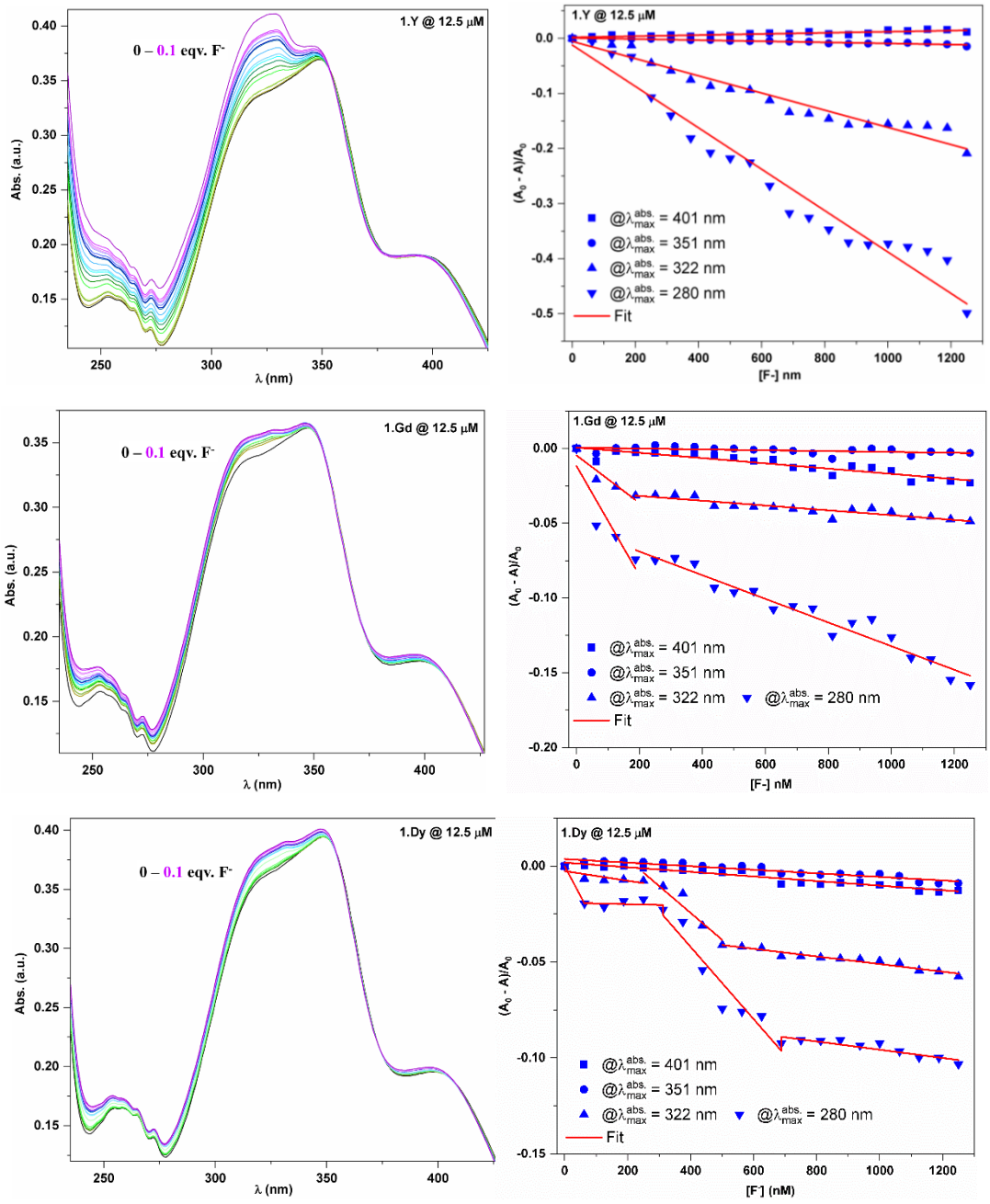

Figure S31: The room temperature UV-vis spectral change (left) and the corresponding calibration plots (right) with 12.5 μM (with respect to Ln centre) methanolic solutions of **1·Dy** (top), **1·Gd** (middle) and **1·Y** (bottom) at 10 minutes time interval upon titration with aqueous methanolic (1:1 v/v) solution of NH_4F in the concentration range 0 – 1250 nM. The relative change in absorbances, $(A_0 – I)/A_0$, at the absorption maxima $\lambda_{max}^{abs.}$ (nm) = 401 (squares), 351 (circles), 322 (up-triangles), and 280 (down-triangles) along with the best fits (the solid red lines) are plotted against the concentration of F^-, where A_0 and A stand for the absorbances of the 12.5 μM solutions of the 1D coordination polymers **1·Ln** (Ln = Y, Gd and Dy) in the absence of NH_4F and in the presence of NH_4F, respectively. The limit of detections (LoD's) for different 1D coordination polymers at different emission maxima are tabulated below (Table S7).

Table S6. The limit of detections (LoD's) of F^- by **1·Dy** at different absorption maximum and different F- concentration domains in the micromolar (μM) to milimolar (mM) range. The calculations are based on the conventional $3\sigma/m$ method where σ stands for the standard deviation of the blank and m stands for the slope of the calibration plots with respect to the relative change in photon counts. The experimental conditions are as described in the figure above (Figure S30).

LoD (μM) [F^-]	$\lambda_{max}^{abs.}$ = 401 nm	$\lambda_{max}^{abs.}$ = 351 nm	$\lambda_{max}^{abs.}$ = 322 nm	$\lambda_{max}^{abs.}$ = 280 nm
12.5 – 250 μM	0.277526	0.543479	6.436616	0.468074
250 – 500 μM	2.259547	3.356639	6.882433	8.284917
500 – 750 μM	0.123881	0.273753	0.459024	0.511415
750 – 3 000 μM	0.899086	2.048592	2.652234	2.197591
12.5 – 3000 μM (av.)	0.89001	1.555616	4.107577	2.865499

Table S7. The limit of detections (LoD's) of F^- by **1·Ln** (Ln = Y, Gd and Dy) at different absorption maximum and different F- concentration domains in the nanomolar (nM) range. The calculations are based on the conventional $3\sigma/m$ method where σ stands for the standard deviation of the blank and m stands for the slope of the calibration plots with respect to the relative change in photon counts. The experimental conditions are as described in the figure above (Figure S31).

LoD (μM) [F^-]	$\lambda_{max}^{abs.}$ = 401 nm	$\lambda_{max}^{abs.}$ = 351 nm	$\lambda_{max}^{abs.}$ = 322 nm	$\lambda_{max}^{abs.}$ = 280 nm
for **1·Y**				
0 – 1250 nM	18.26228876	37.01282186	2.76286781	0.220441439
for **1·Gd**				
0 – 190 nM	10.5	1276.3	6.14641	2.26094
190 – 1250 nM	10.5	1276.3	26.8371	10.4749
0 – 1250 nM (av.)	10.5	1276.3	16.4918	6.36793
for **1·Dy**				
0 – 60 nM	15.4	40	11.95362	2.89985
60 – 250 nM	15.4	40	11.95362	230.11664
250 – 690 nM	15.4	40	2.14038	4.78309
690 – 1250 nM	15.4	40	15.10323	41.7837
0 – 1250 nM (av.)	15.4	40	9.73241	69.89582

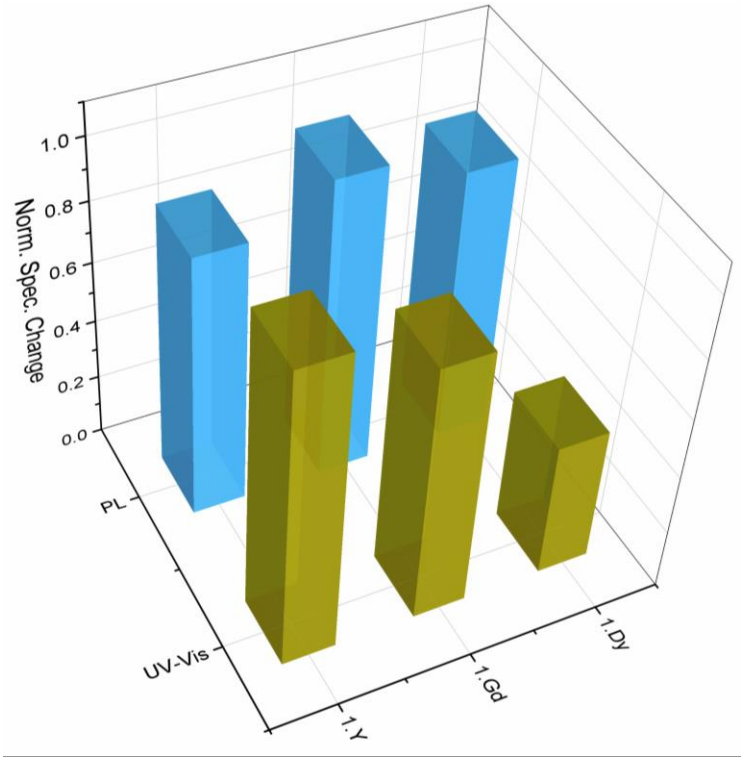

Figure S32: The changes in photon counts relative to **1·Gd**, $(I - I_0)_{\mathbf{1\cdot Gd}}/(I - I_0)_{\mathbf{1\cdot Ln}}$, of the PL spectra at $\lambda_{max}^{em.}$ = 435 nm (cyan), and the changes in absorbances relative to **1·Y**, $(A - A_0)_{\mathbf{1\cdot Y}}/(A - A_0)_{\mathbf{1\cdot Ln}}$, of the UV-Vis spectra at $\lambda_{max}^{abs.}$ = 280 nm (yellow) of the 2 mL of 12.5 μM methanolic solutions of **1·Ln** upon treatment (30 seconds of delay time for PL and 30 minutes of delay time for UV-Vis) with aqueous-methanolic (1:1, v/v) solution of NH_4F (5 eq. for PL and 25 eqv. for UV-Vis) at room temperature.

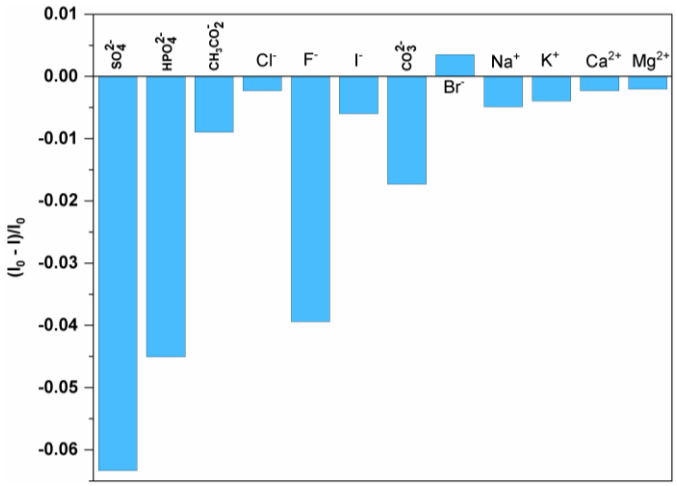

Figure S33: The relative changes in steady-state photon counts, $(I_0 - I)/I_0$, at room temperature and emission maximum $\lambda_{max}^{em.}$ = 435 nm for 12.5 μM (with respect to Ln center) methanolic solution of **1·Dy** at the excitation wavelength of 349 nm upon treatment with 50 equivalents (with respect to the Dy centre in the 1D coordination polymer **1·Dy**) of various anions with the common NH_4^+ cation in aqueous methanolic (1:1 v/v) solutions and various cations with the common NO_3^- anion in aqueous methanolic (1:1 v/v) solutions.

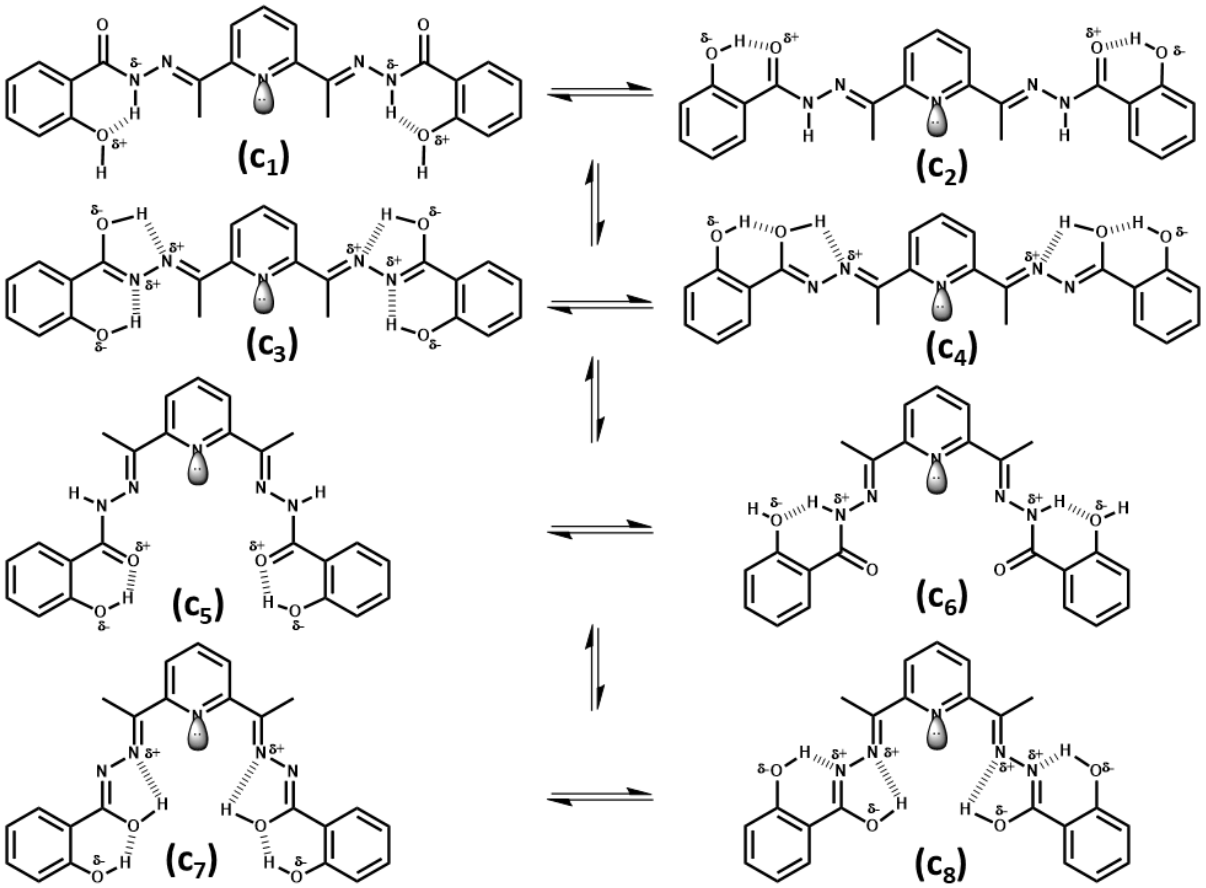

Scheme S1: Schematic chart for the different obvious isomers (conformers and tautomers) of the pristine ligand, **H_4L.**

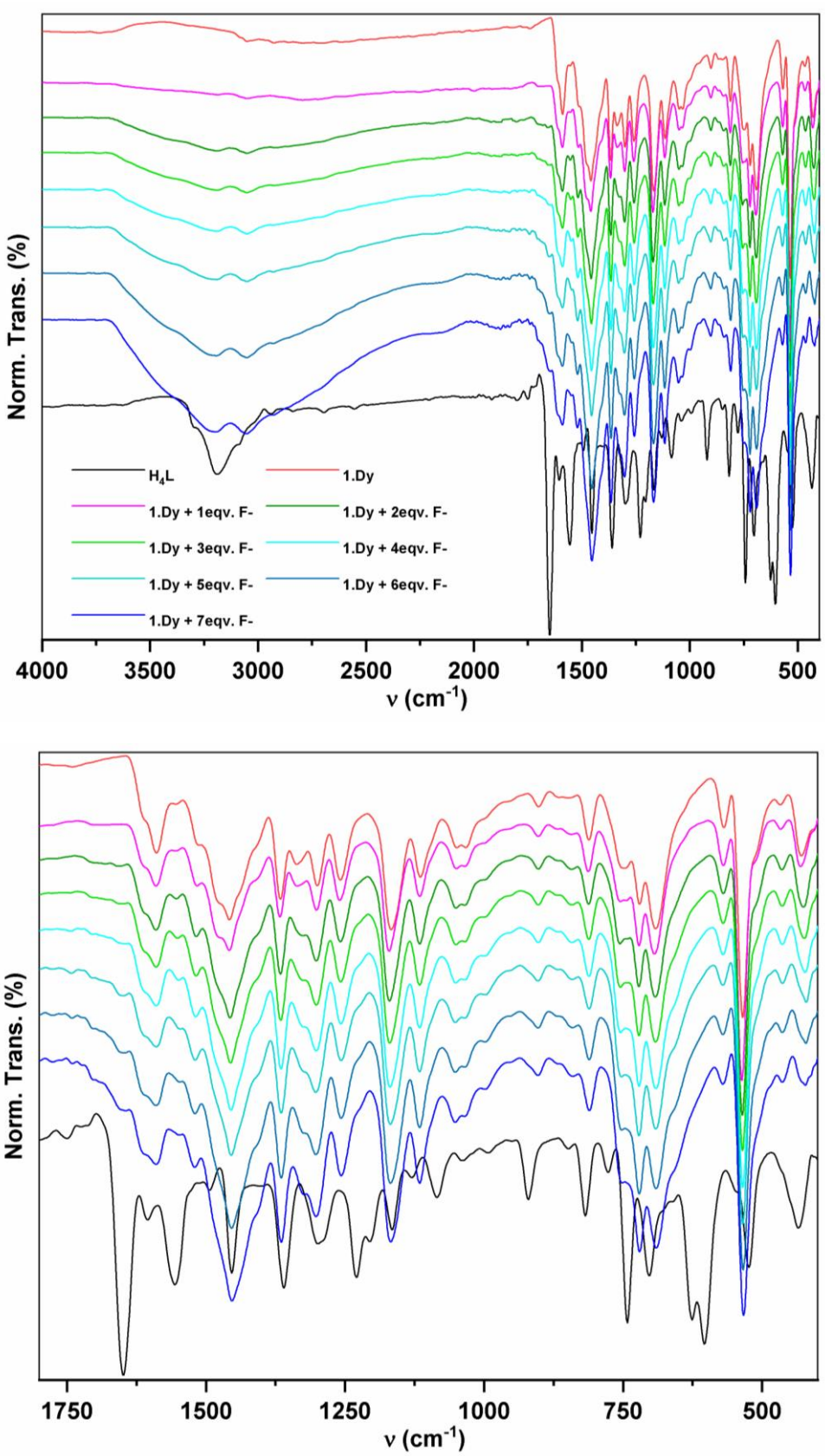

Figure S34: Solid-state FT-IR spectra (full range on the top and expanded at the bottom) of the complex **1.Dy** upon treatment with 0-7 eq. of solid NH_4F at room temperature under aerobic conditions.

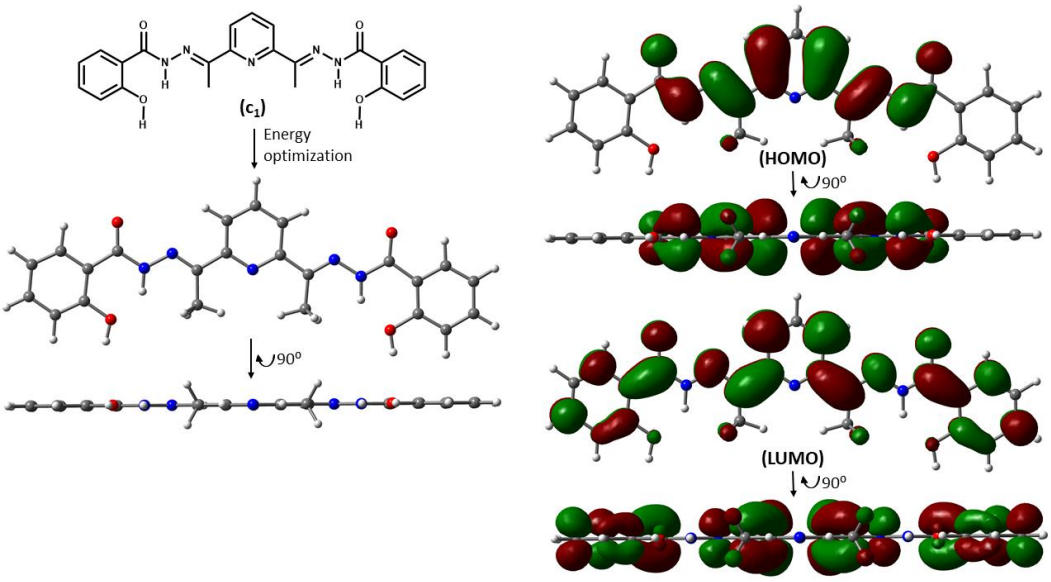

Chart S1: Schematic structure of $\mathbf{c_1}$ (*top-left*) as used for the initial guess in its gas-phase energy optimization; the gas-phase energy optimized geometry of $\mathbf{c_1}$ viewed along the axis perpendicular (*middle-left*) and parallel (*bottom-left*) to the plane of its pyridyl moiety; the isosurfaces (*isovalue* = 0.02; the green and brown coloured surfaces representing the mutually opposite phases of the corresponding wave function) corresponding to the HOMO (*top-right*) and LUMO (*bottom-right*) in the gas-phase energy optimized geometry of $\mathbf{c_1}$.

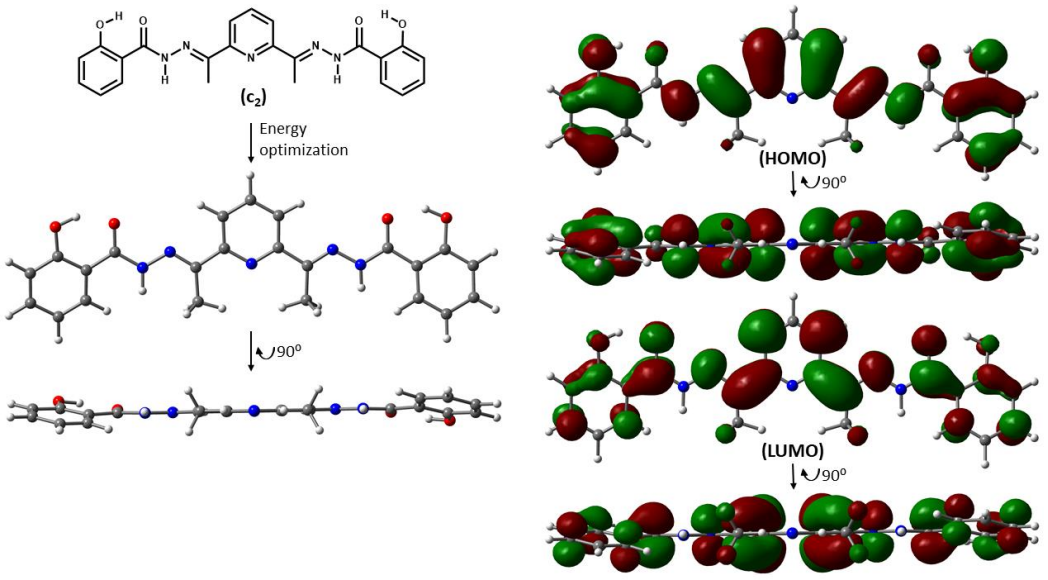

Chart S2: Schematic structure of $\mathbf{c_2}$ (*top-left*) as used for the initial guess in its gas-phase energy optimization; the gas-phase energy optimized geometry of $\mathbf{c_2}$ viewed along the axis perpendicular (*middle-left*) and parallel (*bottom-left*) to the plane of its pyridyl moiety; the isosurfaces (*isovalue* = 0.02; the green and brown colored surfaces representing the mutually opposite phases of the corresponding wave function) corresponding to the HOMO (top-right) and LUMO (*bottom-right*) in the gas-phase energy optimized geometry of $\mathbf{c_2}$.

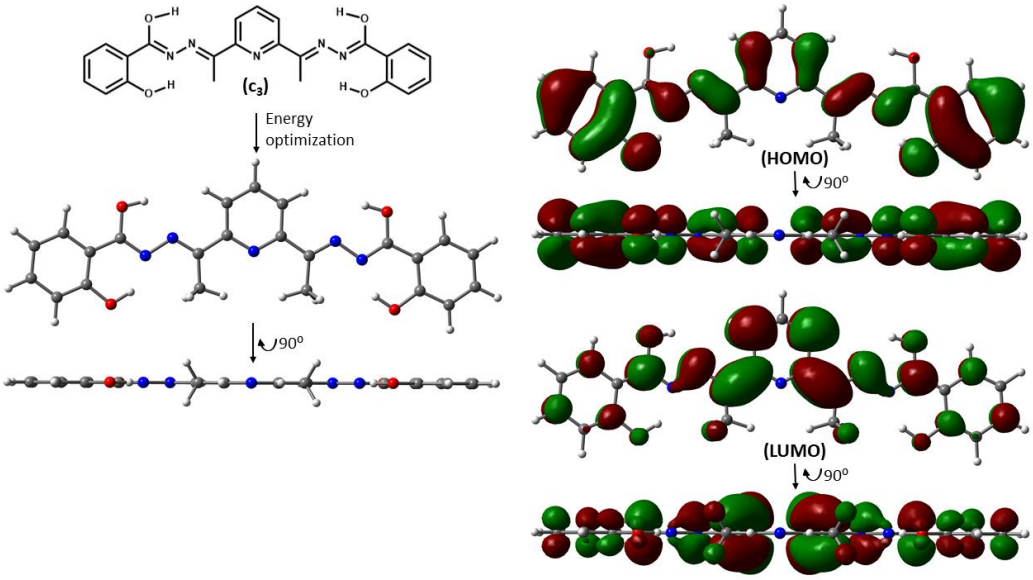

Chart S3: Schematic structure of **c3** (*top-left*) as used for the initial guess in its gas-phase energy optimization; the gas-phase energy optimized geometry of **c3** viewed along the axis perpendicular (*middle-left*) and parallel (*bottom-left*) to the plane of its pyridyl moiety; the isosurfaces (*isovalue* = 0.02; the green and brown colored surfaces representing the mutually opposite phases of the corresponding wave function) corresponding to the HOMO (top-right) and LUMO (*bottom-right*) in the gas-phase energy optimized geometry of **c3**.

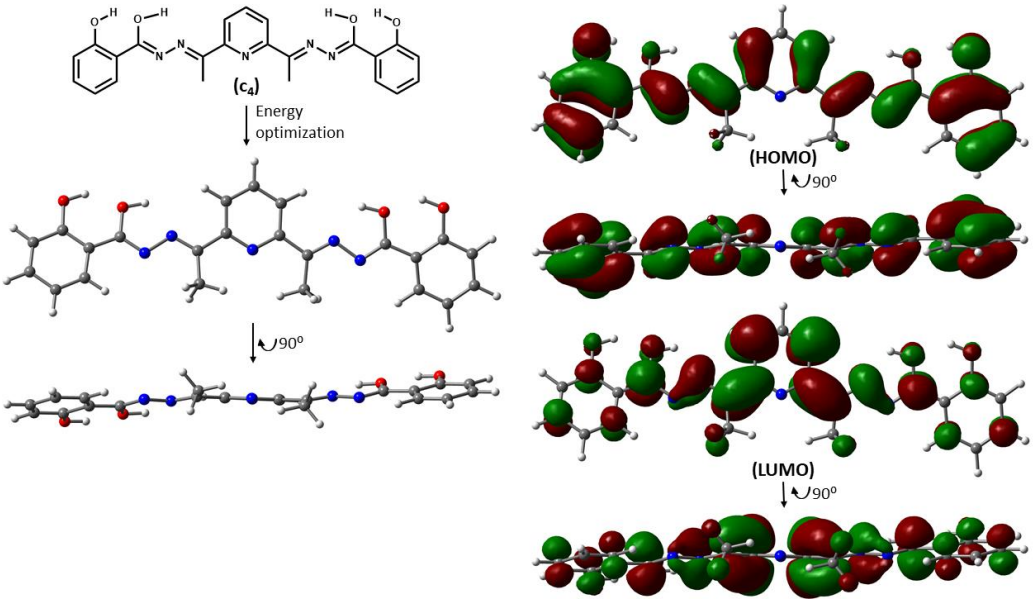

Chart S4: Schematic structure of **c4** (*top-left*) as used for the initial guess in its gas-phase energy optimization; the gas-phase energy optimized geometry of **c4** viewed along the axis perpendicular (*middle-left*) and parallel (*bottom-left*) to the plane of its pyridyl moiety; the isosurfaces (*isovalue* = 0.02; the green and brown colored surfaces representing the mutually opposite phases of the corresponding wave function) corresponding to the HOMO (top-right) and LUMO (*bottom-right*) in the gas-phase energy optimized geometry of **c4**.

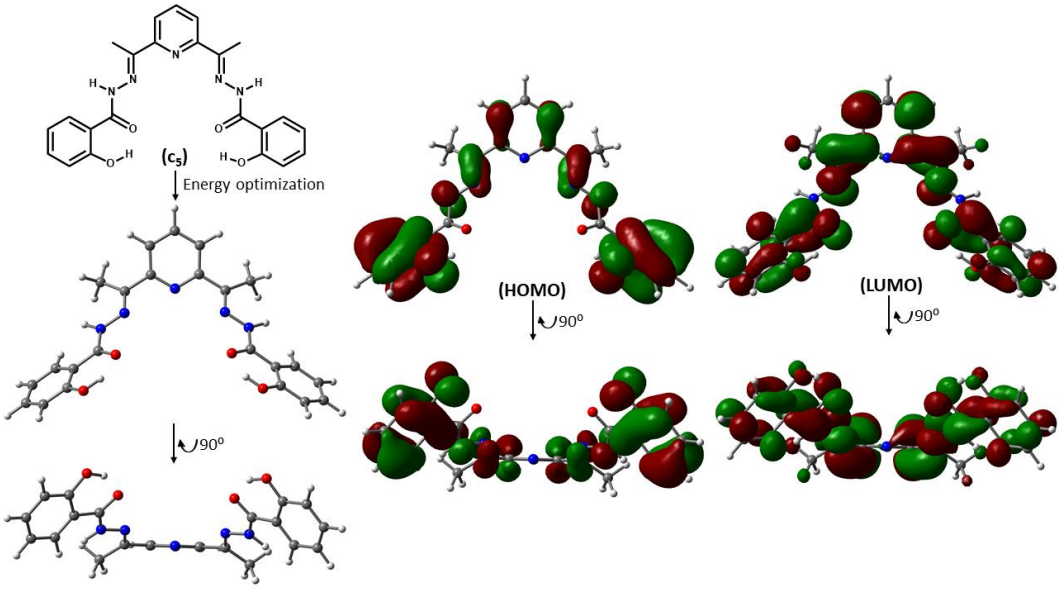

Chart S5: Schematic structure of $\mathbf{c_5}$ (*top-left*) as used for the initial guess in its gas-phase energy optimization; the gas-phase energy optimized geometry of $\mathbf{c_5}$ viewed along the axis perpendicular (*middle-left*) and parallel (*bottom-left*) to the plane of its pyridyl moiety; the isosurfaces (*isovalue* = 0.02; the green and brown coloured surfaces representing the mutually opposite phases of the corresponding wave function) corresponding to the HOMO (top-right) and LUMO (*bottom-right*) in the gas-phase energy optimized geometry of $\mathbf{c_5}$.

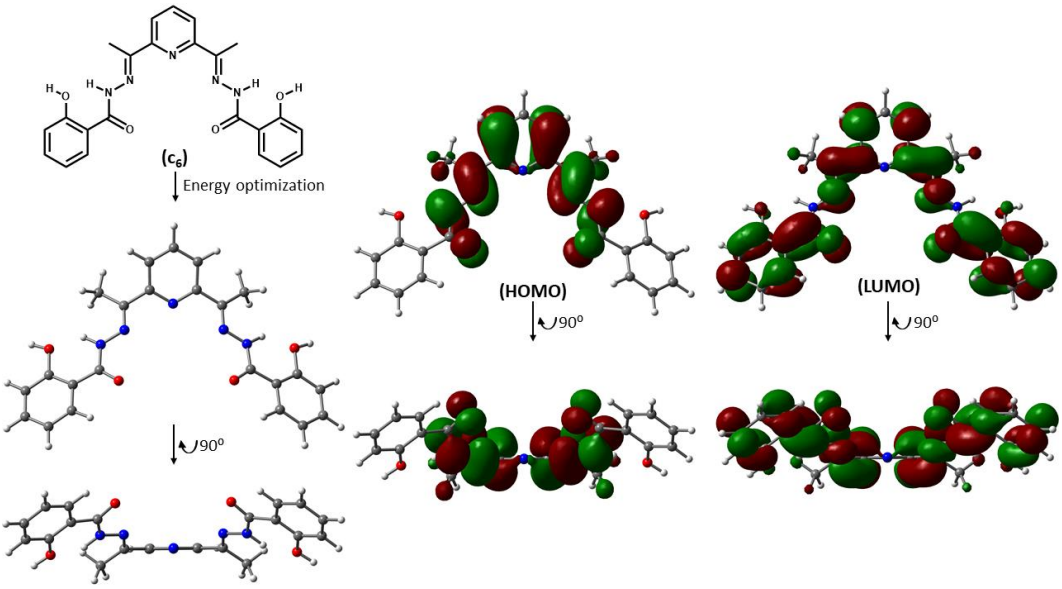

Chart S6: Schematic structure of $\mathbf{c_6}$ (*top-left*) as used for the initial guess in its gas-phase energy optimization; the gas-phase energy optimized geometry of $\mathbf{c_6}$ viewed along the axis perpendicular (*middle-left*) and parallel (*bottom-left*) to the plane of its pyridyl moiety; the isosurfaces (*isovalue* = 0.02; the green and brown colored surfaces representing the mutually opposite phases of the corresponding wave function) corresponding to the HOMO (top-right) and LUMO (*bottom-right*) in the gas-phase energy optimized geometry of $\mathbf{c_6}$.

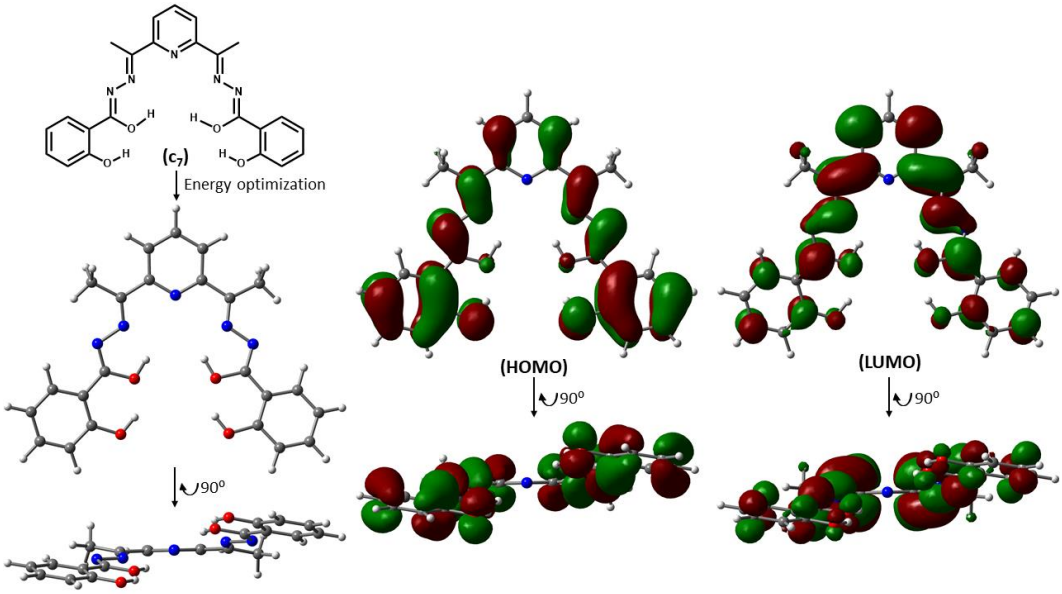

Chart S7: Schematic structure of $\mathbf{c_7}$ (*top-left*) as used for the initial guess in its gas-phase energy optimization; the gas-phase energy optimized geometry of $\mathbf{c_7}$ viewed along the axis perpendicular (*middle-left*) and parallel (*bottom-left*) to the plane of its pyridyl moiety; the isosurfaces (*isovalue* = 0.02; the green and brown colored surfaces representing the mutually opposite phases of the corresponding wave function) corresponding to the HOMO (top-right) and LUMO (*bottom-right*) in the gas-phase energy optimized geometry of $\mathbf{c_7}$.

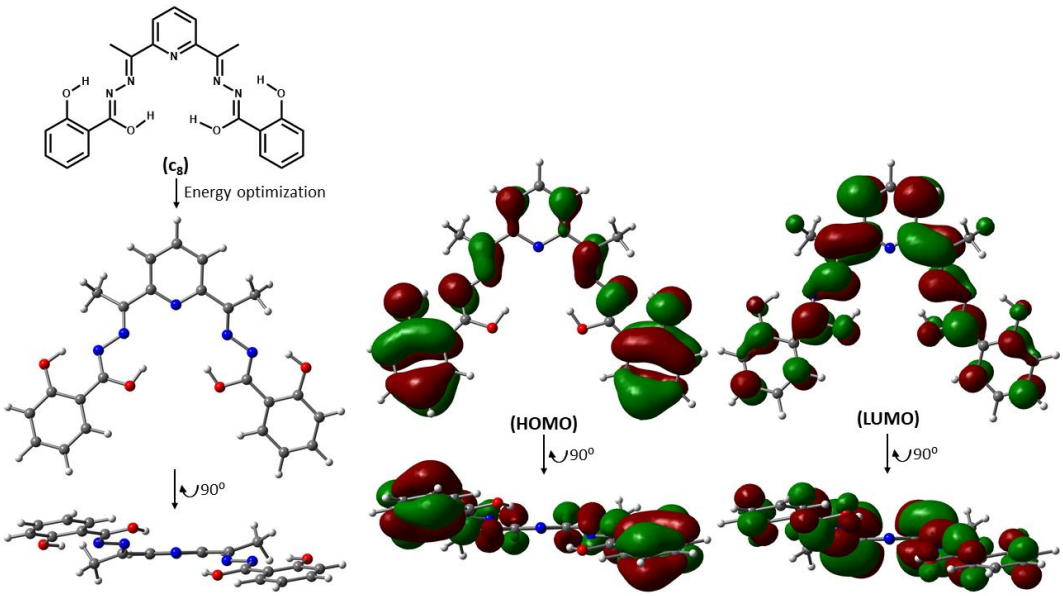

Chart S8: Schematic structure of $\mathbf{c_8}$ (*top-left*) as used for the initial guess in its gas-phase energy optimization; the gas-phase energy optimized geometry of $\mathbf{c_8}$ viewed along the axis perpendicular (*middle-left*) and parallel (*bottom-left*) to the plane of its pyridyl moiety; the isosurfaces (*isovalue* = 0.02; the green and brown colored surfaces representing the mutually opposite phases of the corresponding wave function) corresponding to the HOMO (top-right) and LUMO (*bottom-right*) in the gas-phase energy optimized geometry of $\mathbf{c_8}$.

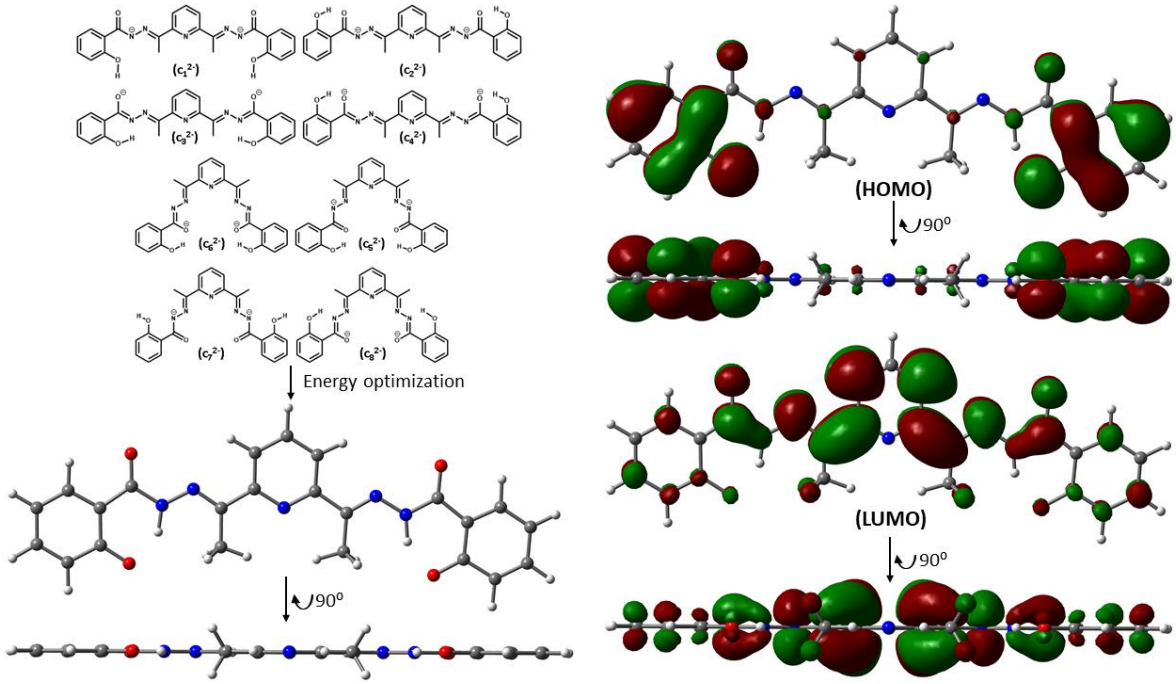

Chart S9: Schematic structures corresponding to the doubly deprotonated forms ($\mathbf{H_2L^{2-}}$) of the ligand (*top-left*) which were used for the initial guesses for the gas-phase energy optimization; the gas-phase energy optimized geometry of $\mathbf{H_2L^{2-}}$ viewed along the axis perpendicular (*middle-left*) and parallel (*bottom-left*) to the plane of its pyridyl moiety; the isosurfaces (*isovalue* = 0.02; the green and brown colored surfaces representing the mutually opposite phases of the corresponding wave function) corresponding to the HOMO (top-right) and LUMO (*bottom-right*) in the gas-phase energy optimized geometry of $\mathbf{H_2L^{2-}}$.

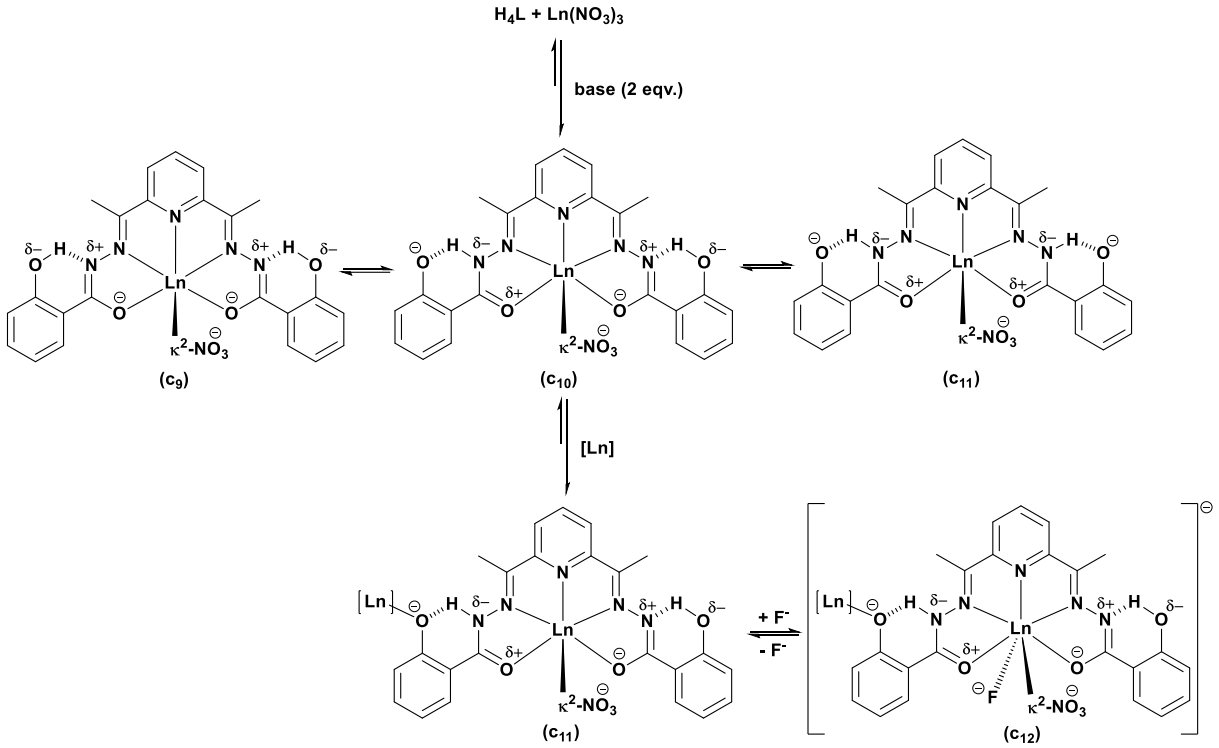

Scheme S2. Schematic representation for the keto-iminolate tautomerization and intramolecular proton transfer in the building-block mimics (omitting TPPO) of the mononuclear complexes (c_9-c_{11}); 1D coordination polymers (c_{12}), and the fluorinated form of the 1D coordination polymers (c_{13})

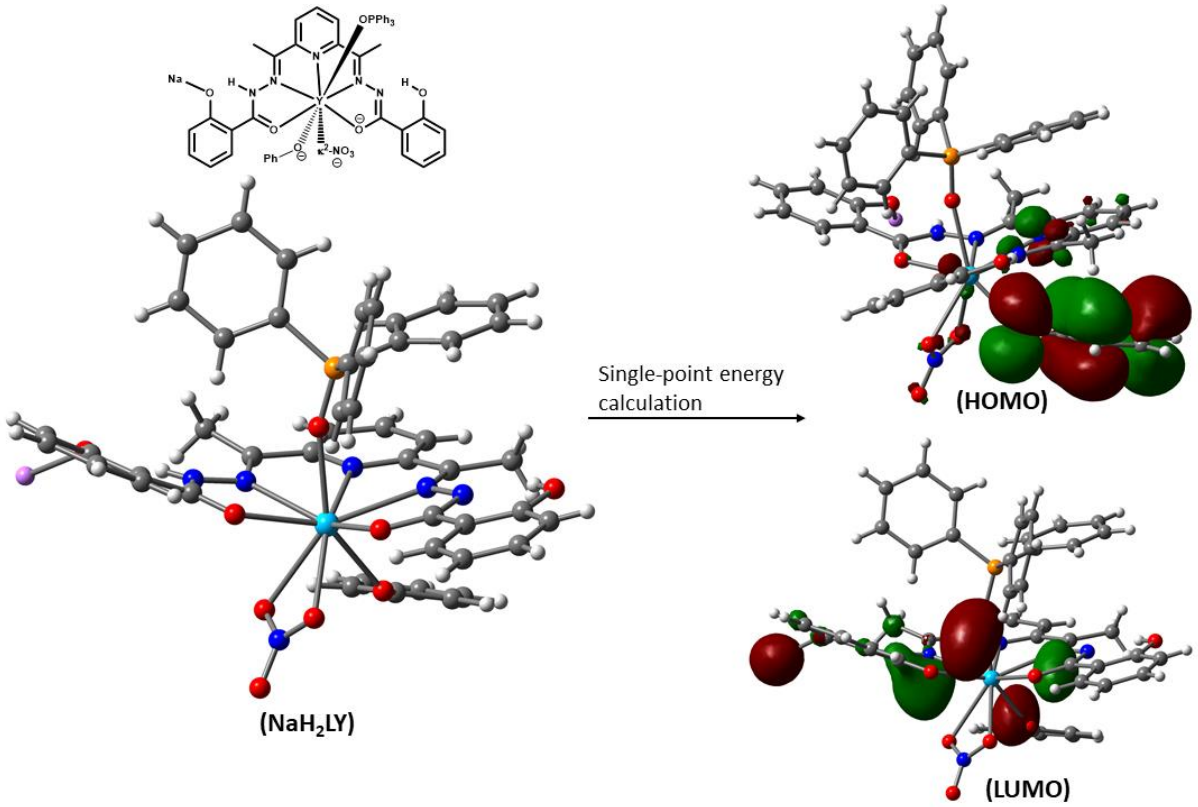

Chart S10: Schematic structure of the hypothetical monomeric model complex **NaH$_2$LY** (*top-left*) representing the building units of the 1D coordination polymer **1·Y**; the corresponding solid-state structure of **NaH$_2$LY** (*bottom-left*) as truncated from the single-crystal X-ray structure of the 1D coordination polymer **1·Y** upon replacing the neighbouring Y(III) ion with Na^+ ion and upon replacing the bridging phenolic group of the neighbouring building unit with the phenolate ion; the isosurfaces (*isovalue* = 0.02; the green and brown colored surfaces representing the mutually opposite phases of the corresponding wave function) corresponding to the HOMO (*top-right*) and LUMO (*bottom-right*) in the solid-state geometry of **NaH$_2$LY** as truncated from **1·Y**.

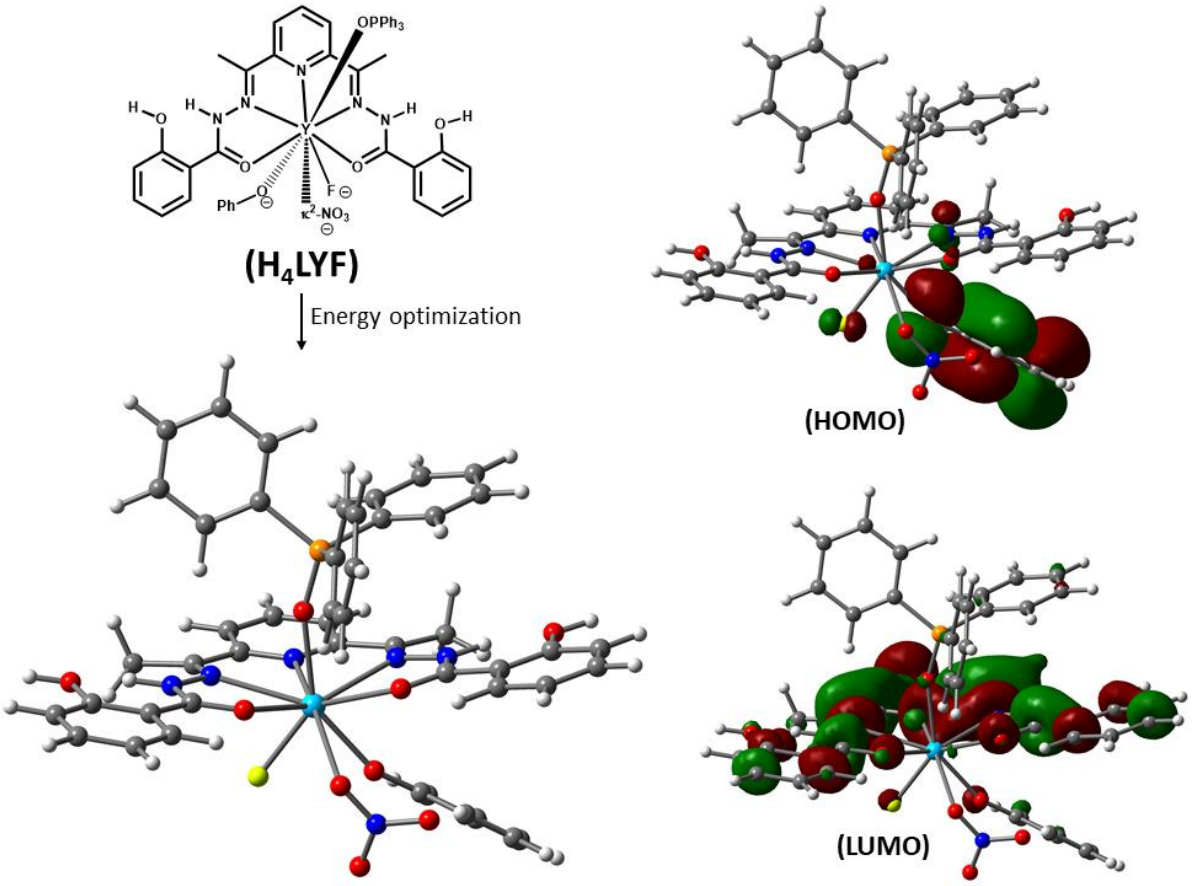

Chart S11: Schematic structures of the hypothetical monomeric model complex **H$_4$LYF** (*top-left*), representing the building units of the fluorinated congener of the 1D coordination polymer **1·Y**, which were used for the initial guesses for the gas-phase energy optimization; the gas-phase energy optimized geometry of **H$_4$LYF** (*bottom-left*); the isosurfaces (*isovalue* = 0.02; the green and brown coloured surfaces representing the mutually opposite phases of the corresponding wave function) corresponding to the HOMO (*top-right*) and LUMO (*bottom-right*) in the optimized geometry of **H$_4$LYF**.

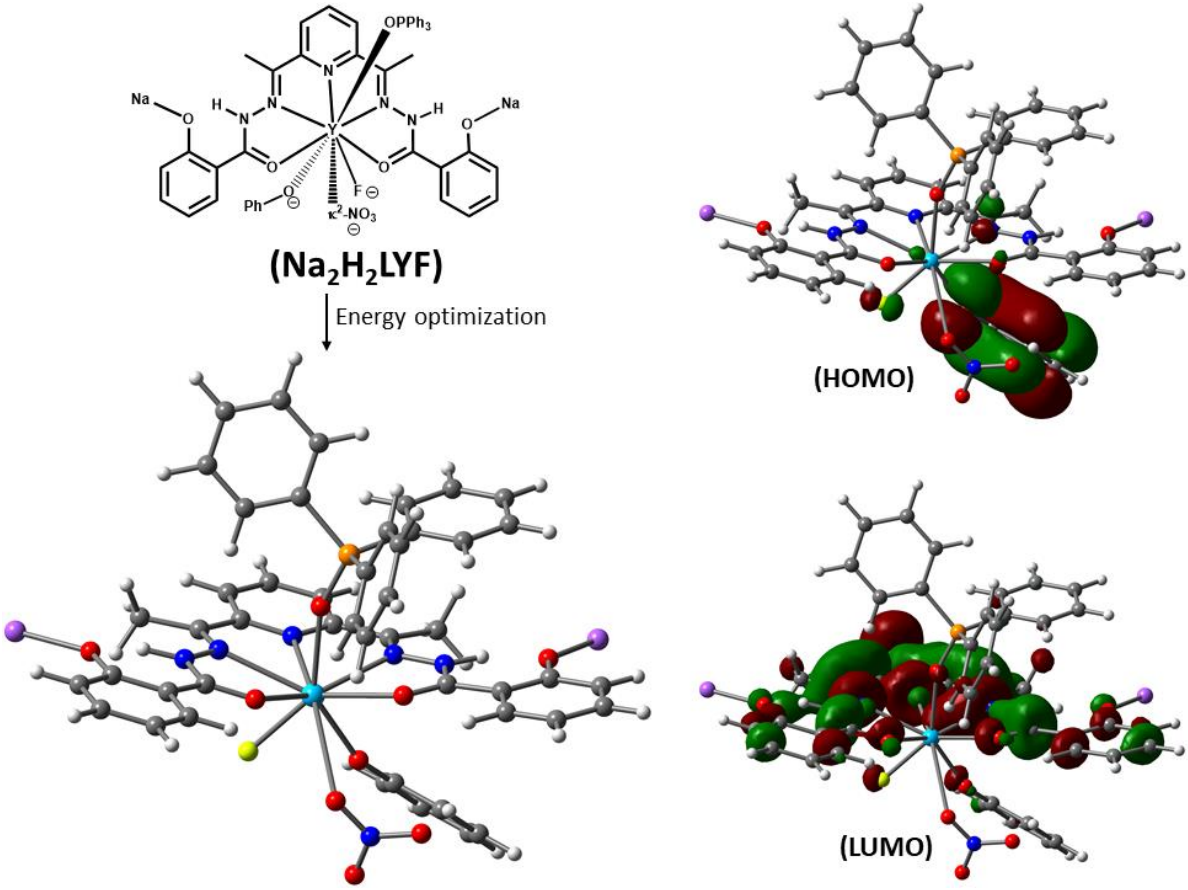

Chart S12: Schematic structures of the hypothetical monomeric model complex **Na_2H_2LYF** (*top-left*), representing the building units of the fluorinated congener of the 1D coordination polymer **1·Y**, which were used for the initial guesses for the gas-phase energy optimization; the gas-phase energy optimized geometry of **Na_2H_2LYF** (*bottom-left*); the isosurfaces (*isovalue* = 0.02; the green and brown coloured surfaces representing the mutually opposite phases of the corresponding wave function) corresponding to the HOMO (*top-right*) and LUMO (*bottom-right*) in the optimized geometry of **Na_2H_2LYF**.

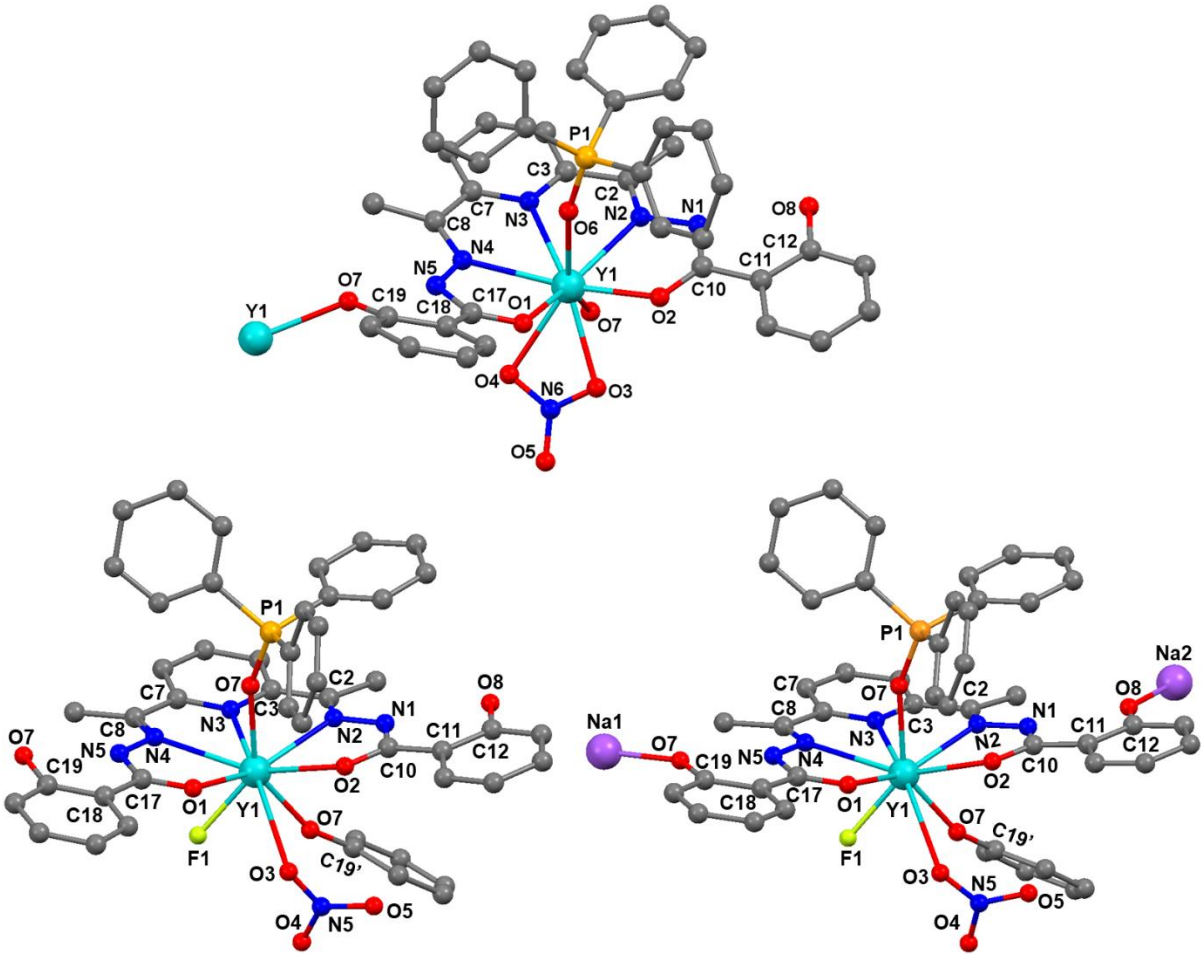

Figure S35: The *ball-and-sticks* representations for the repeat unit of the solid-state single crystal X-ray molecular structure of **1.Y** (*top*), the energy-optimized geometries of the hypothetical monomeric model complexes **H_4LYF** (*left*, *bottom*) and **Na_2H_2LYF** (*right*, *bottom*) representing the fluorinated congener of the 1D CP **1.Y**. The selective atoms are labelled. The H atoms are omitted for clarity. Colour codes: C, grey; N, blue; O, red; F, fluorescent green; P, orange; Na, purple; and Y, cyan. The atomic labels are in accordance with characteristic bond parameters provided in Table S8 below.

Table S8: The characteristic bond parameters associated with the 1D CP **1.Y** and the hypothetical monomeric model complexes **H_4LYF**, and **Na_2H_2LYF** representing the fluorinated congener of the 1D CP **1.Y**. The atomic labels are in accordance with labels as portrayed Figure 35 above.

Bond parameter	1·Y	H_4LYF	Na_2H_2LYF
Y1-O1 (Å)	2.391	2.495	2.477
Y1-O2 (Å)	2.263	2.504	2.519
Y1-O3 (Å)	2.431	3.718	3.517
Y1-O4 (Å)	2.542	-	-
Y1-O6 (Å)	2.357	2.381	2.413
Y1-O7 (Å)	2.356	2.249	2.257
Y1-N2 (Å)	2.472	2.588	2.578
Y1-N3 (Å)	2.512	2.576	2.584
Y1-N4 (Å)	2.535	2.605	2.592
O1-C17 (Å)	1.248	1.276	1.285
O2-C10 (Å)	1.278	1.277	1.284
N1-O8 (Å)	2.594	2.618	2.576
N5-O7 (Å)	2.605	2.619	2.579
Y1-F1 (Å)	-	2.193	2.199
Na1-O7 (Å)	-	-	2.158
Na2-O8 (Å)	-	-	2.155
Y1-O6-P1 (°)	160.1	159.2	158.3
Y1-O7-C19/19’ (°)	131.0	159.0	159.5
O1-C17-N5-N4 (°)	11.863	1.398	2.018
O2-C10-N1-N2 (°)	2.472	3.084	3.144
$Py_{(centroid)} - Ph_{(bridging,\ centroid)}$ (Å)	3.589	6.386	6.177

Table S9: The coordinates of the energy-optimized geometries

c_1:

N	0.0000	0.1092	0.0000	O	-5.9115	-1.7476	0.0000
N	-4.7214	0.2188	0.0000	N	-3.5238	-0.4558	0.0000
C	-7.1694	0.2900	0.0000	C	-7.2246	1.7018	0.0000
C	-1.1705	-0.5730	0.0000	C	-5.9100	-0.4856	0.0000
C	-2.4179	0.2291	0.0000	C	-1.2056	-1.9765	0.0000
H	-2.1605	-2.4781	0.0000	C	-8.4002	-0.4227	0.0000
C	-9.6184	0.2743	0.0000	H	-10.5271	-0.3090	-0.0001
C	-8.4318	2.3845	0.0000	H	-8.4438	3.4651	0.0000
C	-9.6354	1.6599	-0.0001	H	-10.5813	2.1845	-0.0001
C	-2.3427	1.7330	0.0000	H	-1.3036	2.0418	0.0001
H	-2.8247	2.1591	-0.8860	H	-2.8249	2.1591	0.8859
C	-0.0000	-2.6747	0.0000	H	-0.0000	-3.7559	0.0000
O	5.9115	-1.7476	-0.0001	N	4.7214	0.2188	0.0000
N	3.5238	-0.4558	0.0000	C	7.1694	0.2900	0.0000
C	7.2246	1.7018	0.0000	C	1.1705	-0.5730	0.0000
C	5.9100	-0.4856	0.0000	C	2.4179	0.2291	0.0000
C	1.2056	-1.9765	0.0000	H	2.1605	-2.4781	0.0000
C	8.4002	-0.4227	0.0000	C	9.6184	0.2743	0.0000
H	10.5271	-0.3090	0.0001	C	8.4318	2.3845	0.0001
H	8.4438	3.4651	0.0001	C	9.6354	1.6599	0.0001

H	10.5813	2.1845	0.0001	C	2.3427	1.7330	0.0000
H	1.3036	2.0418	-0.0001	H	2.8249	2.1591	-0.8859
H	2.8247	2.1591	0.8860	H	4.7340	1.2279	0.0000
H	-4.7340	1.2279	0.0000	H	6.3145	2.2879	0.0000
H	-6.3144	2.2879	0.0000	O	8.4728	-1.7877	0.0000
O	-8.4727	-1.7877	0.0000	H	7.5522	-2.1669	-0.0001
H	-7.5521	-2.1669	0.0001				

c_2:

N	0.0000	0.0948	0.0000	O	-5.9203	-1.7567	-0.1173
N	-4.7218	0.2032	0.0358	N	-3.5236	-0.4703	0.0271
C	-7.1626	0.2803	0.0852	C	-7.2096	1.6465	0.4400
C	-1.1705	-0.5874	0.0049	C	-5.9108	-0.5015	0.0053
C	-2.4179	0.2147	0.0097	C	-1.2056	-1.9908	0.0044
H	-2.1604	-2.4925	0.0069	C	-8.3883	-0.3768	-0.2063
C	-9.5930	0.3419	-0.1883	H	-10.4994	-0.1943	-0.4268
C	-8.4058	2.3487	0.4686	H	-8.4162	3.3920	0.7500
C	-9.6019	1.6887	0.1411	H	-10.5386	2.2295	0.1578
C	-2.3432	1.7184	-0.0033	H	-1.3042	2.0277	-0.0121
H	-2.8314	2.1376	-0.8891	H	-2.8201	2.1510	0.8824
C	-0.0000	-2.6891	0.0001	H	-0.0000	-3.7703	0.0001
O	5.9202	-1.7567	0.1173	N	4.7218	0.2031	-0.0359
N	3.5236	-0.4703	-0.0271	C	7.1626	0.2803	-0.0852
C	7.2096	1.6465	-0.4399	C	1.1705	-0.5874	-0.0049
C	5.9107	-0.5015	-0.0053	C	2.4179	0.2147	-0.0098
C	1.2056	-1.9908	-0.0043	H	2.1604	-2.4925	-0.0068
C	8.3883	-0.3768	0.2063	C	9.5930	0.3419	0.1883
H	10.4994	-0.1944	0.4267	C	8.4058	2.3487	-0.4685
H	8.4162	3.3921	-0.7498	C	9.6019	1.6887	-0.1411
H	10.5386	2.2295	-0.1577	C	2.3432	1.7184	0.0031
H	1.3042	2.0277	0.0119	H	2.8201	2.1510	-0.8826
H	2.8314	2.1377	0.8889	H	4.7403	1.2125	-0.0062
H	-4.7403	1.2125	0.0061	H	6.3042	2.1649	-0.7289
H	-6.3042	2.1648	0.7291	O	8.4659	-1.7076	0.5125
O	-8.4658	-1.7076	-0.5126	H	7.5646	-2.1196	0.4304
H	-7.5646	-2.1196	-0.4304				

c_3:

N	0.0000	0.1529	0.0000	O	5.7628	1.9741	0.0003
N	4.7110	-0.1211	-0.0001	N	3.5426	0.6635	0.0000
C	7.1220	-0.0045	0.0000	C	7.2530	-1.4202	-0.0004
C	1.1736	0.8290	-0.0001	C	5.8122	0.6115	0.0000
C	2.4134	0.0122	-0.0001	C	1.2041	2.2331	-0.0001
H	2.1518	2.7458	-0.0001	C	8.2880	0.7915	0.0004
C	9.5455	0.2081	0.0004	H	10.4315	0.8270	0.0007
C	8.5294	-1.9984	-0.0003	H	8.5955	-3.0762	-0.0006
C	9.6608	-1.1934	0.0001	H	10.6403	-1.6529	0.0001
C	2.3252	-1.4859	-0.0002	H	1.2899	-1.8042	0.0000
H	2.8312	-1.8973	-0.8763	H	2.8315	-1.8974	0.8757
C	0.0000	2.9327	-0.0001	H	0.0000	4.0140	-0.0001
O	-5.7628	1.9741	-0.0004	N	-4.7110	-0.1212	0.0001
N	-3.5425	0.6635	0.0000	C	-7.1220	-0.0045	0.0000
C	-7.2530	-1.4202	0.0003	C	-1.1736	0.8290	0.0000
C	-5.8122	0.6115	-0.0001	C	-2.4134	0.0122	0.0001
C	-1.2041	2.2331	0.0000	H	-2.1518	2.7458	0.0000

C	-8.2880	0.7916	-0.0002	C	-9.5455	0.2081	-0.0001
H	-10.4315	0.8270	-0.0003	C	-8.5294	-1.9984	0.0004
H	-8.5955	-3.0762	0.0006	C	-9.6608	-1.1934	0.0002
H	-10.6403	-1.6528	0.0002	C	-2.3252	-1.4859	0.0002
H	-1.2898	-1.8042	0.0001	H	-2.8315	-1.8975	-0.8756
H	-2.8311	-1.8973	0.8764	O	6.1712	-2.2573	-0.0008
O	-6.1712	-2.2574	0.0006	H	8.1754	1.8654	0.0006
H	-8.1753	1.8655	-0.0005	H	-5.3297	-1.7087	0.0005
H	5.3297	-1.7087	-0.0009	H	-4.8109	2.2293	-0.0004
H	4.8109	2.2293	0.0003				

c_4:

N	0.0000	0.1706	-0.0001	O	-5.6741	-1.5782	0.3860
N	-4.7026	0.4739	-0.1905	N	-3.5353	-0.3205	-0.0685
C	-7.1255	0.3026	-0.0290	C	-7.2991	1.6620	-0.3756
C	-1.1689	-0.5063	-0.0989	C	-5.7768	-0.2378	0.0445
C	-2.4035	0.3116	-0.1989	C	-1.1994	-1.9104	-0.1070
H	-2.1429	-2.4229	-0.2008	C	-8.2774	-0.4812	0.2343
C	-9.5504	0.0988	0.1472	H	-10.4025	-0.5311	0.3553
C	-8.5611	2.2267	-0.4592	H	-8.6733	3.2680	-0.7258
C	-9.6927	1.4359	-0.1951	H	-10.6824	1.8684	-0.2578
C	-2.3062	1.7901	-0.4355	H	-1.2776	2.0813	-0.6136
H	-2.9353	2.0745	-1.2791	H	-2.6883	2.3374	0.4291
C	-0.0000	-2.6105	-0.0001	H	-0.0000	-3.6918	-0.0001
O	5.6742	-1.5782	-0.3864	N	4.7026	0.4738	0.1903
N	3.5352	-0.3206	0.0678	C	7.1255	0.3026	0.0289
C	7.2989	1.6621	0.3751	C	1.1688	-0.5063	0.0986
C	5.7768	-0.2379	-0.0447	C	2.4035	0.3115	0.1987
C	1.1993	-1.9104	0.1068	H	2.1428	-2.4229	0.2005
C	8.2775	-0.4813	-0.2338	C	9.5505	0.0989	-0.1467
H	10.4026	-0.5311	-0.3543	C	8.5609	2.2269	0.4587
H	8.6730	3.2683	0.7249	C	9.6926	1.4361	0.1952
H	10.6822	1.8686	0.2580	C	2.3064	1.7898	0.4364
H	1.2769	2.0821	0.6070	H	2.6967	2.3378	-0.4241
H	2.9289	2.0723	1.2857	H	6.4127	2.2468	0.5719
H	-6.4129	2.2467	-0.5729	O	8.2434	-1.8136	-0.5801
O	-8.2432	-1.8134	0.5811	H	7.3202	-2.1436	-0.6190
H	-7.3200	-2.1433	0.6197	H	4.7076	-1.7898	-0.3869
H	-4.7075	-1.7898	0.3860				

c_5:

N	18.8544	3.0409	1.9232	O	16.0536	6.0056	-0.9052
N	15.2818	4.8891	0.9597	N	16.4281	4.1374	1.0705
C	13.9729	6.7326	0.0349	C	13.0782	6.7735	1.1274
C	17.6866	2.3657	2.0304	C	15.1790	5.8755	-0.0076
C	16.4256	3.1434	1.9092	C	17.6517	0.9761	2.2564
H	16.7077	0.4481	2.3238	C	13.7021	7.5656	-1.0875
C	12.5397	8.3558	-1.1115	H	12.3643	8.9659	-1.9892
C	11.9373	7.5675	1.1034	H	11.2690	7.5877	1.9569
C	11.6661	8.3535	-0.0316	H	10.7760	8.9738	-0.0598
C	15.2276	2.7539	2.7527	H	15.4631	1.9286	3.4251
H	14.9056	3.5927	3.3872	H	14.3689	2.4527	2.1363
C	18.8558	0.2793	2.3624	H	18.8563	-0.7947	2.5155
O	21.6640	5.9833	-0.9294	N	22.4265	4.8879	0.9517
N	21.2813	4.1342	1.0628	C	23.7341	6.7286	0.0199

C	24.6194	6.7846	1.1194	C	20.0226	2.3668	2.0301
C	22.5322	5.8658	-0.0239	C	21.2829	3.1456	1.9078
C	20.0592	0.9774	2.2565	H	21.0039	0.4506	2.3243
C	24.0107	7.5514	-1.1086	C	25.1700	8.3462	-1.1310
H	25.3501	8.9482	-2.0134	C	25.7571	7.5832	1.0968
H	26.4180	7.6151	1.9557	C	26.0345	8.3586	-0.0439
H	26.9221	8.9825	-0.0711	C	22.4787	2.7631	2.7576
H	22.2440	1.9375	3.4298	H	22.7936	3.6042	3.3925
H	23.3418	2.4654	2.1455	H	23.2209	4.7133	1.5547
H	14.4840	4.7063	1.5558	O	14.5283	7.6415	-2.1710
O	23.1931	7.6127	-2.1995	H	13.2921	6.2045	2.0275
H	24.4000	6.2240	2.0235	H	15.3453	7.0876	-1.9997
H	22.3768	7.0575	-2.0290				

c_6:

N	18.8560	3.1180	1.8892	O	15.9877	6.1312	-0.9158
N	15.2264	4.8877	0.8867	N	16.3940	4.1714	1.0025
C	13.7974	6.6280	-0.0909	C	12.6940	6.4361	0.7642
C	17.6872	2.4457	2.0151	C	15.1017	5.8696	-0.0828
C	16.4213	3.2130	1.8825	C	17.6529	1.0617	2.2764
H	16.7075	0.5378	2.3582	C	13.6889	7.6340	-1.0685
C	12.5435	8.4178	-1.1968	H	12.4936	9.1854	-1.9609
C	11.5383	7.2154	0.6453	H	10.7021	7.0441	1.3188
C	11.4613	8.2071	-0.3343	H	10.5619	8.8079	-0.4202
C	15.2408	2.8488	2.7628	H	15.4933	2.0529	3.4642
H	14.9213	3.7147	3.3598	H	14.3734	2.5232	2.1714
C	18.8560	0.3666	2.3993	H	18.8560	-0.7036	2.5788
O	21.7241	6.1315	-0.9155	N	22.4856	4.8878	0.8867
N	21.3179	4.1714	1.0025	C	23.9146	6.6280	-0.0909
C	25.0181	6.4360	0.7640	C	20.0248	2.4457	2.0151
C	22.6102	5.8697	-0.0827	C	21.2907	3.2130	1.8825
C	20.0591	1.0617	2.2763	H	21.0044	0.5378	2.3581
C	24.0230	7.6341	-1.0684	C	25.1684	8.4179	-1.1967
H	25.2183	9.1855	-1.9608	C	26.1738	7.2152	0.6451
H	27.0101	7.0437	1.3185	C	26.2508	8.2070	-0.3344
H	27.1502	8.8078	-0.4204	C	22.4713	2.8487	2.7626
H	22.2188	2.0528	3.4641	H	22.7909	3.7146	3.3596
H	23.3386	2.5230	2.1712	H	23.2773	4.7322	1.5060
H	14.4347	4.7323	1.5061	O	12.7637	5.4382	1.7501
H	11.9498	5.3953	2.2853	O	24.9484	5.4380	1.7498
H	25.7624	5.3950	2.2850	H	14.5444	7.7699	-1.7198
H	23.1674	7.7702	-1.7196				

c_7:

N	-0.0005	2.8386	-0.0002	O	1.9391	-0.8891	0.6215
N	3.4880	0.6631	-0.1879	N	2.3300	1.4582	-0.0412
C	4.1754	-1.6532	0.1443	C	5.4891	-1.3889	-0.3052
C	1.1584	3.5147	-0.1693	C	3.2074	-0.5694	0.1762
C	2.4048	2.7198	-0.3308	C	1.1892	4.9213	-0.1819
H	2.1182	5.4530	-0.3180	C	3.8502	-2.9725	0.5509
C	4.8268	-3.9774	0.5000	H	4.5407	-4.9691	0.8174
C	6.4472	-2.3882	-0.3517	H	7.4466	-2.1670	-0.6985
C	6.1091	-3.6908	0.0548	H	6.8506	-4.4779	0.0215
C	3.6666	3.3945	-0.7987	H	4.0534	4.0778	-0.0372
H	4.4270	2.6465	-0.9971	H	3.4902	3.9782	-1.7043
C	-0.0005	5.6226	0.0003	H	-0.0005	6.7039	0.0004

O	-1.9387	-0.8893	-0.6205	N	-3.4884	0.6627	0.1879
N	-2.3306	1.4579	0.0414	C	-4.1750	-1.6539	-0.1442
C	-5.4889	-1.3901	0.3049	C	-1.1594	3.5146	0.1693
C	-3.2073	-0.5698	-0.1758	C	-2.4057	2.7196	0.3306
C	-1.1902	4.9211	0.1823	H	-2.1192	5.4528	0.3185
C	-3.8493	-2.9731	-0.5508	C	-4.8255	-3.9783	-0.5002
H	-4.5390	-4.9700	-0.8175	C	-6.4466	-2.3897	0.3510
H	-7.4463	-2.1688	0.6977	C	-6.1080	-3.6922	-0.0554
H	-6.8493	-4.4795	-0.0223	C	-3.6678	3.3942	0.7979
H	-3.4919	3.9787	1.7030	H	-4.4279	2.6460	0.9968
H	-4.0548	4.0766	0.0356	O	2.6114	-3.3556	1.0083
O	-2.6101	-3.3558	-1.0078	H	5.7217	-0.3800	-0.6116
H	-5.7219	-0.3812	0.6113	H	1.9852	-2.5988	1.0095
H	-1.9842	-2.5987	-1.0088	H	1.4170	-0.0388	0.5790
H	-1.4169	-0.0386	-0.5780				

c_8:

N	0.0000	2.5383	0.0001	O	2.0562	-1.1985	-0.7868
N	3.5170	0.4067	0.0854	N	2.3604	1.1941	-0.0441
C	4.3190	-1.8416	-0.3089	C	5.6330	-1.5182	0.1253
C	1.1535	3.2156	0.1981	C	3.2809	-0.8329	-0.3283
C	2.3953	2.4186	0.3809	C	1.1853	4.6216	0.2085
H	2.1130	5.1530	0.3568	C	4.0377	-3.1629	-0.7176
C	5.0245	-4.1367	-0.6983	H	4.7983	-5.1457	-1.0125
C	6.6225	-2.5098	0.1396	H	7.6113	-2.2327	0.4737
C	6.3203	-3.8033	-0.2662	H	7.0935	-4.5600	-0.2493
C	3.6077	3.0486	1.0162	H	3.3294	3.8075	1.7457
H	4.2042	2.2903	1.5172	H	4.2489	3.5208	0.2655
C	0.0001	5.3234	-0.0002	H	0.0001	6.4047	-0.0003
O	-2.0562	-1.1985	0.7869	N	-3.5170	0.4067	-0.0853
N	-2.3604	1.1941	0.0443	C	-4.3190	-1.8416	0.3089
C	-5.6329	-1.5183	-0.1254	C	-1.1535	3.2156	-0.1981
C	-3.2809	-0.8329	0.3284	C	-2.3954	2.4187	-0.3808
C	-1.1852	4.6217	-0.2088	H	-2.1128	5.1531	-0.3571
C	-4.0377	-3.1629	0.7176	C	-5.0245	-4.1367	0.6983
H	-4.7983	-5.1457	1.0126	C	-6.6225	-2.5099	-0.1397
H	-7.6113	-2.2328	-0.4740	C	-6.3203	-3.8033	0.2661
H	-7.0934	-4.5601	0.2491	C	-3.6078	3.0487	-1.0159
H	-4.2490	3.5209	-0.2651	H	-4.2043	2.2904	-1.5168
H	-3.3297	3.8076	-1.7454	H	-5.1798	0.3424	-0.4634
H	5.1798	0.3425	0.4632	O	5.9826	-0.2573	0.5280
O	-5.9826	-0.2574	-0.5282	H	3.0349	-3.3942	-1.0445
H	-3.0349	-3.3942	1.0446	H	1.4798	-0.3917	-0.7396
H	-1.4799	-0.3917	0.7398				

H_2L^{2-}:

N	0.0000	0.2419	0.0000	O	6.0102	2.1022	0.0001
N	4.7269	0.1551	0.0000	N	3.5387	0.8244	0.0000
C	7.1263	-0.0398	0.0000	C	7.0391	-1.4871	-0.0001
C	1.1771	0.9227	0.0000	C	5.9364	0.8455	0.0000
C	2.4302	0.1321	0.0000	C	1.2075	2.3291	0.0000
H	2.1662	2.8240	0.0000	C	8.3858	0.5865	0.0001
C	9.5739	-0.1345	0.0001	H	10.5307	0.3747	0.0001
C	8.2881	-2.1956	-0.0001	H	8.2218	-3.2769	-0.0002
C	9.5081	-1.5445	0.0000	H	10.4262	-2.1264	0.0000
C	2.3807	-1.3720	0.0000	H	1.3492	-1.7081	0.0004

H	2.8949	-1.7834	-0.8743	H	2.8957	-1.7834	0.8738
C	0.0000	3.0240	0.0000	H	0.0000	4.1076	0.0000
O	-6.0102	2.1022	-0.0002	N	-4.7269	0.1551	0.0000
N	-3.5387	0.8244	0.0000	C	-7.1263	-0.0398	0.0000
C	-7.0391	-1.4871	0.0001	C	-1.1771	0.9227	0.0000
C	-5.9364	0.8455	0.0000	C	-2.4302	0.1321	0.0000
C	-1.2075	2.3291	0.0000	H	-2.1662	2.8240	0.0000
C	-8.3858	0.5865	-0.0001	C	-9.5739	-0.1345	0.0000
H	-10.5307	0.3747	-0.0001	C	-8.2881	-2.1956	0.0001
H	-8.2218	-3.2769	0.0002	C	-9.5081	-1.5445	0.0001
H	-10.4262	-2.1264	0.0001	C	-2.3807	-1.3720	0.0000
H	-1.3492	-1.7081	-0.0005	H	-2.8958	-1.7834	-0.8738
H	-2.8948	-1.7834	0.8743	O	5.9037	-2.1505	-0.0002
O	-5.9037	-2.1505	0.0002	H	8.3885	1.6695	0.0001
H	-8.3885	1.6695	-0.0001	H	-4.8322	-0.8868	0.0002
H	4.8322	-0.8868	-0.0001				

H_4LYF:

P	0.9737	2.4062	-0.2576	O	-1.5128	-0.3433	-1.1456
N	0.1456	-0.6028	3.0015	O	2.0586	-1.6445	-0.9071
O	0.9084	0.8496	0.2206	O	6.0092	-1.9974	0.5016
N	3.4511	-1.6210	0.9190	H	4.4050	-1.7360	1.2792
O	-0.1650	-2.7334	-2.9054	C	2.5182	3.1851	0.4358
N	-1.9054	0.0912	1.4430	C	4.1145	-2.4032	-2.6581
H	3.0869	-2.3281	-2.9995	N	-2.8729	0.4466	0.5244
C	1.2351	3.7729	-2.7419	H	1.2892	4.6864	-2.1554
C	-0.9716	-0.0916	3.5977	C	4.3855	-2.1419	-1.2917
C	-2.6027	0.2269	-0.8037	C	3.2325	-1.7851	-0.4266
C	3.7710	-1.5857	3.7487	H	3.5665	-1.9028	4.7727
H	4.2989	-2.4113	3.2574	H	4.4529	-0.7241	3.7900
C	3.6080	2.3469	0.7471	H	3.5261	1.2717	0.6164
C	-2.1402	0.2098	2.7260	C	-0.9956	0.2152	4.9754
H	-1.8846	0.6243	5.4383	C	1.2842	-0.7807	3.7359
C	5.7299	-2.2506	-0.8451	N	2.3730	-1.2748	1.7086
C	-3.5979	0.6663	-1.8135	O	-5.1052	1.6213	-0.1757
C	1.3187	-0.4872	5.1164	H	2.2253	-0.6220	5.6921
C	1.0655	2.5204	-2.1141	C	-4.8114	1.3415	-1.5137
C	5.1350	-2.7545	-3.5501	H	4.9036	-2.9528	-4.5923
C	0.1614	0.0035	5.7385	H	0.1675	0.2347	6.7994
C	1.2752	2.6616	-4.9147	H	1.3554	2.7160	-5.9977
C	1.3379	3.8406	-4.1431	H	1.4675	4.8048	-4.6279
C	3.8217	5.1376	1.0866	H	3.9016	6.2137	1.2178
C	-5.3833	1.4379	-3.8753	H	-6.0723	1.7364	-4.6612
C	-3.4406	0.6740	3.3340	H	-3.6336	0.1618	4.2804
H	-3.4113	1.7542	3.5361	H	-4.2952	0.4730	2.6813
C	2.6222	4.5816	0.6029	H	1.7851	5.2343	0.3694
C	4.8045	2.9083	1.2312	H	5.6450	2.2624	1.4720
C	-1.5045	3.8066	-0.5225	H	-1.4533	3.5867	-1.5850
C	-0.4762	3.3987	0.3507	C	1.1105	1.4144	-4.2820
H	1.0633	0.5034	-4.8728	C	-3.3084	0.3876	-3.1723
H	-2.3829	-0.1289	-3.4025	C	1.0058	1.3399	-2.8794
H	0.8836	0.3761	-2.3968	C	4.9134	4.3032	1.4002
H	5.8386	4.7356	1.7736	C	-5.6966	1.7246	-2.5370
H	-6.6189	2.2414	-2.2813	C	2.5030	-1.2345	3.0097
C	6.4637	-2.8536	-3.0836	H	7.2648	-3.1267	-3.7654

C	-4.1839	0.7670	-4.1969	H	-3.9418	0.5422	-5.2313
C	6.7609	-2.6026	-1.7346	H	7.7816	-2.6785	-1.3669
C	-2.6135	4.5104	-0.0146	H	-3.4036	4.8270	-0.6905
C	-2.6975	4.8027	1.3604	H	-3.5534	5.3493	1.7491
C	-1.6717	4.3851	2.2337	H	-1.7333	4.6078	3.2958
C	-0.5624	3.6818	1.7321	H	0.2244	3.3627	2.4116
O	-1.8197	-2.5913	0.6977	C	-5.3677	-3.4030	0.0362
H	-6.0312	-3.5405	-0.8166	C	-4.0192	-3.0743	-0.1890
C	-3.1186	-2.8925	0.9045	C	-5.8682	-3.5619	1.3483
H	-6.9114	-3.8202	1.5156	C	-4.9862	-3.3898	2.4377
H	-5.3512	-3.5168	3.4562	C	-3.6346	-3.0611	2.2259
H	-2.9558	-2.9454	3.0694	Y	0.0468	-1.3469	0.5375
H	-3.6405	-2.9600	-1.2026	F	0.8378	-3.3331	1.0264
N	-1.2536	-3.4596	-2.8787	O	-2.3352	-3.0367	-3.4824
O	-1.2618	-4.6012	-2.2443	H	-3.7540	0.9059	0.7797
H	6.9590	-2.0937	0.7281	H	-5.9644	2.0778	-0.0483

Na_2H_2LYF:

P	-0.6853	-2.5454	0.2470	O	1.4348	0.1130	-1.3653
N	-0.2645	1.2779	2.6274	O	-2.1953	1.0812	-1.4055
O	-0.8253	-0.9246	0.3213	O	-6.1566	1.5272	0.0335
N	-3.6112	1.3622	0.3942	H	-4.6147	1.4875	0.6722
O	0.0396	2.3542	-3.3272	C	-2.0741	-3.3189	1.2207
N	1.8584	0.4444	1.2523	C	-4.4024	1.0025	-3.2100
H	-3.3875	0.8894	-3.5820	N	2.8656	-0.0208	0.4403
C	-0.8104	-4.5120	-1.8131	H	-0.6901	-5.2513	-1.0252
C	0.9021	1.0792	3.3114	C	-4.5881	1.1818	-1.8128
C	2.5875	-0.2045	-0.8963	C	-3.3933	1.2010	-0.9551
C	-4.0170	1.9329	3.1096	H	-3.9532	2.2107	4.1609
H	-4.4616	2.7817	2.5700	H	-4.7092	1.0820	3.0257
C	-3.2452	-2.5646	1.4353	H	-3.3131	-1.5453	1.0661
C	2.0978	0.6888	2.5180	C	0.9475	1.1666	4.7205
H	1.8727	1.0086	5.2600	C	-1.4276	1.5048	3.3102
C	-5.9218	1.3446	-1.2788	N	-2.5192	1.3469	1.2292
C	3.6687	-0.7729	-1.7172	O	5.2499	-0.9570	0.1409
C	-1.4383	1.5996	4.7193	H	-2.3576	1.7789	5.2614
C	-0.8283	-3.1330	-1.5139	C	4.9542	-1.1282	-1.1608
C	-5.4845	0.9722	-4.0920	H	-5.3248	0.8344	-5.1578
C	-0.2345	1.4424	5.4224	H	-0.2225	1.5148	6.5058
C	-1.1106	-3.9864	-4.1777	H	-1.2182	-4.3163	-5.2082
C	-0.9503	-4.9359	-3.1470	H	-0.9347	-5.9977	-3.3793
C	-3.0658	-5.2108	2.3920	H	-2.9943	-6.2311	2.7602
C	5.6521	-1.8690	-3.4089	H	6.4172	-2.2921	-4.0573
C	3.4575	0.5310	3.1542	H	3.5378	1.0834	4.0912
H	3.6689	-0.5282	3.3629	H	4.2396	0.9092	2.4852
C	-1.9814	-4.6432	1.6967	H	-1.0799	-5.2299	1.5405
C	-4.3260	-3.1370	2.1323	H	-5.2297	-2.5559	2.2984
C	1.9497	-3.6484	0.1517	H	1.8304	-3.6949	-0.9268
C	0.9089	-3.1713	0.9731	C	-1.1332	-2.6121	-3.8714
H	-1.2579	-1.8778	-4.6630	C	3.4193	-0.9690	-3.1016
H	2.4463	-0.6868	-3.4935	C	-0.9929	-2.1808	-2.5381
H	-1.0162	-1.1215	-2.3043	C	-4.2385	-4.4598	2.6102
H	-5.0746	-4.9010	3.1475	C	5.9268	-1.6810	-2.0516
H	6.8978	-1.9529	-1.6409	C	-2.6758	1.5920	2.5059
C	-6.7980	1.1275	-3.5755	H	-7.6508	1.1064	-4.2516

C	4.3884	-1.5121	-3.9481	H	4.1805	-1.6553	-5.0048
C	-7.0099	1.3094	-2.2063	H	-8.0180	1.4296	-1.8135
C	3.1606	-4.0709	0.7330	H	3.9606	-4.4407	0.0970
C	3.3343	-4.0119	2.1290	H	4.2693	-4.3429	2.5754
C	2.2949	-3.5250	2.9487	H	2.4250	-3.4776	4.0268
C	1.0834	-3.1031	2.3734	H	0.2866	-2.7298	3.0126
O	1.5244	2.8289	-0.0771	C	5.0430	3.8643	-0.5579
H	5.8217	3.7927	-1.3164	C	3.7856	3.2879	-0.8084
C	2.7368	3.3665	0.1590	C	5.3059	4.5366	0.6575
H	6.2794	4.9848	0.8435	C	4.2768	4.6253	1.6208
H	4.4565	5.1476	2.5598	C	3.0141	4.0519	1.3820
H	2.2201	4.1395	2.1220	Y	-0.2131	1.3931	0.0462
Na	-7.6219	2.1932	1.4716	H	3.5886	2.7790	-1.7494
F	-1.2015	3.3554	0.1279	N	1.1614	2.9810	-3.5746
O	2.1767	2.3278	-4.0787	O	1.2678	4.2571	-3.3153
H	3.8322	-0.2960	0.7374	Na	6.8608	-1.0179	1.5715

Table S10: The coordinates of **NaH_2LY** as used for the single-point computation

P	0.5890	1.7036	1.4631	O	-1.4047	0.9012	-1.8960
N	-0.5923	-2.0941	1.0785	O	1.9221	-0.2596	-1.9350
O	0.5687	0.6590	0.3999	O	5.5787	-1.7857	-0.5975
N	2.9742	-1.7332	-0.5721	H	3.6929	-2.1471	-0.3450
O	-0.5169	-0.9991	-3.6133	C	2.1542	1.6880	2.3490
N	-2.2916	-0.3137	0.1532	C	4.2929	1.0868	-2.4851
H	3.4879	1.4287	-2.8010	N	-3.0817	0.7314	-0.3281
O	0.5521	-2.7031	-2.8544	C	0.4006	4.4747	1.6263
H	0.4486	4.3563	2.5471	C	-1.8120	-2.0436	1.6582
C	4.2920	-0.1106	-1.7419	C	-2.5032	1.2866	-1.3689
C	2.9935	-0.7088	-1.4636	C	2.8849	-3.4012	1.6943
H	2.5875	-3.8941	2.4622	H	3.3405	-3.9913	1.0909
H	3.4838	-2.7043	1.9733	C	3.2506	1.1123	1.7359
H	3.1539	0.6983	0.9088	C	-2.7419	-1.0169	1.1291
C	-2.1505	-2.8828	2.7045	H	-3.0072	-2.8634	3.0641
C	0.3457	-2.9130	1.6139	C	5.5139	-0.6333	-1.2498
N	1.7536	-2.0770	-0.0547	C	-3.1979	2.4480	-1.9699
O	-5.0160	2.4501	-0.4304	H	-4.5809	1.8201	-0.1352
C	0.0599	-3.7588	2.6604	H	0.7137	-4.3303	2.9952
C	0.4118	3.3544	0.7827	C	-4.3985	2.9530	-1.4976
C	5.4488	1.7511	-2.7487	H	5.4343	2.5342	-3.2493
C	-1.2039	-3.7494	3.2070	H	-1.4163	-4.3222	3.9069
C	0.2212	5.9023	-0.2587	H	0.1824	6.7589	-0.6173
C	0.3176	5.7376	1.1094	H	0.3279	6.4779	1.6724
C	3.5836	2.3416	4.1646	H	3.6975	2.7565	4.9900
C	-4.4174	4.5839	-3.2516	H	-4.8377	5.2945	-3.6800
C	-4.0983	-0.8465	1.7379	H	-4.2129	-1.4812	2.4486
H	-4.1856	0.0430	2.0850	H	-4.7706	-0.9956	1.0662
C	2.3444	2.2802	3.5780	H	1.6139	2.6495	4.0213
C	4.4965	1.1505	2.3448	H	5.2239	0.7364	1.9366
O	0.2226	-2.4864	-4.9873	C	-1.8563	2.3066	2.6585
H	-1.9449	2.9509	1.9935	C	-0.7166	1.5226	2.7035
C	0.1799	4.8088	-1.1032	H	0.0783	4.9254	-2.0202
C	-2.6225	3.0417	-3.1086	H	-1.8157	2.7164	-3.4366
C	0.2911	3.5178	-0.5596	H	0.2836	2.7755	-1.1203
N	0.0874	-2.0789	-3.8448	C	4.6576	1.7759	3.5072
H	5.5075	1.8332	3.8829	C	-4.9895	4.0425	-2.1367

H	-5.7800	4.4012	-1.8027	C	1.7037	-2.7959	1.0028
C	6.6590	1.2479	-2.2645	H	7.4540	1.6895	-2.4582
C	-3.2432	4.1059	-3.7483	H	-2.8611	4.4876	-4.5053
C	6.6793	0.1157	-1.5081	H	7.4882	-0.1737	-1.1516
C	-2.8549	2.1473	3.5765	H	-3.6102	2.6896	3.5374
C	-2.7547	1.2279	4.5180	H	-3.4370	1.1511	5.1452
C	-1.6635	0.3703	4.6046	H	-1.6234	-0.2895	5.2582
C	-0.6007	0.5347	3.6544	H	0.1484	-0.0147	3.6802
O	-2.0220	-2.5057	-1.6254	C	-4.0140	-5.0388	0.1288
H	-4.8947	-5.2077	0.3762	C	-3.7110	-3.8736	-0.6030
C	-2.3726	-3.6151	-0.9900	C	-3.0429	-5.9226	0.4788
H	-3.2570	-6.6821	0.9701	C	-1.7207	-5.6819	0.0977
H	-1.0507	-6.2749	0.3501	C	-1.4091	-4.5840	-0.6451
H	-0.5323	-4.4686	-0.9331	H	-4.4883	-3.1868	-0.8654
Y	-0.2706	-0.9517	-1.1602	Na	6.7106	-3.2756	-0.8644

Table S11: The characteristic computational output parameters regarding different isomers of the pristine ligand, **H_4L**, its doubly deprotonated forms, **H_2L^{2-}**, and the model complexes **NaH_2YF**, **H_4YF** and **Na_2H_2YF**. The energy-optimized ground state electronic energy of the most stable isomer (**c_2**) of the pristine ligand **H_4L** is highlighted in bold with green colour.

	Ground-state energy (Hartree) (ΔE_{ci-c2}; kCal)	**HOMO energy (Hartree)**	**LUMO energy (Hartree)**	**$\Delta E_{LUMO-HOMO}$ (kCal)**
C_1	-1463.649624 (*7.5*)	-0.21452	-0.06774	92.10489034
C_2	**-1463.661515 (*0*)**	-0.23437	-0.08505	93.69874796
C_3	-1463.652503 (*5.6*)	-0.22948	-0.09834	82.29074342
C_4	-1463.6379 (*14.8*)	-0.22822	-0.09578	83.10649732
C_5	-1463.28007 (*239.4*)	-0.22256	-0.06459	99.12664891
C_6	-1463.264868 (*248.9*)	-0.20779	-0.04736	100.6703063
C_7	-1463.626776 (*21.8*)	-0.22491	-0.08822	85.77338703
C_8	-1463.638065 (*14.7*)	-0.2277	-0.08984	86.50756358
H_2L^{2-}	-1462.558863	-0.01074	0.10716	73.9826037
NaH_2LY	-2870.857993	-0.14251	-0.10227	25.25072072
H_4LYF	-2965.431912	-0.19255	-0.09608	60.53521441
Na_2H_2LYF	-2964.794594	-0.19071	-0.09033	62.98875114

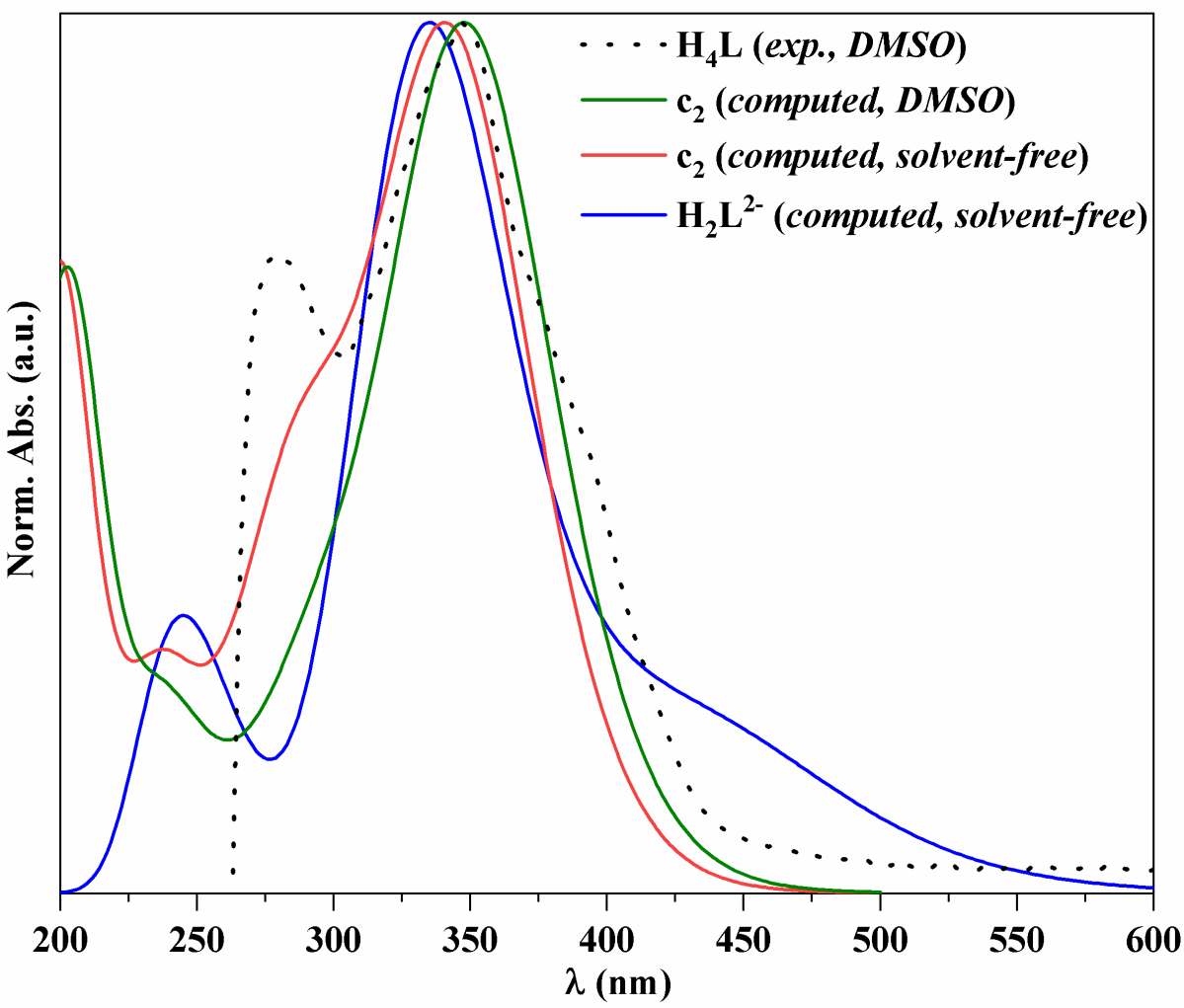

Figure S36: The normalized UV-Vis spectra for the energy optimized geometry of $\mathbf{H_2L^{2-}}$ computed in solvent-free gas-phase (*blue solid line*); the energy optimized geometry of the conformer $\mathbf{c_2}$ computed in solvent-free gas-phase (*red solid line*); the energy optimized geometry of the conformer $\mathbf{c_2}$ computed in gas-phase with self-consistent DMSO solvent environment (*green solid line*); and the DMSO solution (see the experimental section for details) of the *as-synthesized* sample of $\mathbf{H_4L}$ at room temperature (*black dotted line*).

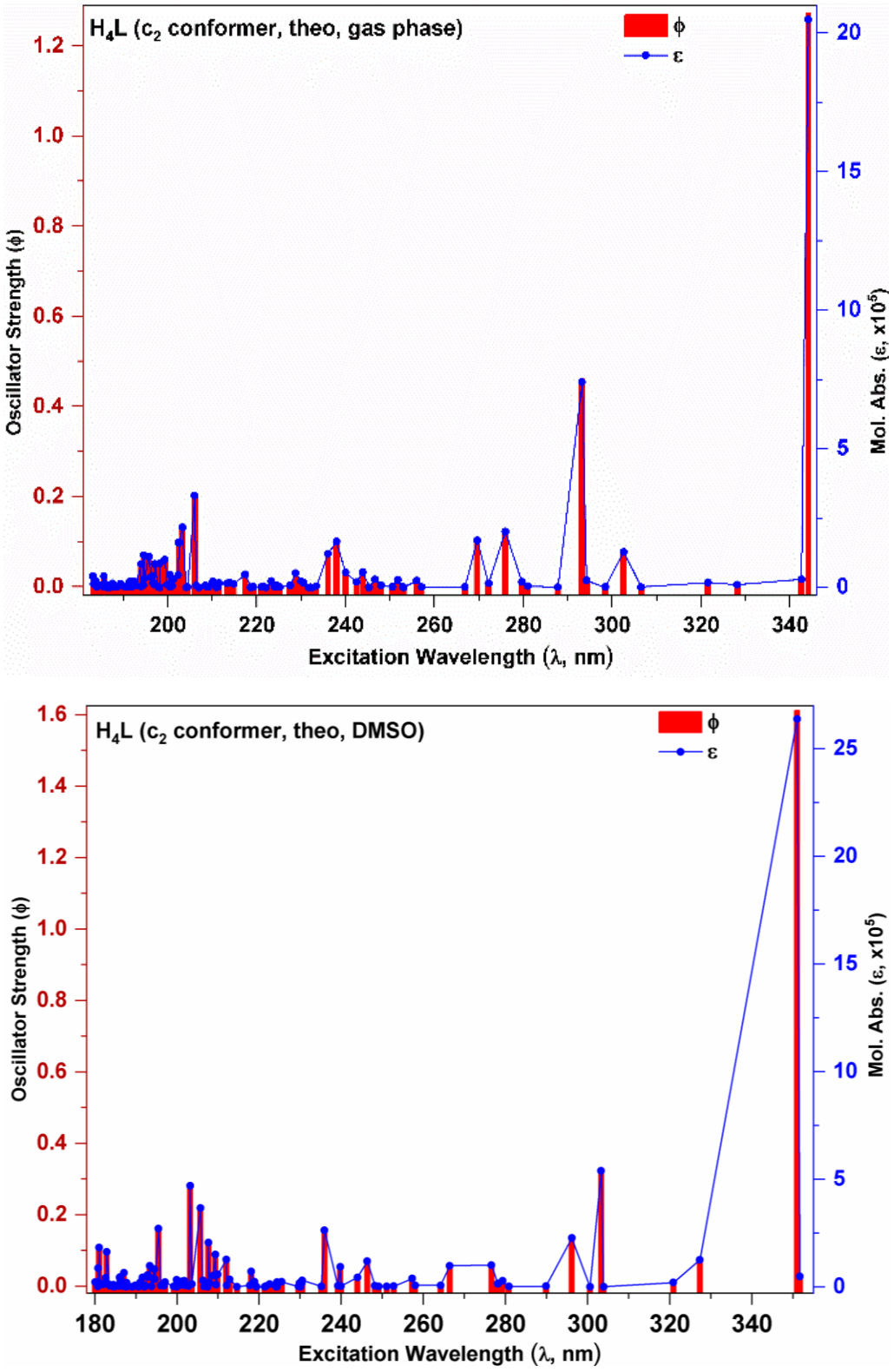

Figure S37: The theoretically predicted molar absorption coefficients (solid blue circles) and the associated oscillator strengths (solid red bars) considering 120 frontier electronic transitions associated with the lowest energy conformer (**c2**) of the pristine ligand **H4L** in solvent free gas phase (*top*) and in gas-phase with self-consistent DMSO solvent environment *(bottom*). The solid blue lines are eye-guides only.

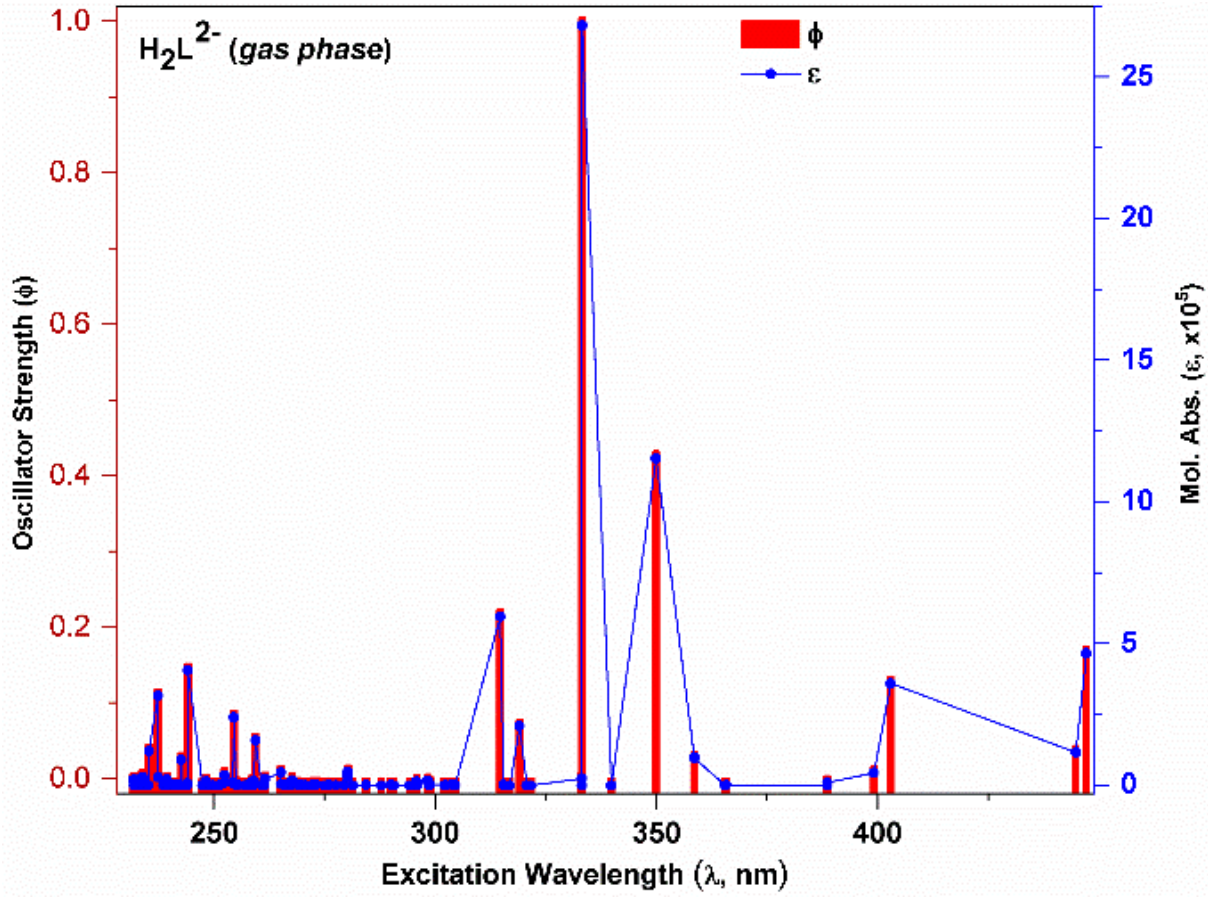

Figure S38: The theoretically predicted molar absorption coefficients (solid blue circles) and the associated oscillator strengths (solid red bars) considering 120 frontier electronic transitions associated with the *energy-optimized* geometry of the hypothetical doubly deprotonated dianionic form (**H_2L^{2-}**) of the pristine ligand **H_4L** in solvent-free gas-phase. The solid blue lines are eye-guides only.

Table S12. The outputs from the *Continuous Shape Measures* (CShM's) analyses employing the SHAPE program based on the Pinsky-Avnir algorithm for the calculation of continuous shape measures for the [LnN_3O_6] nonacoordinate fragments around the Ln centers in the complexes **1·Ln**, and **2·Ln** and the [LnN_3O_5F] nonacoordinate fragments around the Ln centers in the energy optimized geometries of the hypothetical monomeric complexes **H_4LYF** and **Na_2H_2LYF** representing the fluorinated congener of **1·Y**. The coordination geometry with the *minimal distortion paths value* with respect to the ideal topology is highlighted in bold with green text for each metal center.

Complex Polyhedron*	**1·Y**	**1·Gd**	**1·Dy**	**2·Y**	**2·Gd**	**2·Dy**	**H_4LYF**	**Na_2H_2LYF**
EP-9	29.482	29.343	29.375	35.446	35.052	35.293	31.453	30.762
OPY-9	21.338	21.111	21.237	23.271	23.446	23.313	20.638	21.262
HBPY-9	17.492	17.653	17.520	15.420	15.216	15.319	15.491	16.428
JTC-9	14.182	14.514	14.209	16.358	16.348	16.336	15.829	15.508
JCCU-9	7.437	7.510	7.464	8.068	8.127	8.099	7.704	7.279
CCU-9	6.241	6.318	6.254	6.736	6.771	6.762	7.218	6.728
JCSAPR-9	4.063	4.249	4.120	2.746	3.008	2.831	6.403	4.721
CSAPR-9	3.171	3.395	3.230	**1.807**	**2.060**	**1.893**	7.388	5.535
JTCTPR-9	4.200	4.502	4.277	4.086	4.256	4.158	**5.181**	**3.575**
TCTPR-9	4.246	4.325	4.288	2.582	2.796	2.656	7.726	5.694
JTDIC-9	11.371	10.838	11.296	11.310	11.164	11.291	12.377	12.624
HH-9	6.062	6.003	6.036	8.707	8.403	8.656	6.008	6.915
MFF-9	**2.664**	**2.817**	**2.698**	1.843	2.097	1.933	6.081	4.766

*EP-9: Enneagon (*D9h*); OPY-9: Octagonal pyramid (*C8v*); HBPY-9: Heptagonal bipyramid (*D7h*); JTC-9: Johnson triangular cupola J3 (*C3v*); JCCU-9: Capped cube J8 (*C4v*); CCU-9: Spherical-relaxed capped cube (*C4v*); JCSAPR-9: Capped square antiprism J10 (*C4v*); CSAPR-9: Spherical capped square antiprism (*C4v*); JTCTPR-9: Tricapped trigonal prism J51 (*D3h*); TCTPR-9: Spherical tricapped trigonal prism (*D3h*); JTDIC-9: Tridiminished icosahedron J63 (*C3v*); HH-9: Hula-hoop (*C2v*); MFF-9: Muffin (*Cs*).

========== THE END ==========